Tetrahedron 67 (2011) 9233–9264

Contents lists available at SciVerse ScienceDirect

Tetrahedron

journal homepage: www.elsevier.com/locate/tet

Tetrahedron report number 955

Colorimetric metal ion sensors

Navneet Kaur [a,*], Subodh Kumar [b,*]

[a] Department of Chemistry, Panjab University, Chandigarh, 160 014, Punjab, India
[b] Department of Chemistry, Guru Nanak Dev University, Amritsar 143 005, Punjab, India

ARTICLE INFO

Article history:
Received 30 August 2011
Available online 8 September 2011

Contents

1. Introduction

Molecular chemistry has developed a wide range of procedures for creating ever more sophisticated molecules and materials from atoms linked by covalent bonds.[1] Beyond molecular chemistry, supramolecular chemistry aims at constituting highly complex, functional chemical systems from components held together by intermolecular forces. Chemosensors are the molecules of abiotic origin that bind selectively and reversibly with the analyte with concomitant change in one or more properties of the system, such as color (colorimetric chemosensors) or fluorescence (fluorescent chemosensors) or redox potentials (electrochemical sensors) (Fig. 1).[2–7]

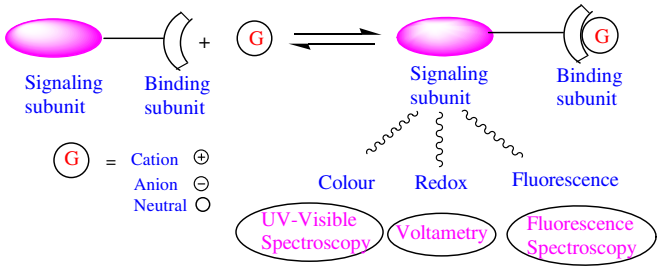

Fig. 1. Schematic presentation of interaction of chemosensor with guest analyte.

Supramolecular chemistry, conceptually founded as a research field in its own right in the 1960s, is a rapidly growing field at the borderline of several disciplines, such as bio(organic) chemistry, material sciences and certainly the classical chemistry topics, i.e., (in) organic and physical chemistry.[8] An early landmark in the development of receptors for group I metal cations was Pedersen's observations of the formation of side products during the synthesis

* Corresponding authors. Tel.: +91 172 2541435; fax: +91 172 2545074 (N.K.); tel.: +91 183 2258802 09x3206; fax: +91 183 2258820 (S.K.); e-mail addresses: neet_chem@yahoo.co.in (N. Kaur), subodh_gndu@yahoo.co.in (S. Kumar).

0040-4020/$ – see front matter
doi:10.1016/j.tet.2011.09.003

of 'metal deactivators' for use in the stabilization of rubber.[9] The ensuing decade brought further notable advances through the use of the principles of shape and size complementarity and Cram's principle of preorganization of binding sites in the design and construction of spherands, cavitands, lariat ethers, and macrocyclic ligands with predetermined selectivity for cations.[10]

Significant contributions by Lehn have transformed the humble beginning of molecular recognition into molecular information, functionalized supramolecular materials, self-organization, self-assembly, and this has been extended to constitutional dynamic chemistry.[11] The trailblazing work of the trio has been recognized by the Nobel Prize in Chemistry in 1987.

The recognition and signaling of ionic and neutral species of varying complexity is one of the most intensively studied areas of contemporary supramolecular chemistry.[12] The dynamic forces viz. dipole–dipole, H-bonding, charge–dipole, cation-π etc. are responsible for reversible substrate–analyte association and, additionally, many of the sensors exploit the dynamic exchange of covalent bonds. In this sensing process, information at the molecular level, such as the presence or not of a certain guest in solution, is amplified to a macroscopic level; hence sensing might open the door to determination (qualitative or quantitative) of certain guests.

Among different types of chemosensors, colorimetric/chromogenic chemosensors are especially attractive because the guest determination can be carried out by the naked eye, without the use of expensive equipment and they also find direct applications in the development of optodes and disposable dip-stick arrays based on absorption changes.[13,14] In colorimetric chemosensors, a bathochromic or hypsochromic shift of absorption spectra or visual color change is affected by the respective increase or decrease in electron densities (Fig. 2) on the chromophore moiety, which is more effectively carried by the association of a charged analyte, i.e., cation or anion than a neutral molecule. So, most of the chromogenic sensors are available for only charged guests.

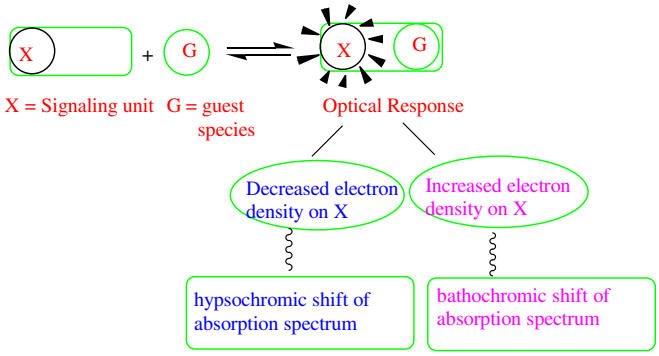

Fig. 2. Schematic presentation of hypsochromic and bathochromic shifts in chemosensors.

In this review, based on the metal ion, colorimetric cation sensors have been classified into different categories:

Alkali and alkaline earth metal ion sensing chemosensors
Cu^{2+} metal ion sensing chemosensors
Hg^{2+} metal ion sensing chemosensors
Ag^{+} metal ion sensing chemosensors
Fe^{2+}/Fe^{3+} metal ion sensing chemosensors
Pb^{2+} metal ion sensing chemosensors
Zn^{2+} metal ion sensing chemosensors
Other transition metal ion sensing chemosensors
Lanthanide sensing metal ions

Amongst all these colorimetric cation sensors, the chemodosimeters use specific reactions between host and metal ions to give new chemical entities with dramatic color changes.

2. Alkali and alkaline earth metal ion sensing chemosensors

A photochromic diarylethene with an imidazole unit (**1**) has been used for the detection of Na^{+}/K^{+} by colorimetric changes and for the detection of Cu^{2+} by fluorescence changes.[15] The absorption spectrum of **1** showed λ_{max} at 318 nm. Addition of Cu^{2+} to a solution of **1** produced a decrease in intensity of the 318 nm band with a concomitant increase in a new one at 370 nm (K_b 3.73×10^4 M^{-1}). Upon irradiation with UV light, absorption of **1** at 318 and 230 nm decreased and two new bands appeared at 545 and 340 nm, which corresponded to structure **2**. Accompanying photocyclization, the color of the solution changed from colorless to purple. Addition of Na^{+} to the solution of **2** produced a decrease in intensity of the 550 nm band in the absorption spectrum with a concomitant increase in a new band at 440 nm. This was accompanied by a strong color change from purple to yellow. Similar results were obtained when **2** formed a complex with K^{+}. The binding constants for 1:1 complex formation were found to be 5.8×10^4 and 6.5×10^4 M^{-1} for Na^{+} and K^{+}, respectively.

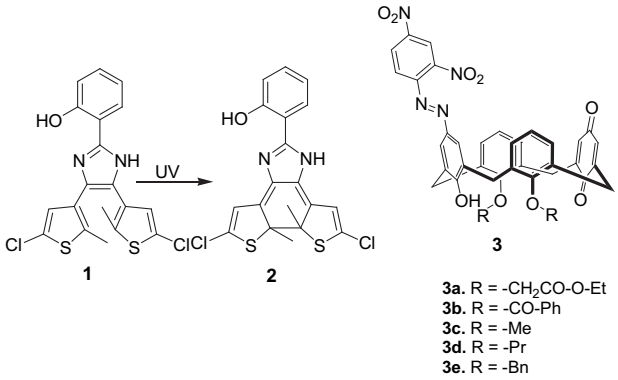

However no color change was observed when **2** bonded with Ca^{2+}, Mg^{2+}, Mn^{2+}, Fe^{2+}, Ba^{2+}, Li^{+}, Cd^{2+}, and Pb^{2+} and no new absorption band was detected, except for a slight decrease in intensity of the 550 nm band. The color changed from purple to gray when **2** bonded with Zn^{2+}, Ni^{2+}, Hg^{2+}, Ag^{+}, Co^{2+}, and Cu^{2+}. The spectral investigations showed that the absorption at 550 nm disappeared and a new absorption was detected when **2** bonded with Zn^{2+}, Ni^{2+}, Hg^{2+}, Ag^{+}, Co^{2+}, and Cu^{2+}. However, the absorption of the 550 nm band experienced a red shift when **2** bonded with Zn^{2+}, Ni^{2+}, Co^{2+}, and Cu^{2+} and the absorption disappeared when **2** bonded with Hg^{2+} and Ag^{+}.

Chawla et al. demonstrated that an azo-calix[4]arene monoquinone (**3a**) exhibited a significant bathochromic shift in its UV–vis spectrum on interaction with K^{+} ions in comparison to its treatment with other alkali metal ions.[16] In $CHCl_3$/MeOH (1:1 v/v), the absorption peak of **3a** at 422 nm shifted bathochromically in the presence of Na^{+} and K^{+} ions with the concurrent appearance of a new absorption band at 604 nm ($\Delta\lambda$=182 nm), while addition of Li^{+}, Rb^{+}, and Cs^{+} ions did not exhibit any significant shift in the absorption maximum of **3a**.

However, chemosensors **3b**–**e** did not exhibit any significant change in their absorption maxima when interacted with alkali metal ions, indicating that the functionality tethered to the lower rim of **3a**–**e** played an important role in the binding of alkali metal ions. The association constant of **3a** in the presence of K^{+} ions was determined as 3.27×10^4 M^{-1}.

In a DMF/NaOH medium, a polyamido–amine dendrimer having sixteen 1,8-naphthalimide fragments in its periphery (**4**) formed a complex only with Li^{+} ions, which was detected by a color change from red to yellow.[17] Without NaOH, **4** absorbed at 439 nm and had an intense yellow color. Upon titration with NaOH, the absorbance at 439 was reduced and marked by the appearance of new bands in the UV region at 335 nm and another in the visible

region with λ_{max} at 531 nm. The color of the solution changed to red. This might be due to deprotonation of the hexylamino substituents at C-4 of the 1,8-naphthalimide units caused by OH^- ions.

On the other hand, in pure DMF solution, deprotonation did not occur, but, after addition of a quantity of NaOH to a solution of **4**, the color changed from yellow to red and other metal ions were then added. Only upon addition of Li^+, the absorption maxima at 335 and 351 nm were decreased, while that at 439 nm increased. This caused the color to change from red to yellow. Addition of Na^+ and K^+ did not result in any color or absorption changes.

However, the UV–vis spectrum of a bisindole bearing calix[4] crown-6 (**6**) in MeCN exhibited λ_{max} at 475 nm.[19] Upon addition of alkaline earth metal ions (Mg^{2+}, Ca^{2+}, Sr^{2+}, and Ba^{2+}) to the solution of **6**, the band at 475 nm decreased along with the appearance of a new band at 538 nm. The color of the solution changed from yellow to scarlet. In addition, chemosensor **6** underwent color and absorption changes with the addition of F^- and $MeCOO^-$ ions in MeCN. As a consequence of the UV–vis spectral behavior of **6** in the presence of Ca^{2+} and F^-, **6** mimicked the function of combinational NOR logic gate.

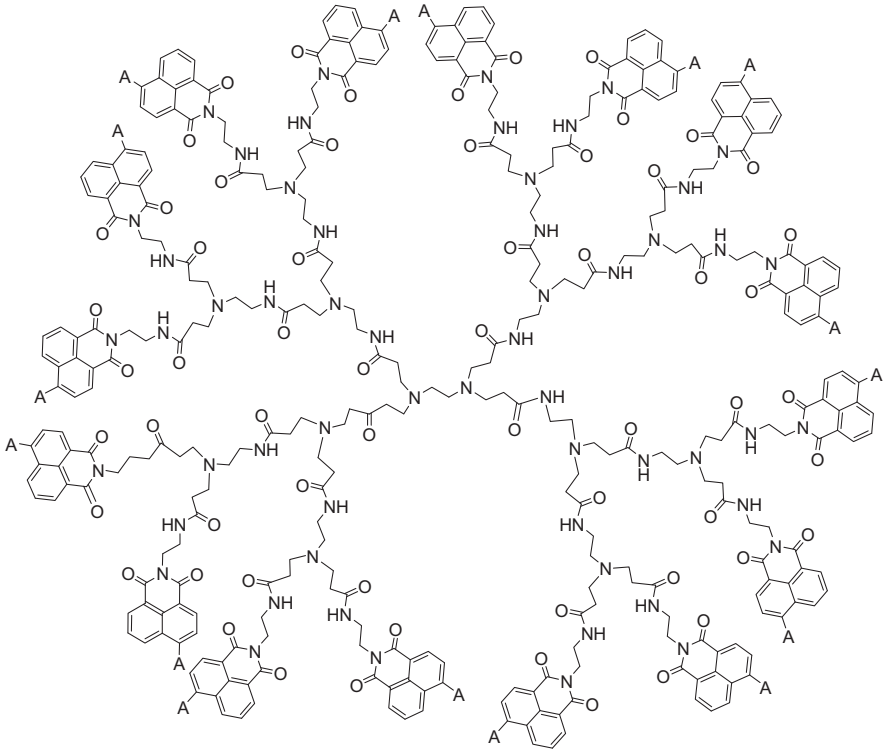

4

Calix[4]arenes **5a**–**e** ($CHCl_3$/MeOH 1:1) exhibited significant bathochromic shifts with Cs^+ (91 nm) and Rb^+ (77 nm) with little or no shifts with Li^+, Na^+, and K^+—the smaller alkali metal ions.[18] Amongst the transition metal ions, only the presence of Pd^{2+} caused a bathochromic shift of 148 nm in **5d**, which was accompanied by a visual color change from yellow to bluish-green. The spectral fitting of Pd^{2+} binding with **5d** showed a 2:1 (Pd^{2+}: **5e**) stoichiometry.

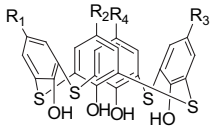

5a. R_1 = Ph-N=N-; R_2 = R_3 = R_4 = H
5b. R_1= R_3 = Ph-N=N-; R_2 = R_4 = H
5c. R_1 = R_2 = R_3 = Ph-N=N-; R_4 = H
5d. R_1 = NSH_2C_3-N=N; R_2 = R_3 = R_4 = H
5e. R_1 = R_2 = NSH_2C_3-N=N-; R_3 = R_4 = H

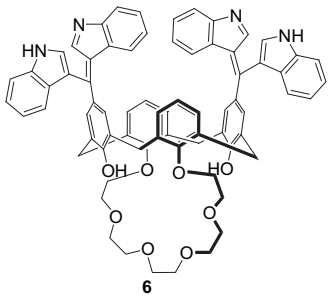

6

Tetrazoles and *para*-substituted phenylazo-coupled calix[4] arenes (**7** and **8**) underwent different absorption changes upon addition of alkaline earth metal ions.[20] The UV–vis absorption maxima of the **7** and **8** showed λ_{max} between 360 and 386 nm. Chemosensor **8a** in MeCN exhibited a remarkable bathochromic shift (from 363 to 533 nm) and a hyperchromic effect toward Ca^{2+}. The color of **8a** changed from colorless to magenta. Medium responses to Cr^{3+} and Pb^{2+} were also found for **8a**. However, no change in the UV–vis spectra was found for the rest of the alkali,

alkaline earth, and transition metal ions. Although **7a** also showed apparent bathochromic shifts toward Cr^{3+} and Ca^{2+}, its association constant was too small to be measured for Ca^{2+} or smaller than that with **8a**. In contrast, the screening of 4-(4-nitrophenyl)azo analogues **7b** and **8b** toward metal ions showed strong bathochromic shifts toward Ca^{2+}, Pb^{2+}, and Ba^{2+}.

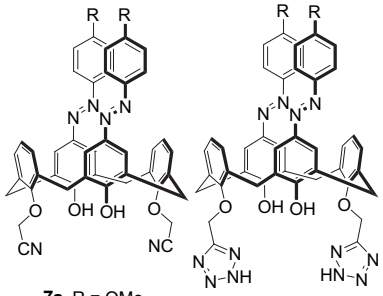

7a. R = OMe
7b. R = NO_2

8a. R = OMe
8b. R = NO_2

A bifunctional chromogenic calix[4]arene (**9**) exhibited an absorption band at 390 nm in MeCN/$CHCl_3$ (1000:4 v/v), which had been found to exhibit remarkable selectivity toward Ca^{2+}, Pb^{2+}, and Ba^{2+} over all other metal ions.[21] The addition of 10 equiv of Ca^{2+}, Pb^{2+}, and Ba^{2+} to a solution of **9** induced a bathochromic shift from λ_{max} 390 to 496, 501, and 485 nm, respectively. Upon interaction with Ca^{2+}, the greenish solution of free **9** turned to a bright-yellow color. The association constants for 1:1 binding were determined to be 1.01×10^5 M^{-1} for **9**·Ca^{2+}, 6.35×10^4 M^{-1} for **9**·Pb^{2+}, and 2.53×10^4 M^{-1} for **9**·Ba^{2+}.

The addition of F^-, AcO^-, and $H_2PO_4^-$ to **9** induced a red shift of the absorption band from 390 nm to 626 nm for F^-, 618 nm for AcO^-, and 622 nm for $H_2PO_4^-$ along with a change in color of the solution from light green to bluish. As a consequence of the UV–vis spectral behavior of **9** toward Ca^{2+} and F^- ions, the chemosensor **9** provided a structure to mimic an INHIBIT logic gate with YES logic function.

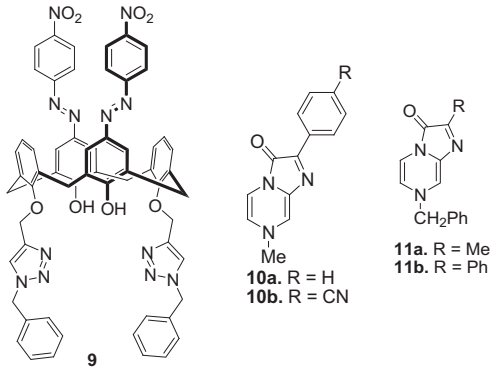

9

10a. R = H
10b. R = CN

11a. R = Me
11b. R = Ph

Hirano et al. studied the metal-ion complexation properties of solvatochromic benzylimidazopyrazinone derivatives (**10** and **11**).[22,23] The UV–vis spectra of **10a** and **10b** derivatives in MeCN exhibited λ_{max} at 501 and 523 nm, respectively. Upon addition of Li^+, Ba^{2+}, Ca^{2+}, Mg^{2+}, La^{3+}, and Sc^{3+} to the solutions of **10a**/**10b**, the absorption band was blue shifted ~25–85 nm, depending upon the Lewis acidity of the metal ion. As the Lewis acidity of the metal ion increased, the Lewis acid/base interactions in the complexes were enhanced, resulting in a blue shift of the λ_{max} values. The solution color of **10b** changed from pink to pale yellow, while that of **10a** changed from red to pale yellow.

The correlations obtained using Fukuzumi parameters indicated that metal–ion complexes of the 2-phenyl derivative **11b** had a wider color variation range and a higher sensitivity to the Lewis acidity of the metal ions compared to those of the 2-methyl derivative **11a**. Ba^{2+}, Li^+, Ca^{2+}, Mg^{2+} formed 1:1 types of complexes with **11a**/**11b**, while La^{3+} and Sc^{3+} formed 2:1 types of complexes.

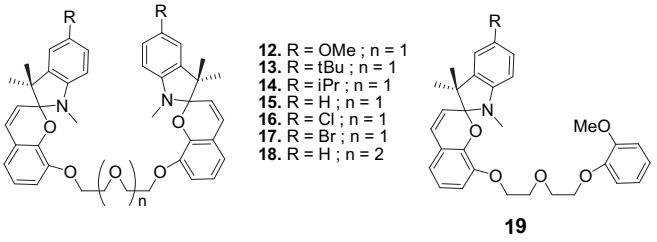

12. R = OMe ; n = 1
13. R = tBu ; n = 1
14. R = iPr ; n = 1
15. R = H ; n = 1
16. R = Cl ; n = 1
17. R = Br ; n = 1
18. R = H ; n = 2

19

A series of oligoether-linked bis(spiropyran) podands [X-BSP (X=MeO, ^{t}Bu, ^{i}Pr, H, Cl, Br), **12**–**19**] had the ability to colorimetrically sense alkaline earth metal ions amongst alkali metal ions.[24] Although chemosensor **15** exhibited no absorption in the visible region in the absence of Ca^{2+}, absorption bands appeared at 397 and 534 nm when Ca^{2+} was present. Similar spectral changes were also observed for chemosensors **12**–**14**, **16**, and **17** upon addition of alkaline earth metal ions, such as Mg^{2+}, Ca^{2+}, Sr^{2+}, and Ba^{2+}, where the solutions of the chemosensor—M^{2+} mixture were deeply colored. Moreover, the color and absorption properties of chemosensors **12**–**19** remained unaffected in the presence of alkali metal ions. However, the selectivity and sensitivity of the bis(spiropyran) podands toward alkaline earth metal ions were tuned by the length of the oligoether moiety and the substituent introduced to the indoline moieties, respectively. In the case of chemosensor **15**, the most intense coloration was observed for Ca^{2+}, whereas Mg^{2+} and Ba^{2+} solutions were less colored, due to the lower stability of these complexes. The absorption maxima of these complexes range from 520 to 550 nm and the solutions were colored from reddish violet (Mg^{2+}) to bluish purple (Ba^{2+}) to purple (Ca^{2+}). On the other hand, the range of λ_{max} in the chemosensor **19** was narrower than that for chemosensor **15** and the λ_{max} of the complexes with Ca^{2+}, Sr^{2+}, and Ba^{2+} was also very similar.

For the chemosensors **12**, **13**, and **14**, λ_{max} was mostly observed within 1 nm of the chemosensor **15**, showing that the introduction of the electron-donating substituents into the indoline moieties hardly affected the λ_{max} of the complexes. However, in chemosensors **16** and **17**, slight bathochromic shifts of λ_{max} by ~10 nm were observed, although the color ranges across the series of metal ions were similar to those observed in podands with the electron-donating groups.

Anthraquinone-based receptors **20a** and **20b** showed selectivity for group IIA metal ions in comparison to group IA metal ions.[25] Receptors **20a** and **20b** exhibited two strong absorption bands at λ_{max} 278 and 427 nm with shoulders at 328 and 369 nm, respectively. Amongst the alkaline earth metal ions, only the addition of Mg^{2+} to solution of **20a** and **20b** in DMF caused a set of new absorption bands in the range 500–575 nm for both the receptors. Consequently, a visual color change from yellow to red was noticed. The visual changes and association constants for **20a** ($K_a=1.02\times10^5$ M^{-1}) were more prominent as compared to **20b** ($K_a=2\times10^4$ M^{-1}).

Squaraine-tethered bichromophoric podand **21** containing five oxygen atoms in the flexible podand moiety was found to specifically bind Ca^{2+} in the presence of other metal ions, such as K^+, Na^+, and Mg^{2+}.[26] The selective binding of Ca^{2+} was clear from the visual color change of **21** from light blue to intense purple blue. Upon gradual addition of Ca^{2+}, the intensity of the absorption maximum at 630 nm decreased with a concomitant hypsochromic shift to λ_{max} 552 nm.

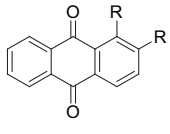

20a. R = OH
20b. R = OMe

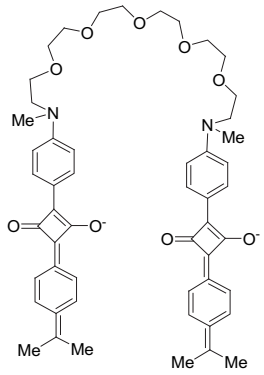

21

Molina et al. invoked the use of azines for the sensing of metal ions via color and redox changes. The absorption spectra of **22** and **23** showed MLCT bands in the region 483–485 nm.[27] On addition of a solution of Mg^{2+} in MeCN into a CH_2Cl_2 solution of **22**, the MLCT band at λ_{max} 483 nm (orange in color) completely disappeared and was replaced by a new band at λ_{max} 564 nm (purple in color). The resulting titration isotherm showed 1:1 binding with K_a 1.02×10^6 M^{-1}. Similarly, a solution of **23** showed a red shift of the absorption band from λ_{max} 485–585 nm with Mg^{2+}. Addition of Na^+, K^+, and Ca^{2+} caused negligible changes in the UV–vis spectra.

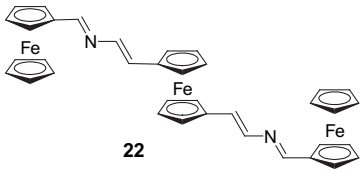

22

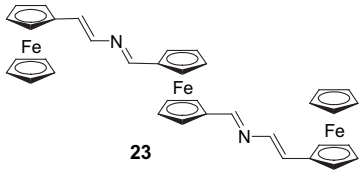

23

The aza-crown ether acridinedione-functionalized gold nanoparticles (**25**) had been investigated as colorimetric and fluorimetric chemosensors for Ca^{2+}/Mg^{2+} by Ramamurthy et al.[28] The absorption spectrum of acridinedione dye (**24**) in MeCN was centered around 360 nm. However, the absorption spectrum of **25** consisted of two bands: (1) the additive absorption spectrum of **24** due to ICT around 360 nm and (2) a broad band in the visible region around 529 nm, which has been attributed to the surface plasmon resonance (SPR) for the stabilized gold nanoparticles. Addition of Na^+/K^+ did not alter the absorption/emission properties of **25**. In contrast, on addition of Ca^{2+}/Mg^{2+} ions, the MeCN solution of **25** showed a red shift in the absorption maximum. The colloidal solution of **25** appeared red and immediately turned to blue upon addition of Ca^{2+}/Mg^{2+}.

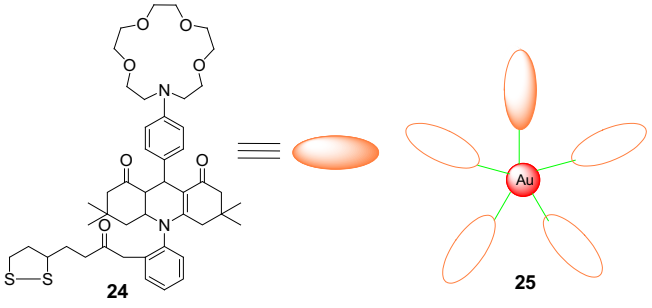

24 **25**

A cooperative effect of bifunctionalized AuNPs on recognition of alkali ions by crown and carboxylate moieties in aqueous media has been reported by Chen and his group.[29] The response time and sensitivity of recognizing alkali metal ions by AuNPs were significantly dependent on the chain length of the crown thiols. Prior to the addition of aggregating alkali metal cations, the solution of (**26**, **27**)-AuNPs appeared ruby red. Upon exposure to 25 μM KCl, the solution of **26a**-AuNPs transformed to blue immediately. However, the response for **26b** and **26c**-AuNPs subjected to the same concentration level of K^+ was slow. For **26c**-AuNPs, upon exposing to 0.10 mM K^+, the color promptly turned purple.

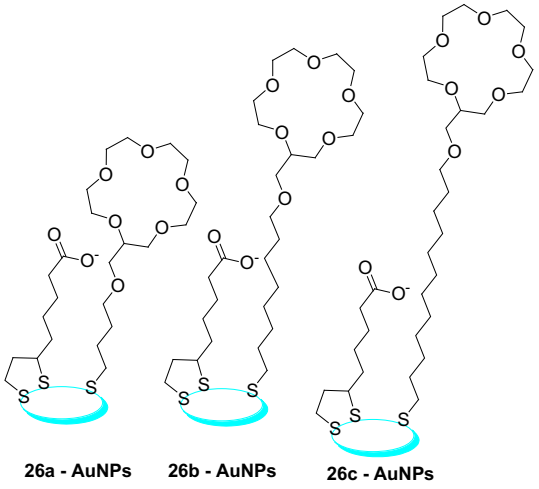

26a - AuNPs **26b - AuNPs** **26c - AuNPs**

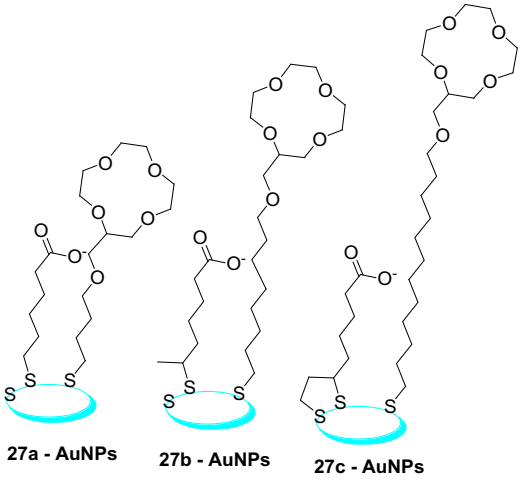

27a - AuNPs **27b - AuNPs** **27c - AuNPs**

27-AuNPs exhibited the same trend of chain-length dependence as **26**-AuNPs. The **27a**-AuNPs showed an intense blue, **27b**-AuNPs were almost unchanged and **27c**-AuNPs gave a deep purple color upon responding to 5.0 mM Na^+. The solutions contained 2.5 mM K^+ as the interfering agent.

The recognition behavior was the best for the shortest crown thiols (**26a** and **27a**-AuNPs, n=4), intermediate for the longest ones (**26c** and **27c**-AuNPs, n=12) and poor for those with eight methylene units (**26b** and **27b**-AuNPs). On the contrary, when the AuNPs were bifunctionalized by thiotic amine and crown thiols, the trend was altered and the sensing performance for the shortest crown thiol (n=4) became the worst.

Fan and his group used unmodified gold nanoparticles as a colorimetric probe for K-DNA aptamers.[30] A solution of unmodified AuNPs was red colored, due to their specific and size-dependent SPR absorption. Addition of salt (K^+) screened electrostatic

repulsion between negatively charged unmodified AuNPs and resulted in aggregation of AuNPs that led to red-to-purple color change. Moreover, Li^+, Na^+, Rb^+, NH_4^+, Ca^{2+}, and Mg^{2+} could not induce a significant color and absorption change of AuNPs.

Dong et al. studied a DNAzyme-based label-free colorimetric method for ultrasensitive detection of K^+, with two G-quadruplex DNAs AGRO100 and human telomeric (HT) DNA as the sensing elements.[31] In the absence of K^+ ions, an AGRO100 and hemin mixture exhibited a catalytic activity largely similar to that of uncomplexed hemin, suggesting no formation of hemin-AGRO100 DNAzyme. The presence of K^+ promoted AGRO100 folding into the G-quadruplex structure and thus allowed the formation of hemin-AGRO100 DNAzyme. The absorbance of the mixture increased sharply. The formed DNAzyme could effectively catalyze H_2O_2—mediated oxidation of ABTS, giving rise to a change in solution color. On the other hand, the presence of Na^+ had little contribution to the DNAzyme activity under same conditions. In contrast to AGRO100, the utilization of HT-DNA for K^+ detection gave a lower sensitivity and poor linearity.

3. Cu^{2+} metal ion sensing chemosensors

N-azo coupled receptors **28a**–**d** possessing amide or urea binding sites[32] showed a highly selective color change from red to yellow on addition of Cu^{2+} amongst Li^+, Na^+, K^+, NH_4^+, Co^{2+}, Cd^{2+}, Pb^{2+}, Zn^{2+}, Hg^{2+}, Fe^{3+}, and Ag^+ metal ions. Solutions of **28a**–**c** in MeCN exhibited an intense absorption band at λ_{max} 480 nm, which on addition of Cu^{2+} resulted in a 160 nm hypsochromic shift. The resulting shifts to shorter wavelengths were attributed to the coordination of Cu^{2+} to the amide carbonyl and to the amino moiety. The log *K* values for the 1:1 complexes are 4.41, 4.39, and 3.38 for **28a**–**c**, respectively. The anchoring of molecular receptor **28d** onto a silica gel plate also showed similar color and UV–vis changes with only Cu^{2+} ions and could detect 10 μM Cu^{2+} in water.

The capture of Cu^{2+} by the receptor[33] **29** resulted in a reduction of the electron-donating ability of the two amino groups conjugated to the naphthalene ring, thus increasing the absorption around 500 nm. Addition of Cu^{2+} to the solution of **29** sufficiently blue shifted the emission from 525 to 475 nm so that the two emission bands are visible. This visible emission change from green to blue allowed Cu^{2+} to be readily distinguished by the naked eye.

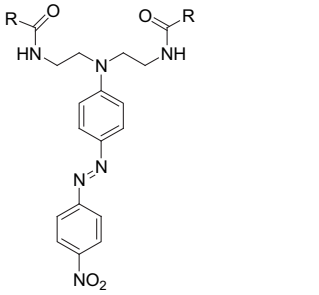

28a. R = $CH(Me)NHCO(CH_2)_{10}Me$
28b. R = $CH(Me)NHCOMe$
28c. R = $(CH_2)_{10}Me$
28d. R = $-NH(CH_2)_3Si(OEt)_3$

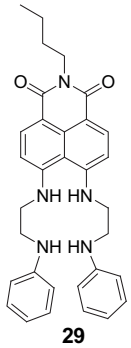

29

Chemosensor **30**, the conjugate of dioxo-tetraamine and 4-amino-1,8-naphthalimide, has found application in the selective estimation of Cu^{2+} amongst heavy-metal ions.[34] The yellow-green methanol solution of **30** (λ_{max} 440 nm) changed to almost colorless on addition of Cu^{2+} (K_a=10,074 M^{-1}) and to orange on addition of Hg^{2+} (K_a=5018 M^{-1}). With the addition of Cu^{2+} to an aqueous methanol solution of **30**, the absorbance at λ_{max} 437 nm decreased with the appearance of a new band at 403 nm. In aqueous methanol, Hg^{2+} did not interfere in the estimation of Cu^{2+}. However, addition of Hg^{2+} to **30** in methanol caused a bathochromic shift from λ_{max} 438–483 nm.

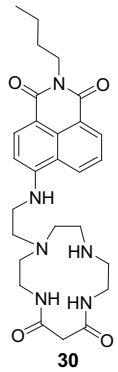

30

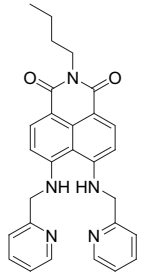

31

Naphthalimide-based chemosensor **31** senses only Cu^{2+} among heavy and transition metal ions by means of a colorimetric (primrose yellow-to-pink) method with a large red shift in emission (green-to-red) attributed to the deprotonation of the secondary amine conjugated to the naphthalimide fluorophore.[35] The absorption spectrum of **31** (10 μM) exhibited λ_{max} at 419 and 458 nm. On addition of 1 equiv of Cu^{2+} to the solution of **31**, the absorbance at 419 nm decreased sharply to its limiting value, while that at 458 nm increased prominently. Furthermore, continuous addition of 1 equiv of Cu^{2+}, the absorbance at 458 nm decreased gradually and an absorption band at 509 nm developed, which induced a color change from primrose yellow to pink.

A similar type of Cu^{2+}-induced deprotonation of the amine NH of 1,8-naphthalimide has been observed in the chemosensors **32**,[36] **33**,[37] and **34**.[38] Chemosensor **32c** underwent a bathochromic shift from 462 to 540 nm with addition of Cu^{2+} along with a color change from yellow to pink. The binding constant of **5c** with Cu^{2+} was calculated to be $7.3\pm0.15\times10^6$ M^{-1}. Similar results were obtained for chemosensor **32b** with a color change from yellow to red. The binding constant of **32b** with Cu^{2+} was $3.77\pm0.29\times10^3$ M^{-1}. However, the Cu^{2+} ion could not induce a change in the UV–vis spectra of **32a**, even at high Cu^{2+} concentration. However, upon addition of Cu^{2+} to the solution of **33**, the band at 514 nm increased in intensity at the expense of the 464 nm band. This 50 nm red shift was associated with a color change from yellow to pink.

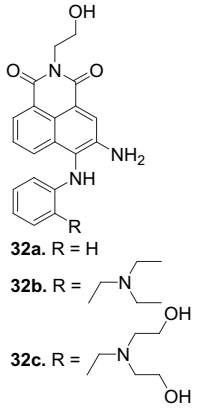

32a. R = H
32b. R =
32c. R =

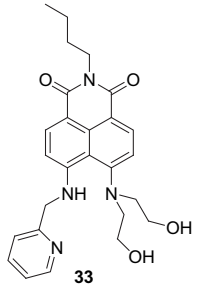

33

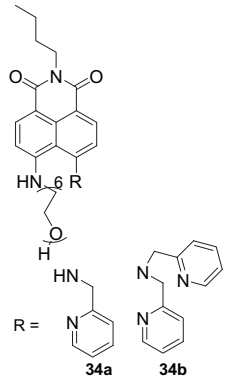

R =

34a **34b**

On the other hand, with the addition of Cu^{2+} to the solution of **34b**, the absorption band at 459 nm decreased and the other two bands at 306 and 504 nm occurred and increased. This was accompanied by a color change from primrose yellow to pink. However, in the absorption spectrum of **34a**, an increasing band around 430 nm was found with the addition of Cu^{2+} (~29 nm blue shift).

Another 1,8-naphthalimide-based perinone dye (**35**) underwent a color change from orange to purple by the addition of Cu^{2+}.[39] The

UV–vis spectrum of the chemosensor **35** in MeCN/H_2O (90:10 v/v) exhibited λ_{max} peaks at 343, 359, and 470 nm. Upon gradual addition of Cu^{2+} to the solution of **35**, the bands at 343 and 359 nm progressively decreased and got slightly shifted, while the band at 470 nm disappeared gradually with simultaneous generation of a new broad band appearing at 557 nm. The association constant for 1:1 binding stoichiometry was found to be 2.16×10^4 M^{-1}.

The absorption spectrum of a perylene-diimide based chemosensor **36**[40] showed two peaks at 491 and 529 nm and the addition of Cu^{2+} showed a remarkable absorption enhancement at 531 nm, while other metal ions induced negligible changes under the same conditions. Moreover, the solution of **36** upon the addition of 20 equiv of Cu^{2+} displayed a distinguishing pink color, compared with the other cations.

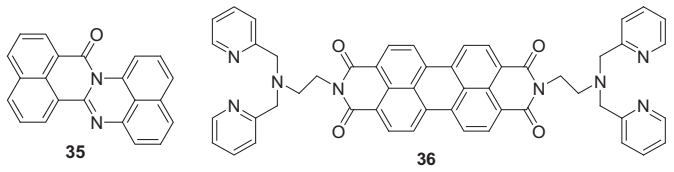

35 **36**

The sensor **37**, possessing oxadiazole and pyrazine heterocycles[41] (H_2O, pH 7.4), underwent a gradual blue shift from λ_{max} 483 to 441 nm with increasing concentrations of Cu^{2+} accompanied by a gradual hypochromic effect.

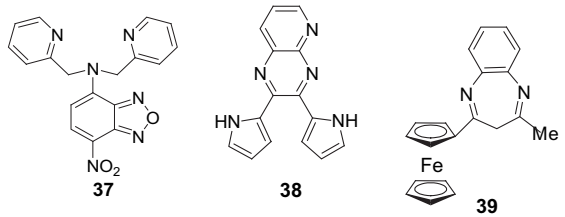

37 **38** **39**

In the dipyrrolylpyrazine derivative **38**,[42] having an additional fused pyridine ring, on addition of Ni^{2+}, Co^{2+}, Cu^{2+}, Zn^{2+}, and Cd^{2+} the absorption band at λ_{max} 420 nm (MeCN) due to free **38** disappeared and a new band appeared at λ_{max} 496 nm. The metal–ion binding is associated with a naked-eye color change from yellowish green to brown. In the case of Cd^{2+}, the color changed to light brown.

The UV–vis spectra of a multichannel signaling cation sensor **39**[43] in MeCN contained a prominent absorption band with λ_{max} at 338 nm and another weaker absorption band at 450 nm. The band at 450 nm of chemosensor **39** was red shifted to 550 nm after addition of 1 equiv Cu^{2+} ion, but more than 1 equiv addition led to quenching of the band at 550 nm and it completely disappeared at 2 equiv addition of Cu^{2+}. Addition of Cu^{2+} ion above 2 equiv did not show any considerable change. The binding constants were calculated as $K_{11}=2.6\times10^3$ M^{-1} and $K_{12}=3.1\times10^3$ M^{-1}, and $\beta_{12}=7.9\times10^6$ M^{-1}. The sequential addition of Cu^{2+} ion from 0 to 1 equiv showed a color change from pale yellow to a deep violet color. After 1 equiv addition, the deep violet color of the solution was gradually reduced and it completely returned to pale yellow.

Torroba et al. reported ferrocene derivatives (**40**–**42**),[44] which were capable of selectively sensing Cu^{2+} and $PhCOO^-$, $MeCOO^-$, and CN^- by cooperative binding of two α,α' groups bonded to the ferrocene nucleus via a naked-eye color change from yellow to colorless. The geometrical constraints and various substitution patterns led these sensors to form complexes of varied stoichiometries with Cu^{2+}, viz. **40**$[Cu^{2+}]_2$, **41**$[Cu_{2+}]_4$ and **42**$[Cu^{2+}]$.

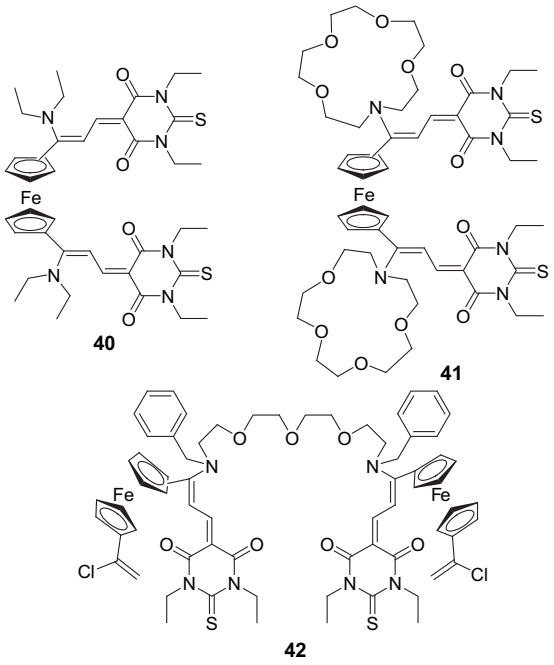

40 **41** **42**

In the case of naphthoquinone derivatives (**43** and **44**),[45] the internal charge-transfer band of **43** and **44** appeared at 532 nm in MeCN. Upon addition of Cu^{2+} to the solution of **43**, a new band appeared at 420 nm, which resulted in a color change of the solution from purple to yellow. Addition of 0.5 equiv Fe^{3+} and Hg^{2+} to the solution of **43** produced a bleaching of the solution, but the band at 420 nm did not appear and the solution remained colorless. Addition of $Cu^{2+}/Fe^{3+}/Hg^{2+}$ to the solution of **44** produced similar changes in the color and absorption spectrum as that observed in the case of **43**. Moreover, addition of Pb^{2+} and Ba^{2+} to the solution of **44** altered the spectrum. Thus, while the presence of Pb^{2+} resulted in complete deactivation of the charge-transfer band, the Ba^{2+} is only able to produce a partial decrease of the intensity of the band at 532 nm.

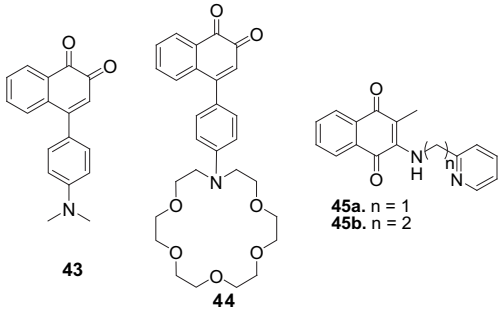

43 **44** **45a.** n = 1 **45b.** n = 2

However, in the case of 1,4-naphthoquinone-based chemosensors **45a** and **45b**, Cu^{2+}-induced deprotonation of the amine NH has been observed.[46] Upon addition of different transition metal ions to solutions of chemosensor **45a** in MeOH/H_2O (4:1 v/v, pH 7.0), Cu^{2+} was the only ion that caused an observable color change from orange to dark blue. In the case of chemosensor **45a**, with increasing Cu^{2+} concentration, the absorbance at 466 nm decreased and a new band centered at 634 nm was formed. Similar changes were observed for chemosensor **45b**. The K_a values for **45a**-Cu^{2+} and **45b**-Cu^{2+} complexes were $1.02\pm0.04\times10^4$ and $8.50\pm0.18\times10^3$ M^{-1}, respectively.

However, when the solvent was changed to MeCN, the only color change was observed when Cu^{2+} was mixed with a solution of chemosensor **45a**. The color changed from orange to blue, but the color rapidly turned orange again, due to the short half life of the deprotonated **45a**-Cu^{2+} complex in MeCN. A reversible color change orange-blue-orange was observed in the **45a**-Ni^{2+} complexes only in methanol.

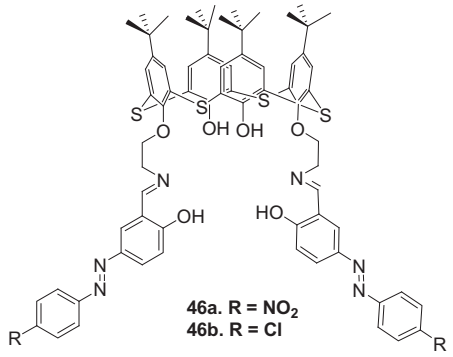

The absorption spectra of thiacalix[4]arene-based imino chemosensors **46a** and **46b** in THF/H_2O (1:1 v/v; pH 7.0 in HEPES) exhibited typical absorption bands at 387 and 351 nm, respectively.[47] The absorption band of chemosensor **46a** underwent a red shift to 451 nm ($\Delta\lambda$=64 nm) along with a color change from light yellow to dark red as 2 mol equiv of Cu^{2+} ion were added, whereas no significant changes were observed upon addition of metal ions, such as Li^+, Na^+, K^+, Cd^{2+}, Ni^{2+}, Zn^{2+}, Ag^+, Pb^{2+}, and Hg^{2+}. This red shift was due to the selective coordination induced deprotonation of the azo-phenol group upon addition of Cu^{2+} ions. Moreover, chemosensor **46b** showed no change in absorption in the presence of any of these ions.

Calix[4]arene-based chromogenic sensors bearing a 9,10-anthraquinone moiety (**47**–**49**) recognized Cu^{2+} amongst other metal ions.[48] The UV–vis spectra of **47**–**49** showed an absorption band at 380 nm in MeCN. On addition of Cu^{2+} to the solution of **47**, a new absorbance band at 450 nm was observed and the color of the solution changed from yellow to red. When Cu^{2+} ions interacted strongly with the lone pair electrons of the carbonyl oxygen atoms along with the aid of the two proximal OH groups of the calix[4]arene platform, then the charge transfer from the 1,8-oxygen atoms to the electron deficient carbonyl group became stronger. However, chemosensors **48** and **49** lacking two proximal OH groups did not show any UV or color changes.

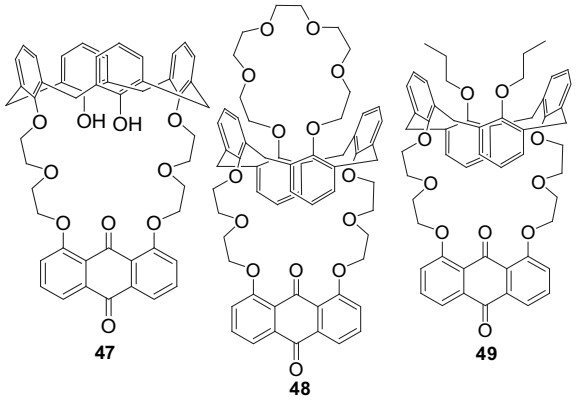

Different anthraquinones bearing electron-rich coordinating sites at 1/1,8 or 1,4 positions for their metal-sensor behavior through color change have been investigated by our group.[49–54] In all the chemosensors, Cu^{2+}-induced deprotonation of the amine NH of anthracene-9,10-dione has been observed, which was responsible for the drastic color changes.

The chemosensors **50a** and **50b** on addition of Cu^{2+} underwent a distinct visual color change from red to blue and a bathochromic shift of λ_{max} from 492 to 600 nm.[49] The presence of alkali, alkaline and transition metal ions like Ni^{2+}, Co^{2+}, Zn^{2+}, Cd^{2+} etc. did not affect the visual color and spectrophotometric changes. However, the sensor **50c** (possessing an additional less basic OH binding site) did not result in any color change or spectrophotometric change on addition of Cu^{2+} or other metal ions.

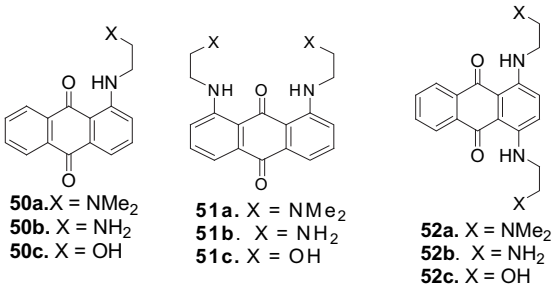

The solution of **51a** and **51b**[50] on gradual addition of Cu^{2+} showed a gradual decrease in absorbance at λ_{max} 535 nm with the concomitant appearance of two new absorption bands at λ_{max} 715 and 800 nm with a gradual increase in intensity with increase in concentration of Cu^{2+}.[28] This caused a color change from magenta to purple to blue. However, no absorption or color changes were observed upon addition of any metal ions to a solution of **51c**.

However, the addition of Cu^{2+} to chemosensors **52a** and **52b** caused a switching of the absorption bands from 585 and 630 to 665 nm with a respective bathochromic shift of 80 and 35 nm.[51] However, on changing the pH of the solution to 9.0, a new band at 725 nm was observed. This resulted in a visible change in color from blue to turquoise blue. No absorption or color changes were observed upon addition of Cu^{2+} to the solution of **52c**.

When the colorless Cu^{2+} solution was added to the red solution of chemosensors **53a**/**53b** at pH 7.0±0.1 (10 mM HEPES in MeOH/H_2O 3:1 v/v), the color changed to blue immediately.[52] The complex remained stable up to pH 11.00 beyond, which the Cu^{2+}-**53b** complex cleaved to form the free ligand and $Cu(OH)_2$.

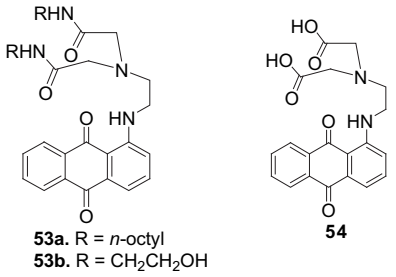

On the other hand, chemosensor **54** (pH 7.0±0.1; 10 mM HEPES in MeOH/H_2O 3:1 v/v) exhibited λ_{max} at 490 nm and, on addition of Cu^{2+} (1 equiv), new absorption band at 600 nm appeared, which induced a color change from red to blue. However, addition of Ni^{2+} and Zn^{2+} showed a lowering in absorption (10–15%) at 495 nm without the appearance of the new absorption band and addition of Co^{2+}, on prolonged standing (~12 h), resulted in a change in color from red to blue. This was associated with a new red-shifted absorption band at 600 nm, but with a significantly lower epsilon value (ε 323) than observed in the case of Cu^{2+} (ε 2070).

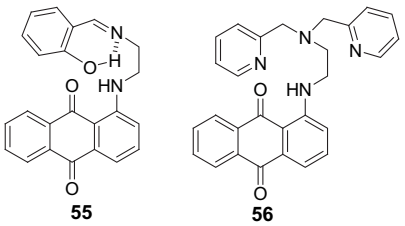

Chemosensor **55**[53] (red, λ_{max} 500 nm) exhibited red-shifted spectral responses and characteristic color changes only on addition of Cu^{2+} (blue, λ_{max} 600 nm) and Ni^{2+} (green, λ_{max} 750 nm), whereas on addition of other metal ions the absorbance spectra of **55** remained unaffected.

On the other hand, the solution of **56** ($MeOH/H_2O$ 4:1 v/v, 10 mM HEPES, pH 7.0±0.1) on addition of solutions of Co^{2+}, Ni^{2+}, and Cu^{2+} showed visible color changes from red to blue and their UV–vis spectra exhibited differently red-shifted absorption bands.[54] Moreover, chemosensor **56** (red, λ_{max} 510 nm) at pH 4.0 (acetic acid–sodium acetate buffer) underwent characteristic color changes only on addition of Co^{2+} (blue, λ_{max} 620 nm), Ni^{2+} (yellowish pink, λ_{max} 380, 460, and 510 nm) and Cu^{2+} (yellow, λ_{max} 460 nm).

Diaminoanthraquinone-linked polyazamacrocycles (**57** and **58**) have been shown to be colorimetric sensors for different transition metal ions in aqueous solution by Guilard et al.[55] The UV–vis spectrum of **57** in $MeOH/H_2O$ solution (1:1 v/v) displayed λ_{max} at 562 nm. Complexation of Cu^{2+} ions induced a red shift of λ_{max} ($\Delta\lambda$=94 nm) and Al^{3+} ions led to a blue shift ($\Delta\lambda$=26 nm). Other metal ions had only a slight influence on the color and absorption changes.

However, in the case of **58a**, the color changed from violet to pink in the presence of Pb^{2+} (hypsochromic shift of 30 nm) and to blue (bathochromic shift of 103 nm) after the addition of Cu^{2+} ions. Equimolar amounts of Al^{3+}, Zn^{2+}, Ni^{2+}, and Cd^{2+} did not change the color of the sensor solution. However, a 100-fold excess of these metals induced a color change from violet to lilac.

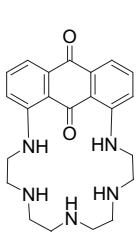

57

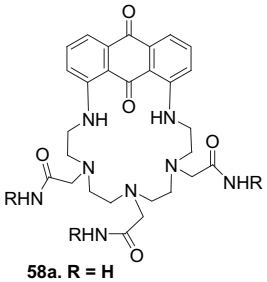

58a. R = H
58b. R = $CH_2P(O)(OEt)_2$

On the other hand, the freely soluble chemosensor **58b** underwent a blue shift of 47 nm upon binding with Pb^{2+} ions in water buffered with HEPES (pH=7.4) along with a color change from violet to pink. The Cd^{2+}-induced spectral changes (blue shift of 44 nm) were similar, but a four-fold excess of Cd^{2+} ions was needed to achieve complete coordination. The complexation of Cu^{2+} ions by chemosensor **58b** was complete after the addition of 1 equiv of the metal salts, but led to a strong red shift ($\Delta\lambda$=97 nm) of the absorption band. Alkali and alkaline earth metal ions in 100-fold excess did not show substantial binding affinity to chemosensor **58b**, but the addition of 100-fold excess of Al^{3+} and Zn^{2+} ions led to a change in color of the solution to violet, whereas Ni^{2+} and Cd^{2+} also taken in 100-fold excess gave pink solutions.

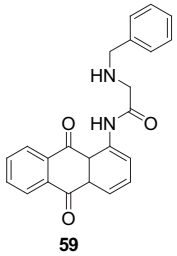

59

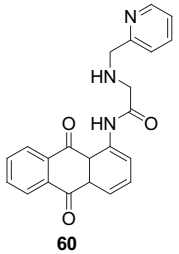

60

A similar Cu^{2+}-induced deprotonation of an amide group of 9,10-anthraquinone based chemosensors **59** and **60** has been demonstrated by Wu et al.[56] When different alkali, alkaline earth, and transition metal ions were added to solutions of chemosensors **59** and **60** in $MeOH/H_2O$ (4:1 v/v, 20 mM HEPES buffer, pH 7.0), only Cu^{2+} was unique in producing a ~76 nm red shift (from 397 to 473 nm), which resulted in a visible color change from yellow to dark red. Addition of Ni^{2+} to chemosensor **60** caused an 86 nm red shift (from 397 to 483 nm), which resulted in a color change from yellow to red. The addition of Co^{2+} to chemosensor **60** resulted in a blue shift and a color change from yellow to pale green, resulting in significant green light emission. The K_a values obtained for **59**-Cu^{2+} and **60**-Cu^{2+} complexes were 8470 and 18,667 M^{-1}, respectively.

Squaraine-based chemosensor **61**[57] had a very strong absorption band centered at 514 nm in HEPES/THF (60:40 v/v, pH 7.4), which shifted to a new position at 675 nm along with a color change from pink to blue. The Job's plot revealed a 1:1 stoichiometry with a stability constant of 1.9×10^6 M^{-1}.

On the other hand, chemosensor **62** with two butyl chains underwent an 86 nm red shift upon addition of Cu^{2+} along with a color change from bright purple to blue-black. Chemosensor **62** could be employed as a Cu^{2+}-selective probe in the fluorescence imaging of living cells.

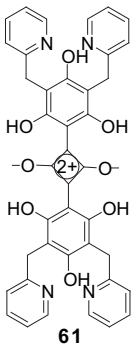

61

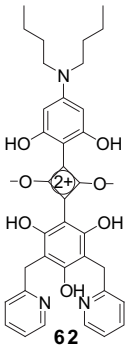

62

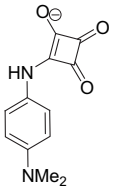

63

The UV–vis spectra of a minimalist squaramide[58]-based chemodosimeter **63** recorded in $MeCN/H_2O$ (1:1 v/v) exhibited an absorption band at λ_{max} 325 nm. Upon addition of Cu^{2+} to the solution of **63**, the initially colorless solution became deep purple, due to the appearance of a strong absorption band around 536 nm. This band was solvent and time dependent.

1-Dicyanomethylene-2-chloro-3-aminoindene derivatives (**64**–**68**)[59] have been found to possess colorimetric applications in cation and anion sensing. Addition of different metal ions to a MeCN solution of chemosensor **64** resulted in a change of color in the presence of Sc^{3+}, Sn^{2+}, Al^{3+}, and especially Fe^{3+} and Cu^{2+}. The UV–vis spectrum of chemosensor **64** showed an intense band with λ_{max} at 550 nm. Addition of increasing amounts of these cations resulted in the quenching of this band, accounting for the bleaching observed in the presence of some of the cations. Chemosensor **64** lost the color in the presence of only CN^- along with disappearance of the absorbance in the 550 nm region.

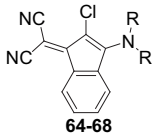

64-68

Chemosensor	R_2NH	Chemosensor	R_2NH
64			
65	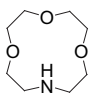	**67**	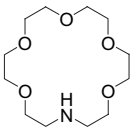
66	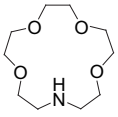	**68**	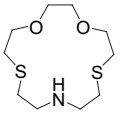

On the other hand, macrocyclic derivatives **65** and **66** did not show immediate color changes in the presence of the usual cations, showing partial decolorization after 20 min in the presence of Sc^{3+}, Sn^{2+}, Al^{3+}, Fe^{3+}, and Cu^{2+}. Chemosensor **67** showed only partial decolorization in the presence of Pb^{2+} and Fe^{3+}. Instead, chemosensor **68** underwent color changes in the presence of Hg^{2+}

(decolorization) and Cu^{2+} (purple to yellow). When Cu^{2+} was added to the solution of **68**, the band centered at 550 nm decreased along with the appearance of a new band at 478 nm.

A solution of quinoline-indene derivative (**69**) in MeCN/H_2O (1:1 v/v) displayed a strong purple color with λ_{max} 545 and 393 nm.[60] Addition of Cu^{2+} resulted in a dramatic change of color from purple to orange along with diminished absorbance at 550 nm. The data gave a 1:1 binding model with an association constant of log K=4.23±0.04. A slight discoloration was observed after the addition of 5 or more equiv of Fe^{3+} or, to a lesser extent, of Hg^{2+} to the solution of **69**. The binding constants for the 1:1 models of complexation of **69** and Fe^{3+} or Hg^{2+} were log K_{Fe3+}=3.44±0.44 and log K_{Hg2+}=3.17±0.01.

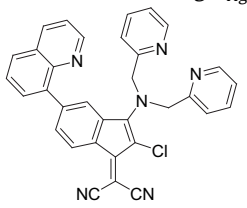

69

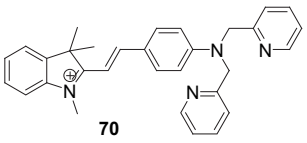

70

When merocyanine dye **70**[61] was treated with various metal ions in the aqueous buffer, only Cu^{2+} ions caused a distinct color change from reddish-purple to yellow along with a blue shift from 504 to 410 nm in the presence of 4 equiv of Cu^{2+} ions. The chemosensor **70** has been used for estimating Cu^{2+} ions within living cells.

Dichlorofluorescein derivatives with two aza-crown ether binding units (**71a** and **71b**)[62] underwent absorption changes with the addition of Cu^{2+}. Chemosensor **71a** exhibited an intense absorption band at 509 nm with a shoulder around 480 nm in an aqueous 50% DMSO solution. Upon interaction with Cu^{2+} ions, **71a** exhibited a significantly diminished absorption around 501 nm. The decreased absorption and slight blue shift from 509 to 501 nm resulted in a change of solution color from yellow to almost colorless. With Pb^{2+} ions, the absorption also decreased significantly and the solution color changed from yellow to light pink. Chemosensor **71b** exhibited similar changes in the absorption spectrum as those observed for chemosensor **71a**, but the Cu^{2+} selectivity of **71b** was less pronounced, compared with **71a**.

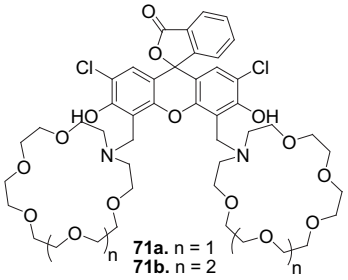

71a. n = 1
71b. n = 2

The 2-aza-1,3-diene moiety in **72** with a putative cation-binding site along with a pyrene unit has been shown to bind selectively with Hg^{2+} and/or Cu^{2+} amongst other metal ions. The UV–vis spectrum of **72** in MeCN exhibited bands at λ_{max} 256, 331, and 413 nm.[63] Addition of only Cu^{2+} resulted in decreased absorbance at λ_{max} 331 and 413 nm with two new bands at λ_{max} 372 and 493 nm causing a color change from yellow to orange. The resulting titration showed a 1:1 stoichiometry with K_a 3.6×10^6 M^{-1}.

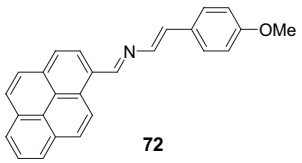

72

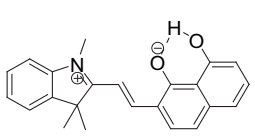

73

In methanol, the absorption maximum of chemosensor **73** appeared at 565 nm. With the addition of Cu^{2+} to chemosensor **73**, the original peak vanished with the appearance of a new peak at 636 nm.[64] The color of the solution changed from blue to cyan. However, upon addition of Cu^{2+} to a solution of chemosensor **73** in phosphate buffer saline (PBS, pH 9.18), the intensity of the absorption maximum at 548 nm was gradually reduced, while a new absorption band appeared at 670 nm with a red shift of 122 nm. This caused a color change from purple to blue.

Tunable photochromism of spirobenzpyrans (**74a** and **74b**) has been observed by Chan's group via selective Cu^{2+}-ion coordination. Metal-chelation modulation affects the equilibrium of the spiro and mero forms.[65] The absorption spectrum of **74a** and **74b** in 50% ethanol/water (v/v) solution at pH 7.04 exhibited strong absorptions in the visible region at 540 and 453 nm. Upon gradual addition of Cu^{2+} to the solution of **74b**, dramatic increases in the absorbance at both 453 and 384 nm were observed up to concentration of 0.5 equiv relative to the host concentration; On further increasing the Cu^{2+} concentration, the two peaks changed into one absorption peak at 418 nm, concomitant with the increased intensity. This absorption change was accompanied by a color change of the solution of **74b** from colorless to red.

On the other hand, in a 50% ethanol/water solution, **74a** was red violet and no significant color change could be observed upon the addition of any metal ions. Although **74a** showed a maximal response toward Cu^{2+}, the enhancements in absorbance at the two wavelengths (396 and 540 nm) were smaller than that of **74b** by Cu^{2+}. Chemosensor **74b** has been used to measure serum divalent copper values.

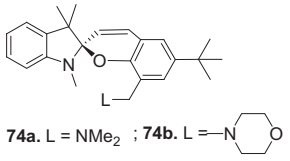

74a. L = NMe_2 ; **74b.** L =

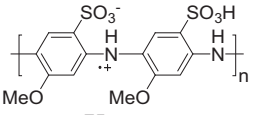

75

Hirao et al. studied the conformational change from extended coil to compact coil induced by the addition of Cu^{2+} to the aqueous emeraldine salt of poly(2-methoxyaniline-5-sulphonic acid) (**75**).[66] The sharp peak around 475 nm attributed to the polaron band was characteristic of the extended coil conformation. The broad peak around 750 nm attributed to the localized polaron band was characteristic of the compact coil conformation. An increase of the peak at 750 nm for the compact coil conformation was observed in the case of Cu^{2+}, Ru^{3+}, Ag^{+}, and Hg^{2+}, where the color of the solution changed from yellow/green to blue. However, the most remarkable changes were observed in the case of Cu^{2+}, the addition of which to a solution of **75** at pH 8.8 resulted in decreased intensity of the polaron band at 471 nm, which completely disappeared after 2 h. Concomitantly, a broad peak around 650 nm appeared and grew gradually with red shifting. The color changed from yellow-green to green within 1 min and then blue within 10 min. After stirring for 24 h, a weak broad shoulder appeared at 540 nm, probably consistent with the oxidation to the pernigraniline state. A catalytic amount of Cu^{2+} was enough to generate the conformational change from the extended to compact coil. However, when the reaction was carried out under argon, the conformational change proceeded very slowly and higher amounts of Cu^{2+} were needed.

The absorption spectrum of phenothiazine-pyridyl chalcone (**76**) displayed a CT band at 434 nm.[67] The addition of Co^{2+}, Zn^{2+}, and Ni^{2+} induced a marginal red shift of 2–4 nm, accompanied by a slight decrease in the band intensity by 5–20%. In addition, these cations also displayed a weak shoulder in the region 540–550 nm. However, addition of Cu^{2+} to a solution of **76** resulted in a decrease in absorbance at 434 nm with a new red-shifted ICT band, which increased in intensity at 560 nm. The red shift of 126 nm resulted in a color change from deep yellow to blue.

A simple heterocyclic molecule, *N*,*N*-dimethyldipyrromethane (**77**),[68] demonstrated a high chromogenic selectivity for Cu^{2+} over

other cations. The UV–vis spectrum of **77** showed a $\pi\rightarrow\pi^*$ absorption band at 223 nm. The addition of Cu^{2+} resulted in the appearance of a peak at 481 nm along with a color change from colorless to intense yellow. Moreover, the **77**-Cu^{2+} complex displayed an ability to detect CN^- from water.

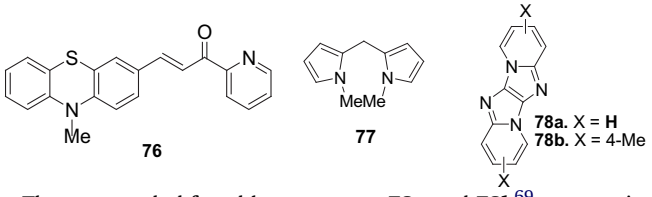

The π-extended fused heteroarenes **78a** and **78b**[69] gave optical responses to metal ions, particularly Cu^{2+}. Chemosensor **78a** displayed λ_{max} at 386 nm in MeCN, the intensity of which gradually decreased and, concomitantly, a new increasing absorption band at 486 nm appeared with Cu^{2+}. When the concentration of Cu^{2+} was further increased, the absorbance at 486 nm began to decline along with a small absorption peak at 525 nm appearing. Hg^{2+} and Fe^{2+} induced a slightly blue-shifted absorption of **78a** with nearly no change in molar absorption coefficient. The colorless solution of **78b** in MeCN changed immediately to a red or yellow color upon addition of different concentrations of Cu^{2+}.

The rotaxane dye **79** having 8-hydroxyquinoline as coupling component exhibited different color changes upon the addition of different metal ions.[70] However, with Cu^{2+}, the color shift depended upon pH, an 80 nm red shift from λ_{max} 440–520 nm with color change from orange to red (pH 7.5) as well as a ~40 nm blue shift from λ_{max} 560 to 520 nm with color change from blue to red (pH 11) being observed. Ni^{2+} and Zn^{2+} imparted a similar, but comparatively weak, red shift at pH 7.5. However, these two metals did not impart a blue shift at pH 11. Under acidic conditions (pH 5), an identical spectral response to that of pH 7.5 was observed.

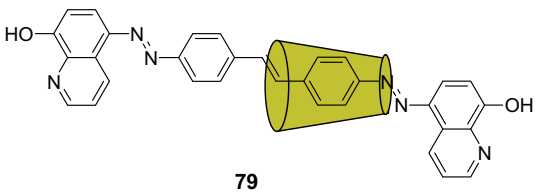

Coumarin pyridyl ketone **80** showed ion discrimination by exhibiting different extents of bathochromic shifts.[71] In MeCN/H_2O (95:5 v/v), chemosensor **80** displayed an intense ICT absorption band in the visible region, which peaked at 465 nm. However, a 118 nm red shift in the absorption was observed in the presence of Cu^{2+}. Similar 80 and 55 nm red shifts were observed upon addition of Ni^{2+} and Cd^{2+}, respectively, to the solution of **80**. The yellow color of the chemosensor **80** changed to blue, purple and orange with the addition of Cu^{2+}, Ni^{2+}, and Cd^{2+}, respectively. The log *K* values based on a 1:1 binding mode were calculated as 4.94 for Cu^{2+}, 3.84 for Ni^{2+}, and 2.98 for Cd^{2+}.

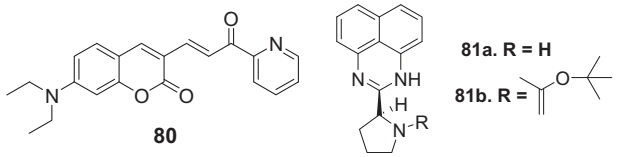

The absorption spectrum of 1,8-diaminonaphthalene-based chemosensor **81a** in MeCN/H_2O (80:20 v/v) exhibited λ_{max} at 328 nm.[72] On addition of 5 μM Cu^{2+} to the solution of **81a**, the absorbance at 328 nm gradually disappeared and a new band appeared around 540 nm that increased progressively, thereby inducing a promising color change from colorless to purple. However, with the addition of solutions up to 15 μM Cu^{2+}, the peak at 328 nm almost disappeared and, again, a significant red shift of the peak from 540 to 650 nm was observed, the intensity of which increased very sharply. This resulted in a naked-eye color change from purple to blue. This red shift occurred due to deprotonation of the secondary amine of the pyrimidine ring.

However, in the chemosensor **81b**, having a sterically hindered protected *N-tert*-Boc group, only the purple color appeared initially. Since the bulky carbamate group restricted the metal–ion coordination with the pyrrolidinium nitrogen, no blue color was observed upon addition of excess Cu^{2+} and the purple color just deepened.

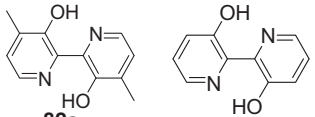

Different 2,2′-bipyridine-3,3′-diols (**82a** and **82b**) have been used for sensing Cu^{2+} by observing changes in the absorption and emission spectra.[73] UV–vis spectroscopy measurements in MeCN displayed typical ligand-centered electronic $\pi\rightarrow\pi^*$ transition bands with a maximum absorption wavelength at 349 nm for **82a** and 342 nm for **82b**. With the addition of Cu^{2+}, a new MLCT band was formed and a decrease in the $\pi\rightarrow\pi^*$ band was observed. This change was accompanied with a color change from colorless to yellow. Binding constant values based on a 1:1 complexation mode were calculated as $3.09\times10^5\pm1.2$ for **82a** and $1.44\times10^7\pm1.4$ for **82d**. The changes observed in the absorption spectrum and color were due to linking of Cu^{2+} to the 2,2′-bipyridine and an oxygen atom from the hydroxyl group.

A colorimetric method using diphenylcarbazide (DPC, **83**)-immobilized sol–gel matrices has been developed by Guan et al.[74] The metal–ion indicator DPC was immobilized in the silica matrices and a cellulose acetate/nitrate membrane was used as the substrate to provide the silica matrices with a support skeleton with a large pore size. With the interaction of Cu^{2+} with **83**, a purple complex was formed, which exhibited a kinetic response for Cu^{2+} ions in the range of 0.16–1.6 μM.

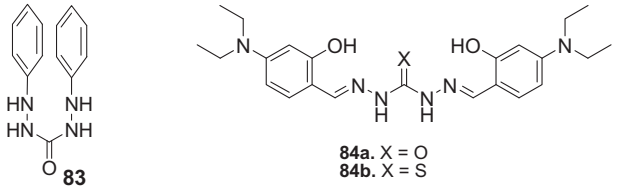

Highly conjugated chemosensors **84a** and **84b** could selectively sense Cu^{2+} by colorimetry with remarkable red shifts, compared with other transition metal ions in MeCN and aqueous media, respectively.[75] Upon addition of 2 equiv of Cu^{2+} to the solution of **84a**, the initial absorbance at 365 nm decreased while a new prominent peak was observed at 450 nm along with a color change from light green to primrose yellow. However, with further addition of Cu^{2+} (up to 5 equiv), the absorbance at 450 nm decreased with the appearance of a characteristic new band at 535 nm. This induced a color change from primrose yellow to pink. On the other hand, with the addition of 2 equiv of Cu^{2+} to **84b**, a 541 nm red shift was observed with the appearance of a new NIR peak at 936 nm. This changed the color of the solution from light green to purple.

1-Phenyl-1,2-propanedione-2-oxime thiosemicarbazone (**85**)[76] has been used to prepare a novel sensing membrane (optode) for the determination of Cu^{2+} by immobilization on a triacetylcellulose membrane. Upon interaction with Cu^{2+}, the membrane made up from **85** became colored, which resulted in an increase in the absorbance at 401 nm.

A colorimetric 3-nitro-4-ethylenediamido-nitrobenzene (**86b**)[77] displayed high selectivity and sensitivity for Cu^{2+}. In the UV–vis spectrum, the absorption peaks of **86b** in MeOH/H_2O (1:1 v/v, pH 7.6) at 348 and 416 nm gradually reduced in intensity with the formation of two new absorption bands at 376 and 525 nm upon

addition of Cu^{2+} along with a naked-eye color change from yellow to red. However, for **86a** no metal ion sensing was observed.

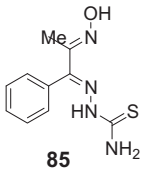

85

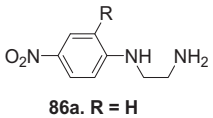

86a. R = H
86b. R = NO_2

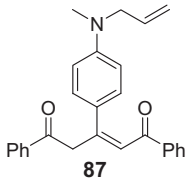

87

Pentenedione derivative **87** was covalently attached to polystyrene, silica, zeolite Y, and poly(ethylene glycol).[78] All the solids changed the color from yellow to red upon contacting with an aqueous solution of Fe^{3+}, Cu^{2+}, and Pb^{2+}.

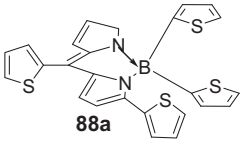

88a

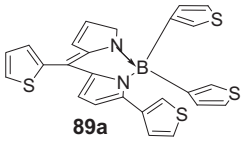

89a

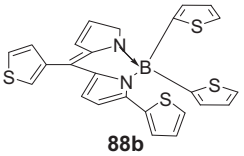

88b

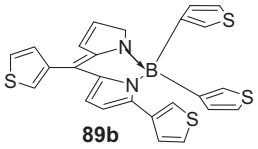

89b

The UV–vis spectra of tetrathienyl-substituted BODIPY-type complexes (**88** and **89**)[79] gave λ_{max} values of 397 and 563 nm for **88a**, 386 and 539 nm for **89a**, 370 and 553 nm for **88b** and 363 and 531 nm for **89b**. With the addition of only Cu^{2+} to the solution of **88b**, a rapid color change from pink to colorless was observed. In the spectra for **89a** and **88b**, growth of the shoulder (hump on left side centered at 531 nm for **88a** and 522 nm for **88b**) gave way at high Cu^{2+} concentration to a lower-energy hump, a band similar to that in the original chemosensor. The Cu^{2+}-titration spectra involving **89a** and **89b** retained their general shape, but became broad and slightly red shifted upon significant Cu^{2+} addition.

The absorption spectrum of **90** showed λ_{max} at 537 nm, the intensity of which decreased with the addition of Cu^{2+} along with the concomitant appearance of a new band at 565 nm.[80] However, upon addition of NaCN to solution of **90**+Cu^{2+}, an absorption wavelength-ratiometric behavior in the reverse direction was observed.

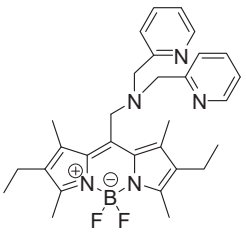

90

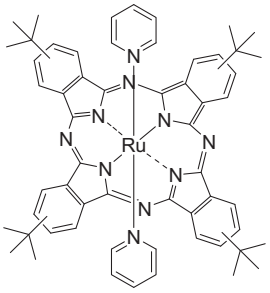

91

The UV–vis spectrum of a colorimetric molecular probe based on Ru(II)-phthalocyanine (**91**) had maxima of absorbance in MeCN at λ=318, 383 and 625 nm, corresponding to B, CT, and Q bands, respectively.[81] Addition of Cu^{2+} to the MeCN solution of **91** led to a decrease in the absorption of the Q band, along with the formation of two new bands with maxima centered at 535 and 700 nm, resulting in a dramatic color change of the solution from cyan to violet.

Cu^{2+}-induced ring opening of spirolactam derivatives has been observed in different rhodamine derivatives (**92**–**104**).[82–92] All of these chemodosimeters exhibited only a very weak band above 500 nm, which was ascribed to traces of the ring-opened form of rhodamine. Upon addition of Cu^{2+}, the absorbance was significantly enhanced above 500 nm, suggesting the clear formation of the ring-opened amide form of rhodamine. This absorption change was accompanied by a color change from colorless to pink along with a strong fluorescence. Moreover, in all cases, the color and absorption changes were reversible, as reversed by the addition of EDTA.

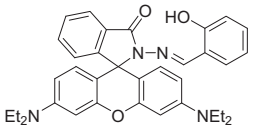

92

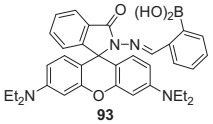

93

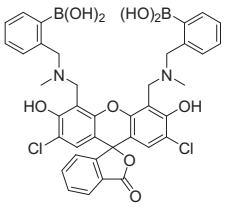

94

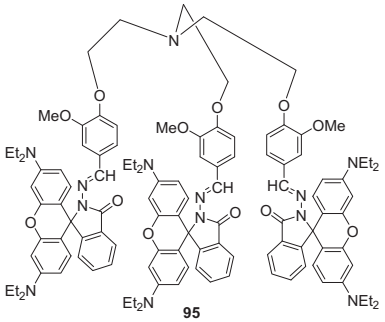

95

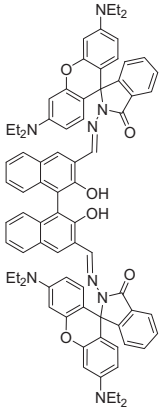

96

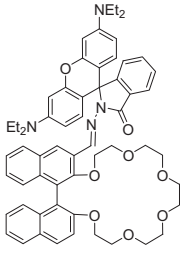

97

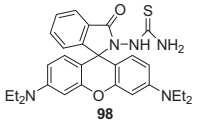

98

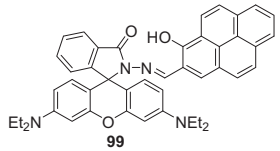

99

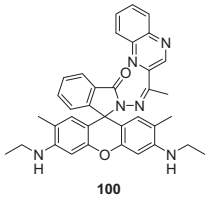

100

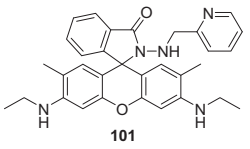

101

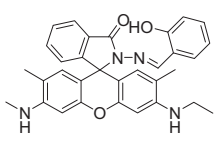

102

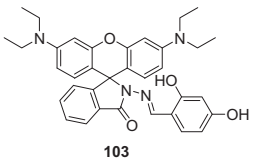

103

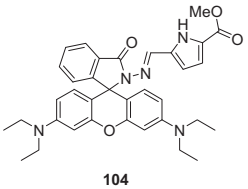

104

Yen et al. developed a colorimetric chemosensor based on a thiourea featuring a pyrene unit (**105**) for the sensing of Hg^{2+} and Cu^{2+} ions through two different color changes in aqueous solution.[93] The absorption spectrum of **105** showed typical pyrene absorption bands in the region of 235–350 nm, which were responsible for its pale-yellow color. Upon addition of Hg^{2+} ions to a solution of **105** in a mixed solvent (DMSO/H_2O 4/1 v/v, pH 7.8), the absorption peaks initially at 278 and 334 nm were gradually decreased, while two new peaks at 284 and 361 nm were evolved. The color of the solution changed from pale yellow to brown. On the other hand, upon treatment with Cu^{2+} ions, the absorption peaks at 278, 334 and a shoulder peak at 388 nm were gradually increased, while the peak at 348 nm was gradually decreased. The color of the solution changed from pale yellow to green-yellow. Alkali, alkaline earth, and other transition metal ions did not result in any absorption or color changes. The distinct color and absorption changes of **105** were caused by the Hg^{2+}-induced transformation of the thiourea function into urea group.

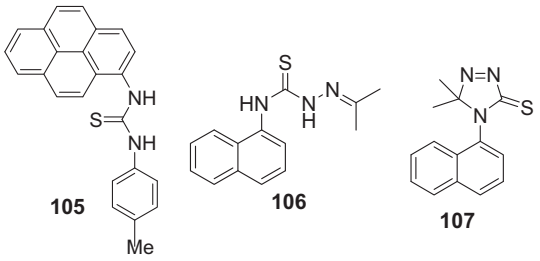

A colorless and weakly fluorescent thiosemicarbazene (**106**) underwent an oxidative cyclization into a colored and highly fluorescent rigid 4,5-dihydro-5,5-dimethyl-4-(naphthalen-5-yl)-1,2,4-triazole-3-thione (**107**).[94] In the UV–vis spectrum, the absorption intensity decreased at 267 nm with increased intensity concomitantly at 328 and 242 nm. This red shift was accompanied by a color change from colorless to yellowish orange.

Directed assembly of DNA-functionalized gold nanoparticles formed by the ligation process has been used for sensing Cu^{2+} ions.[95] The ligation product was designed as a linker to assemble AuNPs, giving blue-colored aggregates. If no Cu^{2+} was present, no aggregation occurred and the color remained red. The dispersed AuNPs had an extinction peak at ~532 nm, which rendered the nanoparticles a characteristic red color. In the presence of Cu^{2+}, the ligation product was formed and AuNPs were assembled, giving increased extinction at the 700 nm region along with a change of the color to blue.

Tan's group developed an allosteric dual-DNAzyme unimolecular probe (combination of D-DNAzyme and H-DNAzyme) for the colorimetric detection of Cu^{2+}.[96] The H-DNAzyme transduced the Cu^{2+}-sensing events through the catalyzed H_2O_2-mediated oxidation of 3,3′,5,5′-tetramethylbenzidine to the blue product, a bisazo benzidine compound. The reaction could be halted with 2 M H_2SO_4 resulting in a yellow-colored product, after which a colorimetric readout at λ=450 nm was recorded.

Another gold nanoparticle (**109**)-based colorimetric sensing of Cu^{2+} has been described by Li et al.[97] The AuNPs displayed a typical plasmon peak at 515 nm. The DPPCA (**108**) showed a characteristic absorption at 550 nm. The DPPCA-AuNP (**109**) composite exhibited λ_{max} at 525 nm. Upon addition of the Cu^{2+} ion to **109** composite, the **108** and AuNPs were separated from each other and the solution displayed the characteristic absorption of **108** at 545 nm. The typical plasmon peak of AuNPs was undetectable, due to strong absorbance of **108** in the region from 500–550 nm. The absorption of the solution was shifted to longer wavelength and resulted in a purple-to-orange color change.

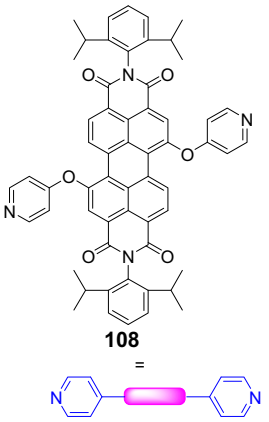

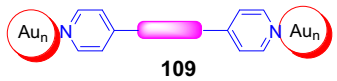

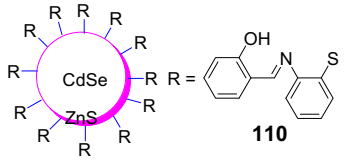

The incorporation of an organic chemosensor onto the surface of a preformed CdSe/ZnS quantum dot (QD) resulted in a nanocrystal hybrid (**110**) with selectivity for both Cu^{2+} and Fe^{3+} ions.[98] Chemosensor **110** in buffered THF/H_2O (80:20 v/v) was characterized by two UV bands, one centered at 275 nm and the other at 355 nm. Addition of Fe^{3+} resulted in a substantial increase in absorbance of these bands, while the addition of Cu^{2+} caused a substantial bathochromic shift of both bands to 295 and 410 nm, respectively. With Fe^{3+}, the color changed from colorless to orange and Cu^{2+} caused a color change from colorless to green. In contrast, the addition of other ions had a negligible effect on the UV–vis spectra of **110**.

BODIPY-functionalized AuNPs (**111**)[99] have been used as a selective fluorochromogenic chemosensor for imaging Cu^{2+} in living cells. The absorption spectrum of free **111** showed a single visible absorption band at 598 nm (ICT band). When Cu^{2+} was added gradually, the λ_{max} showed a 98 nm blue shift with an isosbestic point at 521 nm and the color of the solution turned from light blue to pale yellow. Fluorescence quenching was observed in the fluorescence spectra upon addition by Cu^{2+}. The Job's plot using the fluorescence changes indicated 1:1 binding for **111** with Cu^{2+} with an association constant of 6.3×10^4 M^{-1}. However, no significant spectral changes were observed upon addition of the other metal ions. Chemosensor **112**, devoid of AuNPs, underwent color and spectral changes with addition of Cu^{2+}, but unlike **111**, chemosensor **112** showed quenching effects with Fe^{2+} as well as Cu^{2+}. Chemosensor **111** has been used as an imaging material for Cu^{2+} in living cells.

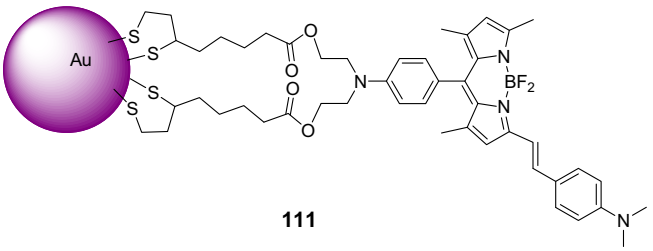

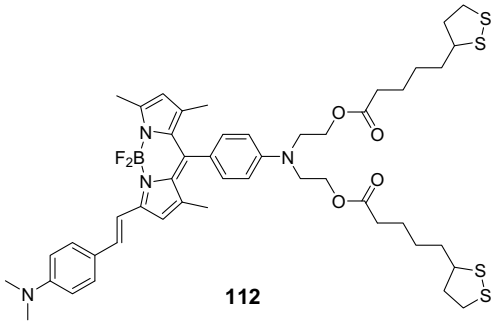

4. Hg^{2+} metal ion sensing chemosensors

Huang et al. described anthraquinone derivatives possessing two urea/thiourea groups at the 1,2 positions for selective estimation of Hg^{2+} and Hg^{2+}/Ag^{+}, respectively. Thiourea derivative **113a**[100] possessed an intensive absorption band at 458 nm in DMSO/MeCN (1:9 v/v). A new absorption band centered at λ_{max} 400 nm arose when more than 1 equiv of Hg^{2+} was added. This blue shift of 58 nm was responsible for the color change from golden to yellow. However, upon adding Ag^{+} to a solution of **113a**, the absorption band of **113a** was broadened and the edge of the absorption band was extended to 650 nm corresponding to the naked-eye color change from golden to orange-red.

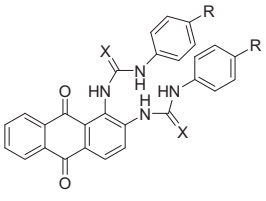

113a. X = S, R = NO_2
113b. X = O, R = NO_2
113c. X = O, R = H
113d. X = O, R = NMe_2

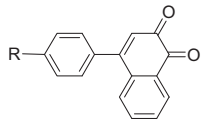

114a. R = NMe_2

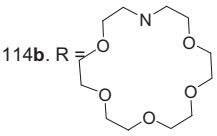

114b. R =

On the other hand, the urea-appended anthraquinone derivative[101] **113b** showed a red shift of the absorption band from λ_{max} 420 to 488 nm in DMSO/MeCN (1:9 v/v) upon addition of Hg^{2+}. Importantly, the presence of other metal ions, such as Cu^{2+}, Ag^{+}, Cd^{2+}, Cd^{2+}, Cr^{3+}, Fe^{3+}, Ni^{2+}, and Zn^{2+} did not affect the selectivity of **113b** for Hg^{2+}. However, the weakened push–pull mechanism in **113c** and **113d**, due to lack of the electron-withdrawing nitro group, is responsible for the negligible color changes observed on addition of Hg^{2+} to solutions of **113c** and **113d**.

However, chemosensors **114a** and **114b** were highly colored receptors with a broad band centered at λ_{max} 534 and 532 nm, respectively.[45] Compound **114a** on addition of Cu^{2+} (1 equiv) and Fe^{3+} and Hg^{2+} (0.5 equiv) showed disappearance of the 535 nm band with appearance of a yellow color (at 420 nm) or complete bleaching of the color. Other metal ions did not bring about any change in the absorption spectrum of **114a**. However, **114b** underwent similar changes with a number of metal ions, viz. Fe^{3+}, Hg^{2+}, Cu^{2+}, Pb^{2+}, and Ba^{2+}, which was attributed to increased complexation of **114b**, due to the presence of the 18-crown-6 macrocycle.

An unsymmetrical cationic squaraine dye (**115**)[102] underwent a color change from green (λ_{max}=770 nm) to pink (λ_{max}=551 nm) upon addition of Hg^{2+} in CH_2Cl_2. Similar observations were made on addition of Pb^{2+} with a maximum at 549 nm. However, with addition of Cu^{2+} ions to **115** in CH_2Cl_2, a small hypsochromic shift from 770 to 750 nm was observed and there was no perceivable color change of the solution.

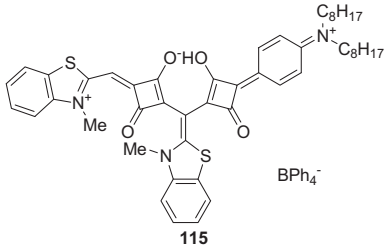

115

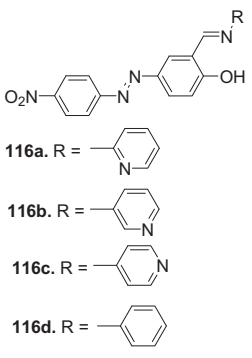

116a. R =
116b. R =
116c. R =
116d. R =

A series of azobenzene dyes (**116a–d**) showed a selective colorimetric and ratiometric response toward Hg^{2+}.[103] The UV–vis absorption spectrum of **116a** displayed absorption peaks at 451 and 383 nm. Upon addition of Hg^{2+} to the solution of **116a**, the 383 nm band was blue shifted to 364 nm. The decrease of the band at 451 nm was responsible for the change of color from orange to pale yellow. The other chemosensors **116b–d** showed a similar type of spectral and color changes. Zn^{2+}, Cu^{2+}, Pb^{2+}, Mn^{2+}, and Ni^{2+} also influenced the color.

Lee et al. showed simple salt-induced color switching in solutions of sensor[104] **117** (λ_{max} 480 nm, red color) with Hg^{2+}, Cu^{2+}, and Fe^{3+}. The cations induced a large hypsochromic shift for Hg^{2+} ($\Delta\lambda$=133 nm) and Cu^{2+}/Fe^{3+} ($\Delta\lambda$=74 nm), resulting in a color change from red to pale yellow. Job's plots revealed the formation of a 1:1 complex with log *K* 6.02, 5.12, and 5.08 for Hg^{2+}, Cu^{2+}, and Fe^{3+}, respectively. However, the color change for **117** with Hg^{2+} was affected by the counter-anion. The addition of NO_3^- or ClO_4^- resulted in hypsochromic shifts to λ_{max} 367 and 350 nm (pale yellow). However, no color changes were observed upon addition of Cl^-, Br^-, I^-, $MeCOO^-$, SCN^- or SO_4^{2-}. This was attributed to the significant coordinating ability of these anions to Hg^{2+} ions.

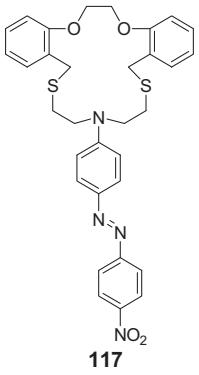

117

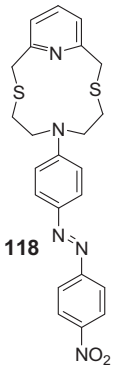

118

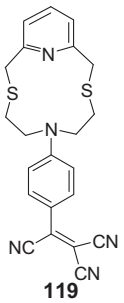

119

In MeCN, chromogenic N_2S_2-donor macrocycles **118** and **119** exhibited intense CT absorption bands at 480 nm (orange red) and 520 nm (pink red), respectively.[105] For **118**, the large metal-induced hypsochromic shifts for Hg^{2+} ($\Delta\lambda$=137 nm) and Cu^{2+} ($\Delta\lambda$=74 nm) resulted in color changes from red to colorless and pale yellow, respectively, whereas no significant color change was observed upon addition of Li^+, Na^+, K^+, Ba^{2+}, Ni^{2+}, Zn^{2+}, Ag^+, Cd^{2+}, and Pb^{2+} metal ions, except Al^{3+} (changed to pink red). Similar results were obtained for **119**. The 1:1 association constant values (log *K*) for the **118** and **119** complexes were 6.37 and 4.91 for Hg^{2+}, respectively.

2,4,6-Triphenylthiopyrylium functionalized with an aza-oxa-thia macrocycle (**120**)[106] selectively recognized Hg^{2+} ions by color change and Cu^{2+} ions by a remarkable significant emission enhancement. The MeCN solution of chemosensor **120** showed a blue coloration with absorption peaks at 400 and 575 nm. Al^{3+}, Cu^{2+}, and Fe^{3+} gave a small hypochromic effect of the CT band that did not induce any remarkable change in the color of the solutions. However, the presence of Hg^{2+} ions resulted in a large hypochromic effect on the band centered at 575 nm, together with a hypsochromic shift of 40 nm, resulting in color modulation from blue to faint yellow.

The UV–vis spectrum of chemosensor **121** with two dithia-dioxa-aza macrocycles on the BODIPY chromophore in THF/H_2O (30:70 v/v; pH 7.2) was characterized by a very intense band centered at 606 nm, which was responsible for the purple color of the solution.[107] Upon adding Hg^{2+} to the solution of **121**, the intensity of the absorption band at 606 nm gradually decreased, followed by the formation of a new band centered at 564 nm, along with a color change from purple to red pink.

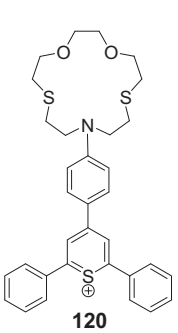
120

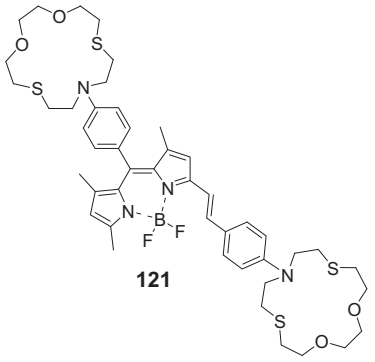
121

The Ru complex **122**[108] showed a larger color change from dark green (λ_{max} 625 nm) to pink (λ_{max} 560 nm) upon addition of Hg^{2+} salts. TiO_2 dye-**122** films on dipping in Hg^{2+} solution underwent similar color changes as observed in solution phase.

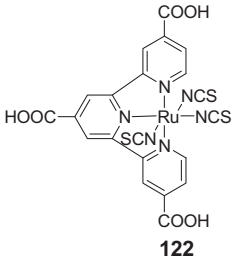
122

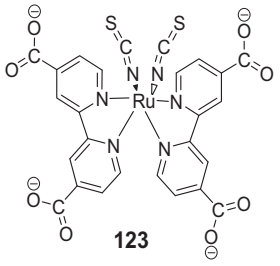
123

A ruthenium dye monolayer (**123**) immobilized onto metal oxide ultrathin film pre-coated cellulose nanofibres of natural cellulose substances underwent a color change from purple (λ_{max}=520 nm) to orange (λ_{max}=480 nm) when dipped into Hg^{2+} ion solution.[109] However, for $(TiO_2)_{15}$/**123** hybrid film-modified quartz plates, no conspicuous color change was observed by exposing them to Hg^{2+} aqueous solutions, due to their much lower surface area, compared with the cellulose substances. Except for Hg^{2+}, no color change was observed for the $(TiO_2)_{15}$/**123**-modified filter paper upon exposure to aqueous solutions of other metal ions.

A solution of Ru-DTTP complex[110] **124** in DMF/EtOH (1:1 v/v), on addition of Hg^{2+}, showed a blue-shifted MLCT absorption band from λ_{max} 570 to 500 nm along with a naked-eye color change from blue to pink.

$Ir(dtp)_2(acac)$ **125**[111] in the absorption spectrum displayed an MLCT transition at λ_{max} 480 nm, which on addition of increasing amounts of Hg^{2+} in MeCN showed a gradual decrease in intensity with the concomitant emergence of a new band at λ_{max} 420 nm with a color change from orange to yellow green with the formation of a 1:1 complex (K=1.5×10^4 M^{-1}).

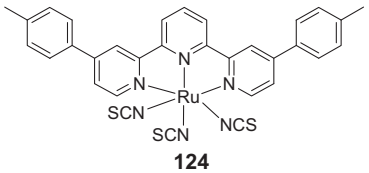
124

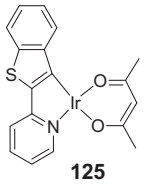
125

The UV–vis spectrum of sensor **126**[112] based on a coumarin platform coupled with a tetramide functionality (λ_{max} 430 nm) exhibited a gradual shift to shorter wavelengths with sequential addition of Hg^{2+} in a phosphate-buffered water solution of **126** along with a color change from yellow to almost colorless. A Job's plot indicated a 1:1 stoichiometry with K_a 4.41±0.02.

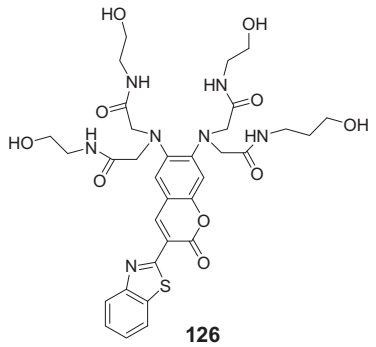
126

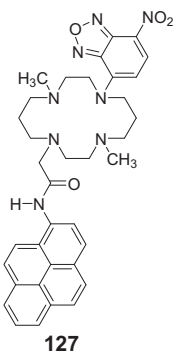
127

The UV–vis spectrum of **127** (MeCN/H_2O 9:1 v/v; pH 4.8) showed two broad absorption bands around 342 and 484 nm, typical of pyrene and NBD subunits, respectively.[113] Upon complexation with Hg^{2+} ions, a slight blue shift in the absorption band of the NBD region was observed with some splitting of the pyrene absorption bands. This shift resulted in a color change from light orange to yellow. The addition of Cu^{2+} ions caused an increase in absorbance in the pyrene region with a pronouncedly reduced absorbance with a blue shift.

Another NBD-derived chemosensor[114] (**128a**) exhibited a characteristic ICT absorption band centered at 455 nm in ethanol. With the addition of Hg^{2+}, the absorbance at 455 nm decreased, while a new band appeared at 493 nm. Such a red shift (38 nm) led to a solution color change from light yellow to light orange. The large association constant was found to be 3.23×10^6 M^{-1} for a 1:1 binding stoichiometry. Chemosensor **128b** with a more rigid distal amino group displayed almost the same photophysical properties as that of **128a**. However, the binding constant of **128b** with Hg^{2+} ($\sim$1×10^5 M^{-1}) was one order of magnitude lower than that of **128a**.

Addition of Hg^{2+} to a solution of the 1-hemocyanine dye (**129**)[115] (ethanol/H_2O 1:10 v/v; pH 7.0) caused a hypsochromic shift of the absorption band with a color change from red to greenish yellow.

A hemicyanine-based water-soluble chemosensor **130** underwent a selective color change from red to colorless with the addition of Hg^{2+}.[116] The absorbance at 542 nm in aqueous ethanol and 529 nm in water decreased sharply, while that at 412 nm in aqueous ethanol and 404 nm in water increased significantly due to the addition of Hg^{2+}.

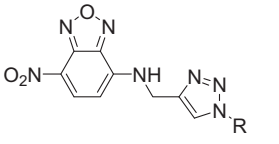
128a. R =

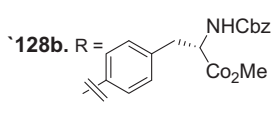
`128b. R =

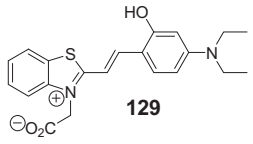
129

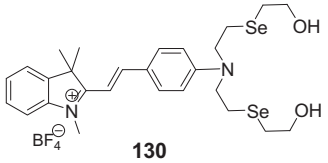
130

The addition of Hg^{2+} in water to a solution of terpyridine-possessing molecules (**131**)[117] in DMSO/H_2O (1:3.5 v/v) caused the immediate appearance of a pink color. Conversely, addition of other metal ions to solutions of **131** resulted in little or no color change, except for Cu^{2+}, which turned the solution slightly blue.

The absorption spectra of a donor–π–acceptor (D–π–A) alternative copolymer of carbazole and thieno[3,4*b*]pyrazine (**132**)[118] in THF solution (containing 0.3% MeCN) displayed two absorption peaks at 306 and 452 nm. Upon addition of Hg^{2+} ions to the

solution of **132**, the 452 nm absorption peak decreased and a new shoulder peak at 570 nm appeared along with a color change from yellow green to dark blue.

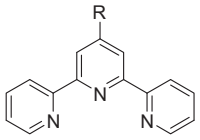

131a. R = H
131b. R = OBu
131c. R = $(OCH_2CH_2)_nOMe$
131d. R = MMA-based polymer

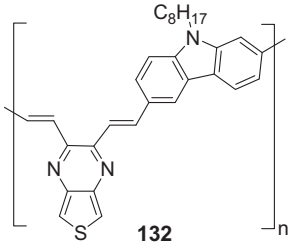

132

Another polymer containing benzo[2,1,3]thiadiazole (**133**)[119] has been found to selectively detect Hg^{2+} ions by undergoing a color change from yellow to violet. The absorption spectra of **133** in $CHCl_3$ displayed an intense absorption band at 510 nm and two weak absorption bands at 326 and 345 nm. With the addition of Hg^{2+}, the absorbance at 510, 326, and 345 nm decreased and the wavelengths of the three bands were red shifted significantly, especially the band at 510 nm. In dilute $CHCl_3$ solution, the polymer chains were well separated and took on a random distribution of conformations along the backbone and consequently, interchain interactions were minimal. After the addition of Hg^{2+}, the coordination of Hg^{2+} to the sulfur atom of the polymer backbone joined the different polymer chains and led to inter-polymer π-stacking aggregation, which resulted in the red shift of the absorption spectra.

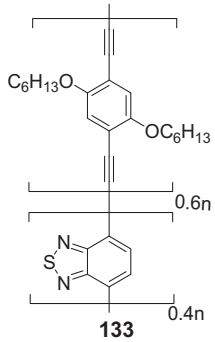

133

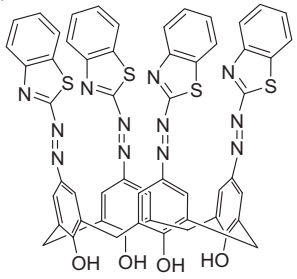

134

The absorption spectrum of a calix[4]arene derivative containing benzothiazole azo groups at the upper rim (**134**)[120] had a maximum absorption peak at 369 nm. When chemosensor **134** was treated with a series of heavy-metal ions, bathochromic shifts were observed only for Hg^{2+} ($\Delta\lambda$=149 nm) and Pb^{2+} ($\Delta\lambda$=19 nm) ions. However, dramatic color changes from light orange to reddish were observed only in the presence of Hg^{2+}.

Another calix[4]arene **135a** containing an azo functionality underwent a bathochromic shift with a color change from yellow to red upon addition of Hg^{2+}.[121] The addition of Pd^{2+} also resulted in a red shift with a color change from yellow to light purple. Similar bathochromic shifts and color changes have been reported for **135b** on addition of Hg^{2+} and Pd^{2+}.

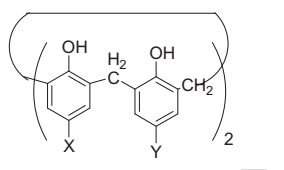

135a. X = H; Y = —N=N— $H_2C{=}HCH_2CS$

135b. X = Y = —N=N— $C_{16}H_{33}S$

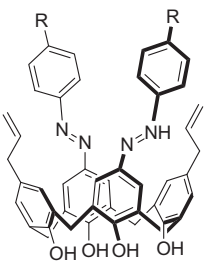

136a. R = H
136b. R = OMe
136c. R = NO_2

On the other hand, the absorption spectra of calix[4]arenes with either 4-methoxyphenylazo (**136b**) or 4-phenylazo (**136a**) on the upper rim[122] showed substantial bathochromic shifts ($\Delta\lambda$=128–162 nm) upon addition of soft metal ions Hg^{2+}, Cu^{2+}, and Cr^{3+}. The light yellowish solution of **136b** turned into a bright red color upon complexation with Hg^{2+}. No shifts in the absorption spectra were observed for **136c** when different metal–ion solutions were added. These results pointed out that contrary to the usual binding of calixarenes at the lower rim phenolic OH groups, the calixarenes **136a** and **136b** bind at the diazo part to bring about significant color changes with metal ions.

The yellow solution of cyclotriveratrylene (**137**)[123] exhibited a broad band around 450 nm. Upon addition of Hg^{2+} ions, the absorption band at 450 nm changed to a new prominent one at 490 nm with a somewhat larger absorbance. The significant red shift ($\Delta\lambda$=40 nm) resulted in a color change from yellow to red orange.

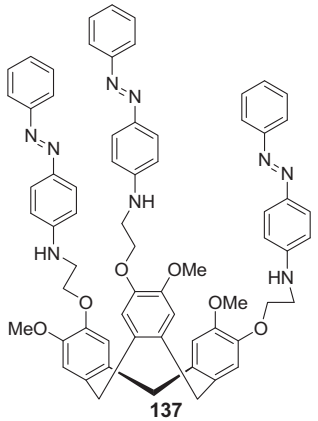

137

In chemosensors **138**–**141**,[124] the linkage of thiazole rings through the 2 and 5 positions can be used for differential analysis of heavy-metal ions. The presence of Hg^{2+} and Pb^{2+} ions induced a red shift of the LE bands of **138** (λ_{max} 449 nm) and **139** (λ_{max} 459 nm) to 514 and 485 nm, respectively. However, bis(ferrocenyl)thiazole **140** revealed red shifts of the LE bands upon addition of Zn^{2+}, Cd^{2+}, Hg^{2+}, Ni^{2+}, and Pb^{2+} ions. Bis(ferrocenyl) compound **141** showed red shifts of the LE band by 79–85 nm and color changes from orange to blue on addition of Zn^{2+}, Cd^{2+}, and Ni^{2+}, whereas the Hg^{2+} and Pb^{2+} metal ions promoted a higher red shift by 109 nm and a color change from orange to green.

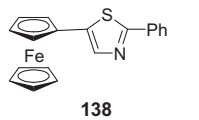

138

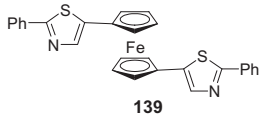

139

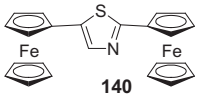

140

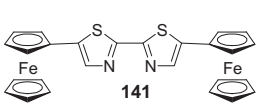

141

A chemosensor, **142**, based on a ferrocene azaquinoxaline dyad, recognized Hg^{2+} in an aqueous environment as well as Zn^{2+} and Pb^{2+} metal ions in MeCN solution.[125] In pure MeCN, the absorption spectrum of **142** was characterized by an HE absorption at 335 nm and an LE band at 516 nm. Addition of Hg^{2+} ions to the solution of chemosensor **142** caused a progressive appearance of a new strong

band located at 376 nm and a red shift of the LE band to 628 nm. This red shift was responsible for a perceptible change of color from pale orange to deep green. The binding constant for 1:1 stoichiometry was calculated to be $K_a=1.1\times10^4$ M^{-1}.

On the other hand, addition of Pb^{2+} ions to a solution of **142** caused a red shift of the LE band by $\Delta\lambda=90$ nm, which was responsible for the change of color from pale orange to purple. The LE band of chemosensor **142** was red shifted ($\Delta\lambda=42$ nm) upon addition of Zn^{2+} with a concomitant color change from pale orange to purple. Binding assays suggested a 2:1 (chemosensor/metal ion) binding model with $\beta=5.42\times10^9$ M^{-2} for Pb^{2+} and $\beta=6.5\times10^9$ M^{-2} for Zn^{2+} ions. By contrast, addition of Cu^{2+} ions to the solution of **142** produced the same perturbations in its absorption spectrum as those observed when **142** was electrochemically oxidized.

Moreover, addition of Hg^{2+} ions to a solution of **142** in MeCN/H_2O (3:7 v/v) induced a red shift of the two absorption bands from 345 to 368 nm ($\Delta\lambda=23$ nm) and from 539 to 612 nm ($\Delta\lambda=73$ nm) ($K_a=2.51\times10^3$ M^{-1}). These changes were responsible for the change of color from pale orange to deep green.

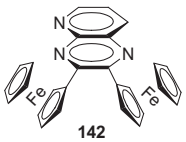

142

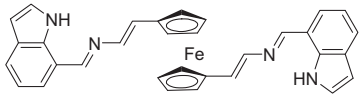

143

The absorption spectrum of another ferrocene-based chemosensor (**143**) displayed an HE band at 354 nm and an LE band at 452 nm in MeCN.[126] Addition of Hg^{2+} ions to the solution of **143** caused the disappearance of the LE band at $\lambda=452$ nm along with a progressive appearance of a new band located at $\lambda=572$ nm. In addition, a decrease of the initial HE band at 354 nm, with the concomitant appearance of a new band at 424 nm, was observed. These changes were responsible for the change of color from orange to deep green. A Job's plot suggested a 1:1 binding model with $K_{as}=6.06\pm0.5\times10^4$ M^{-1}. However, Cu^{2+} induced the oxidation of the chemosensor.

Molina's group described the Hg^{2+} binding with different chemosensors having naphthyl-, pyrenyl- or ferrocenyl subunits directly linked to a 2-aza-1,3-butadiene moiety (**144**–**147**).[127] Chemosensors **144**–**147** underwent a red shift with the addition of Hg^{2+} in MeCN solution. Moreover, these changes also resulted in a variation of the color of their solutions from orange, in the free chemosensors, to purple, for Hg^{2+}-complex. However, chemosensors **148**, with no redox subunit, underwent significant changes upon addition of Cu^{2+} and Hg^{2+} ions, while the similar chemosensor **149** did not show either optical or fluorescence selectivity for any of the metal ions.

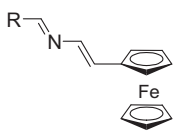

144. R = 2-naphthyl
145. R = pyrenyl

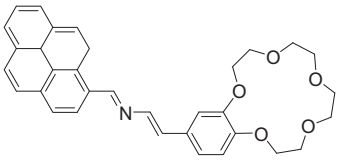

148

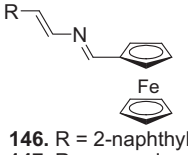

146. R = 2-naphthyl
147. R = pyrenyl

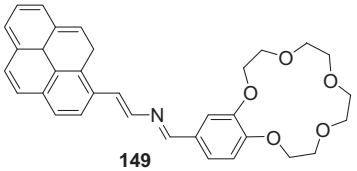

149

The addition of Hg^{2+} to a solution of **150** in MeCN/H_2O (7:3 v/v) caused the appearance of a new band at λ_{max} 521 nm and the disappearance of the initial band at 476 nm, which was responsible for change of color from yellow (neutral azine) to deep purple (complexed azine).[128] However, a solution of **151** caused a bathochromic shift of 51 nm along with a color change from pale yellow to deep orange on addition of Hg^{2+}. The absorption spectral data indicate a 1:1 binding model with K_a 4.35×10^5 M^{-1} (for **150**) and 9.79×10^7 M^{-1} (for **151**) in MeCN.

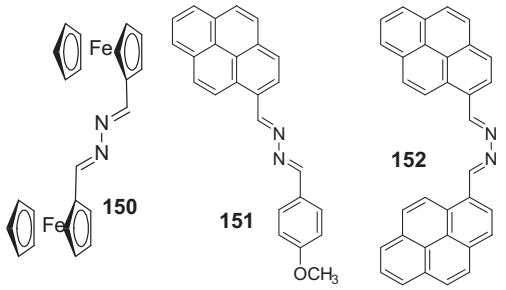

1,4-Bis(1-pyrenyl)-2,3-diaza-1,3-butadiene **152**[129] (MeCN) on addition of Hg^{2+} and Cu^{2+} showed the appearance of a new band at λ_{max} 515 nm. This red-shifted (94 nm) LE band was responsible for a color change from yellow to deep pink. Analysis of the absorption spectral data confirmed a 1:1 binding model and K_{Hg2+} 9.70×10^6 M^{-1} and K_{Cu2+} 6.9×10^6 M^{-1}.

The absorption spectrum of coumarin azine derivative (**153**)[130] in MeCN/H_2O (99:1 v/v) showed an intense band that appeared in the visible region and peaked at 490 nm. A small decrease at 490 nm accompanied by an increase at 565 nm was observed in the presence of Pb^{2+}, while upon addition of Fe^{3+} a new band was observed at wavelength 450 nm. However, it was found that the maximum absorption of chemosensor **153** shifts from 490 to 565 nm ($\Delta\lambda=75$ nm) upon addition of Hg^{2+} along with a color change from orange to purple.

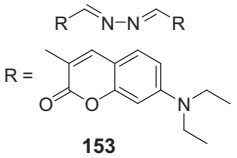

153

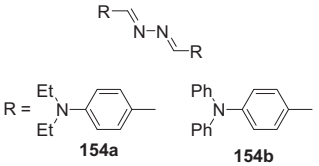

154a 154b

Upon addition of Hg^{2+} ions to a solution of the chemosensor **154a**, a new band at 496 nm appeared with the disappearance of the initial band at 393 nm.[131] This bathochromic shift of 103 nm caused the color of the solution to change from pale yellow to red. The new band was ascribed to MICT absorption. The binding constant for a 1:1 binding manner was calculated to be 2.6×10^4 M^{-1}. However, weak MICT absorptions were also observed with Zn^{2+}, Co^{2+}, and Mg^{2+}. With the addition of Cu^{2+}, a new peak in the UV–vis spectrum was observed at 336 nm with the disappearance of the absorption at 393 nm, due to decomposition of **154a**. On the other hand, upon addition of Hg^{2+} ions to a solution of chemosensor **154b**, the absorption at 400 nm decreased gradually with the observation of a new absorption at 500 nm and the color of the solution changed from pale yellow to red. The binding constant in this case was found to be 6×10^4 M^{-1}.

In the case of **155**,[63] the addition of Cu^{2+} and Hg^{2+} caused a red shift in its LE bands by 92 and 96 nm, respectively, with a color change from yellow to deep orange. These experiments revealed 1:1 stoichiometry with K_{Cu2+} 8.55×10^5 M^{-1} and K_{Hg2+} 2.36×10^5 M^{-1}.

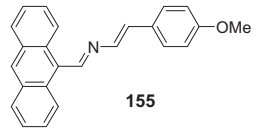

155

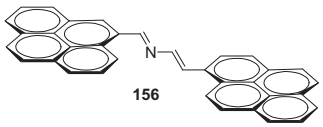

156

The UV–vis spectrum of **156**, made up of two pyrene units connected by a 2-aza-1,3-butadiene ionophore, in MeCN was dominated by the typical pyrene absorption bands appearing in the region 233–393 nm.[132] Stepwise addition of Cu^{2+} and Hg^{2+} ions induced the appearance of a new LE absorption band at λ 528 nm with a decrease in intensity of the bands at λ 233–393 nm. These changes are accompanied by a simultaneous change of color of the solution from yellowish to deep pink. Analysis by Job's plot gave a 1:1 stoichiometry for the complexes formed with corresponding binding constants $K_a=1.3\times10^6$ M^{-1} and $K_a=1.2\times10^6$ M^{-1} for Cu^{2+} and Hg^{2+}, respectively.

The chemosensor **157**, on addition of Hg^{2+}, exhibited a red shift of 73 nm from λ_{max} 445–518 nm and the color changed from yellow to red, which could be observed by the naked eye.[133] However, on addition of Cu^{2+} to **157**, a new band centered at λ_{max} 383 nm appeared. It showed a hypsochromic shift of 62 nm and the color of **157** changed to colorless.

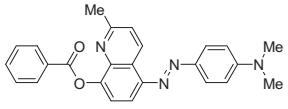

157

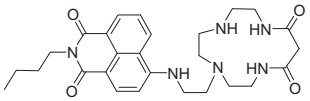

158

A yellow-green methanol solution of chemosensor **158**,[34] a conjugate of a dioxo-tetraamine and a 4-amino-1,8-naphthalimide (λ_{max} 440 nm), changed to almost colorless on addition of Cu^{2+} (K_a=10,074 M^{-1}) and to orange on addition of Hg^{2+} (K_a=5018 M^{-1}). With addition of Cu^{2+} to an aqueous methanol solution of **158**, the absorbance at λ_{max} 437 nm decreased with the appearance of a new band at 403 nm. In aqueous methanol, Hg^{2+} did not interfere in the estimation of Cu^{2+}. However, addition of Hg^{2+} to **158** in methanol caused a bathochromic shift from λ_{max} 438–483 nm.

The highly selective Hg^{2+}-promoted desulphrization of thioamides and thiosemicarbazides to the respective guanidine and oxadiazole derivatives is another chemical reaction, which has received attention for the development of chemosdosimeter-based sensors (**159**–**173**).[132,134–146] In all these chemodosimeters, almost no absorption above 400 nm was observed. However, with the addition of Hg^{2+}, ring opening of the rhodamine derivative occurred, which resulted in a large enhancement above 500 nm along with a color change from colorless to pink/red.

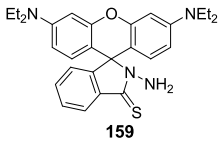

159

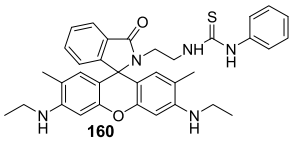

160

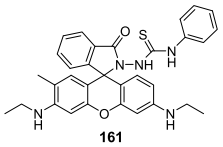

161

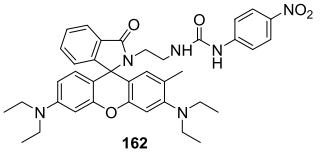

162

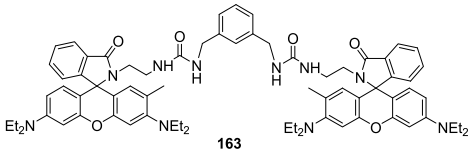

163

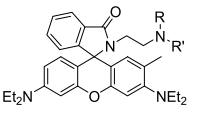

164. R = $(HO)_2B$ R' = H

164b. R = R' = $(HO)_2B$

164c. R = R' =

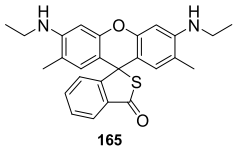

165

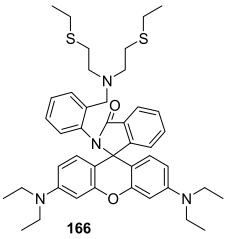

166

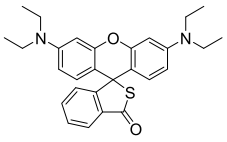

167

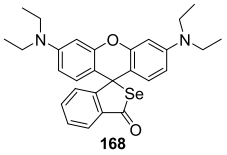

168

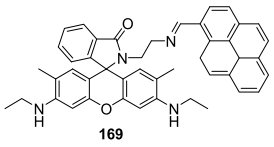

169

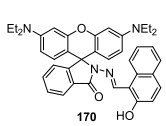

170

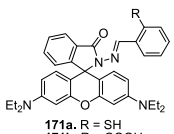

171a. R = SH
171b. R = COOH

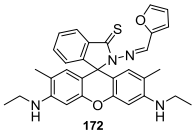

172

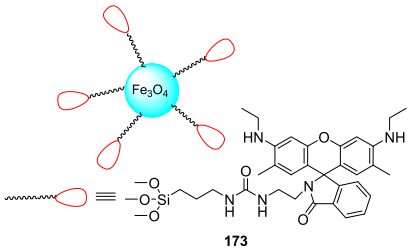

173

Another Hg^{2+}-triggered guanylation has been observed in the naphthalimide derivative **174**.[147] The addition of Hg^{2+} ions to a solution of **174** in MeCN/H_2O (4:1 v/v) transformed the thiourea unit of the chemodosimeter **174** under aqueous conditions into an imidazoline moiety, that is, a much weaker electron-donating group and reduces electron delocalization within the chromophore. This reduced electron delocalization is associated with a hypsochromic shift of the absorption maximum from λ_{max} 435 nm

(for **174**, fluoresces yellowish green color) to 350 nm (for imidazoline derivative, fluoresces blue color).

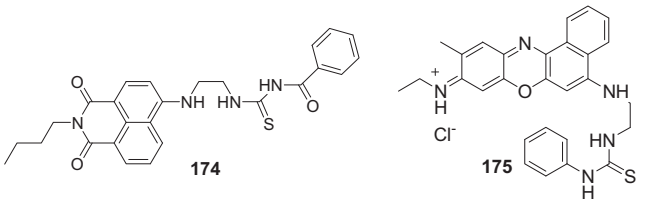

A Nile blue-based chemodosimeter **175**[148] revealed two absorption maxima at 630 and 592 nm. Upon addition of Hg^{2+} ions, the maxima were shifted to 583 and 546 nm, respectively, due to Hg^{2+}-induced desulphurization-based cyclization along with naked-eye color changes.

Due to Hg^{2+}-induced desulfurization of tricarbocyanine dyes (**176a** and **176b**),[149] the λ_{max} of both chemosensors underwent a large red shift of ~165 nm along with a color change from deep blue to pea green.

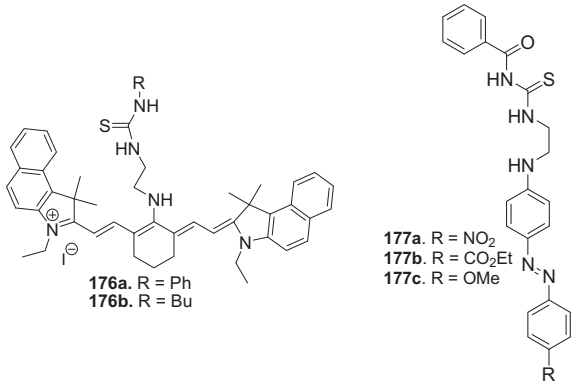

Azo-component-containing chemodosimeters (**177a**–**c**) showed a blue shift in the UV–vis spectra upon addition of only Hg^{2+}.[150] This blue shift was assigned to Hg^{2+}-induced cyclization of the chemodosimeter followed by desulphurization into an imidazoline moiety, which would decrease the intramolecular charge-transfer property of the azo chromophore.

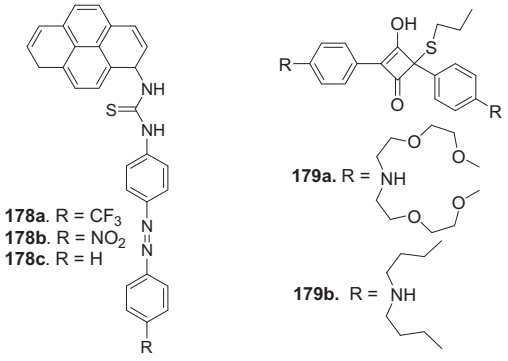

Azo dye with a pyrene unit **178a** exhibited absorption peaks at 279, 350, and 397 nm.[151] Upon addition of Hg^{2+}, the absorption peaks initially at 279 and 350 nm were gradually increased and red shifted to 285 and 368 nm, respectively. The color of the solution changed from gold to pale yellow. The distinct color change of **178a** was caused by the Hg^{2+}-induced transformation of the thiourea functionality into a urea group. Moreover, replacing the 4-trifluoromethylazobenze group by either a more electron-withdrawing group, 4-nitrobenzene (chemosensor **178b**, color change from golden to yellow), or a less electron withdrawing group, azobenzene (chemosensor **178c**, pale yellow to light golden yellow), resulted in similar photochemical changes upon Hg^{2+} introduction as observed in the case of chemosensor **178a**.

Chemodosimeter **179a** showed two overlapping bands at ~265 and 305 nm.[152] Addition of Hg^{2+} ions to a solution of **179a** resulted in a dramatic change of color from colorless to blue, owing to the appearance of a new and intense absorption band at 642 nm. Chemodosimeter **179b** containing hydrophobic *n*-butyl chains was adsorbed or anchored on suitable supports to be used as dipstick assays for rapid screening of Hg^{2+} ions.

The UV–vis spectrum of thiomethoxychalcone-based chemodosimeter **180** showed an HE band at 344 nm and an LE band at 480 nm.[153] The gradual addition of Hg^{2+} up to 0.5 equiv caused the appearance of a new peak at 565 nm with a concomitant decrease in the HE band intensity at 344 nm and the LE band at 480 nm. These changes were accompanied by a color change from orange to purple. A further addition caused a decrease in the intensity at 565 nm and a gradual red shift of the 344 nm HE band to 356 nm, with up to 1 equiv of Hg^{2+}, to generate a new absorption band at 444 nm. A further addition of Hg^{2+} above 1 equiv led to a gradual red shift of the 356 nm band to 362 nm upon addition of 2 equiv of Hg^{2+}.

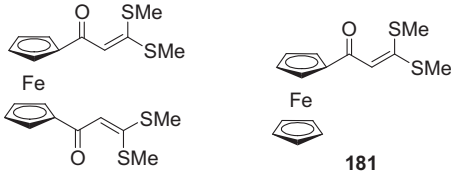

On the other hand, in the case of **181**, the HE band was observed at 326 nm along with the LE band at 466 nm. Addition of Hg^{2+} to a solution of **181** led to the appearance of a new peak at 600 nm with up to 1 equiv of Hg^{2+} with a concomitant decrease at 326 and 466 nm with a color change from orange to purple.

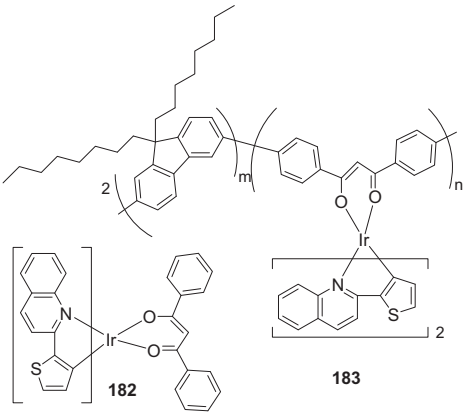

The mechanism of decomposition of iridium complexes induced by the coordination of Hg^{2+} has been demonstrated by Huang et al.[154] The UV–vis spectrum of complex **182** in MeCN showed intense absorption bands at 280–400 nm and weak bands at 400–550 nm. Upon addition of Hg^{2+} to the solution of **182**, the absorption band at 518 nm decreased with the appearance of a new band at 440 nm, which induced an evident color change from red to yellow. On the other hand, with the addition of Hg^{2+} to a solution of the conjugated polymer **183** in THF, the absorbance at 378 nm decreased and that at 418 nm increased, resulting in a solution color change from orange to yellow.

Tian et al. synthesized and studied selective chemodosimeters for Hg^{2+} ions based on the Hg^{2+}-promoted intramolecular cyclic guanylation of thiourea connected with 1,8-naphthalimide (**184**) and its immobilization on the surface of gold nanoparticles (AuNPs) (**185**).[155] In DMSO/H_2O (1:1 v/v) solution, **184** displayed a main absorption band at 446 nm and an emission maximum at 542 nm.

Upon addition of Hg^{2+}, the 446 nm band decreased significantly along with the growth of a new absorption band at 348 nm.

However, a suspension of CHD-AuNPs (**185**) in MeCN displayed two main bands at 380 and 509 nm. Upon addition of Hg^{2+} to a solution of **185**, a considerable increase including overall absorption wavelengths of less than 500 nm was observed, while the absorbance at 520 nm remained nearly unaffected with much less increment. As a result, the initial two main bands at 380 and 509 nm gradually disappeared and a new shoulder peak at 430 nm appeared. Through reacting with Hg^{2+}, **185** exhibited a color change from yellowish brown to yellow. Moreover, a yellowish brown suspension of **185** in water showed low sensing ability, which was improved by using an anionic surfactant SDS and the spectral modifications closely resembled those observed in the MeCN suspension.

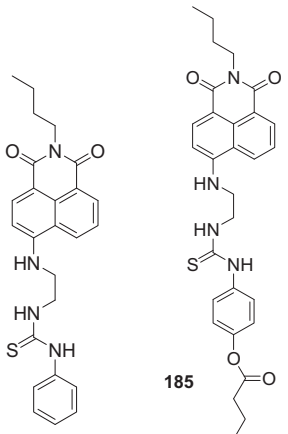

184

185

Tseng et al. investigated the effects of metal ions on the colorimetric sensitivity of polythymine oligonucleotide (T_{33})-gold nanoparticles (AuNPs) toward Hg^{2+} in phosphate-buffer saline (PBS) solution.[156] The SPR peak of T_{33}-AuNPs was located at 520 nm, indicating that highly charged T_{33} were indeed adsorbed on the surface of AuNPs, thereby preventing the AuNPs from salt-induced aggregation. Upon addition of Hg^{2+} ions to a solution of 0.75 nM T_{33}-AuNPs, 0.2× PBS, and 0.2 mM Mn^{2+}, a decrease in the SPR peak at 520 nm was observed along with the formation of a new red-shifted band, thus improving the color sensitivity and accelerating the color change.

Another aggregation-induced color change upon addition of Hg^{2+} invoked the use of mercaptopropionic acid-modified gold nanoparticles (MPA-AuNPs).[157] A 3.0 nM suspension of MPA-AuNPs in 50 mM Tris borate buffer (pH 9.0) displayed an extinction band at 520 nm. Upon addition of Hg^{2+} ions to this solution, the signal underwent a red shift with decreased extinction, while the intensity of the signal at 650 nm increased. The color of the solution changed from red to purple upon addition of Hg^{2+} ions.

DNA-functionalized gold nanoparticles have been used for the colorimetric detection of Hg^{2+} ions in aqueous media.[158] Two types of thiolated-DNA sequences (probe A: 5′HS-C_{10}-A_{10}-T-A_{10}3′; probe B: 5′HS-C_{10}-T_{10}-T-T_{10}3′) have been used, which are complementary except for a single thymidine–thymidine mismatch. DNA-AuNP aggregates formed from probes A and B (1.5 nM each) gave an SPR peak at 525 nm. Without Hg^{2+}, the aggregated melted with a dramatic purple-to-red color change at about 46 °C (T_m). However, in the presence of Hg^{2+}, the aggregates melted at temperatures higher than 46 °C along with a color change because of the strong coordination of Hg^{2+} to the two thymidines that make up the T–T mismatch, thereby stabilizing the duplex DNA strands containing the T–T single base mismatches. Indeed, at 47 °C, only the aggregate solution containing Hg^{2+} was purple, whereas all of the others had turned bright red. Pb^{2+} is the only other metal ion that influenced the T_m of the aggregate, but only by a negligible amount ($\Delta T_m \sim 0.8$ °C).

Deng et al. synthesized a homogeneous Hg^{2+} sensor based on a DNA assembly with T–T mismatched base pairs as Hg^{2+} ion recognition sites and the interactions between two G-quadruplex halves for signal transductions.[159] In the absence of Hg^{2+} ions, the hairpin structure based on the nucleic acid strand would be destabilized into an unstructured random coil, which was flexible enough to combine and form an intact peroxidase-active G-quadruplex upon hemin binding. The catalytic activity of the re-formed G-quadruplex was responsible for the oxidation of 2,2′-azino-bis(3-ethylbenzothiazoline-6-sulphonic acid) diammonium salt (ABTS) into a blue-green colored cationic radical, $ABTS^{\bullet+}$, in the presence of H_2O_2 as an oxidant. However, the presence of Hg^{2+} ions facilitated the formation of intrastrand T-Hg^{2+}-T complexes and thus prevented the G-quadruplex from being correctly formed. This led to a decreased output that can be quantified at λ=418 nm.

Wang et al. introduced a label-free colorimetric method for the selective detection of aqueous Hg^{2+} using Hg^{2+}-modulated G-quadruplex based DNAzymes with many T-residues, AGRO100 and G4-2S as the sensing elements in low and high-salt conditions, respectively.[160] The uncomplexed hemin had a Soret absorption band centered at 397 nm. After incubation with the folded AGRO100, a noticeable hyperchromicity was observed in the hemin Soret band. The absorption center shifted to 404 nm, accompanied by an observable increase in the absorption intensity. This was consistent with the binding of AGRO100 to hemin. However, in the presence of Hg^{2+}, there was little hyperchromicity in the hemin Soret band, suggesting no binding interaction between AGRO100 and hemin. As a result of Hg^{2+} inhibition, a sharp decrease in the catalytic activity toward the H_2O_2-mediated oxidation of ABTS was observed, accompanied by a change in solution color. Similar results have been found for another bimolecular DNA G-quadruplex G4-2S with the only difference that G4-2S was found to need a high salt concentration (at least 20 mM K^+) to remain stable.

Another Hg^{2+}-induced conformational change of ssDNA and dsDNA and interaction with AuNPs has been demonstrated by Yang et al.[161] The stabilized gold colloids exhibited the nanoparticle characteristic SPR peak at 520 nm and appeared pink red. On increasing the salt concentration of the solution (0.1 M NaCl), this 520 nm band was shifted to long wavelength concomitant with a color change of the solution from pink red to blue gray. However, in the presence of the ssDNA strand in the colloidal solutions, the intrinsic absorption peak at 520 nm and pink-red color of the AuNPs was displayed.

For dsDNA, the colloidal solution of the AuNPs displayed a blue gray color with a broad absorption between 600 and 800 nm. In the absence of Hg^{2+}, the mixture of a solution of AuNPs and **186** in 0.1 M NaCl displayed λ_{max} at 520 nm, indicating that, at this salt concentration, the free **186** existed in the single-stranded form and was adsorbed on the surfaces of AuNPs to protect the AuNPs against salt-induced aggregation. In the presence of Hg^{2+} ions, AuNPs displayed a blue-gray color concomitant with a broad absorption between 600 and 800 nm. This result implied that binding of Hg^{2+} with **186** formed a double-stranded structure, which reduced the interaction with AuNPs and lost the ability to disperse the aggregated nanoparticles.

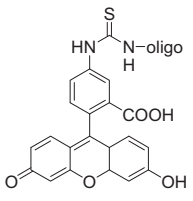

186

Liu et al. utilized a combination of oligonucleotides and AuNPs, which readily detected Hg^{2+} in aqueous solution.[162] The basic design consisted of two types of DNA-functionalized AuNP probes (probe A and probe B) and an appropriate oligonucleotide linker (probe C). In the absence of Hg^{2+}, these three probes did not form DNA-AuNP aggregates because of a lower-melting temperature T_m than the operating temperature, due to mismatches formed in the DNA duplexes. Upon addition of an aqueous solution of Hg^{2+}, a clear red to purple-pinkish colorimetric response occurred within 5 min. The UV–vis spectrum of the solution also showed a bathochromic shift of the AuNPs from 520 to 565 nm, indicating the formation of particle aggregates via an Hg^{2+}-induced hybridization event.

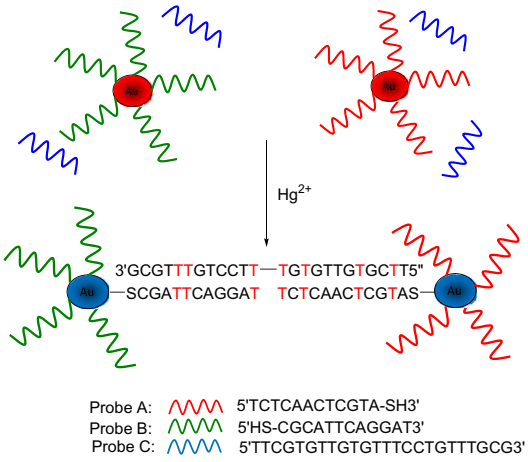

Yang et al. demonstrated a colorimetric detection method for Hg^{2+} ions with a tunable detection range based on DNA oligonucleotides and unmodified gold nanoparticles (DNA1 (5′-ATGTCACGTTATTGCATTCG-3′)/DNA2 (5′-CGATTGCTAT ATCGGTCAT-3′)/AuNPs) sensing systems.[163] In the absence of Hg^{2+} ions, a characteristic surface plasmon resonance absorption band of AuNPs was observed in the spectra at ~520 nm and the color of the solution remained red after the addition of a salt ($NaClO_4$). However, in the presence of Hg^{2+} ions, a shoulder absorption band at 700 nm appeared and increased and the absorbance at 520 nm decreased. Correspondingly, the color of the solution turned to blue gray. Hg^{2+} ions could stabilize DNA duplexes with T–T mismatches, and thus DNA1 and DNA2 could hybridize in the presence of Hg^{2+}, due to the formation of T-Hg^{2+}-T base pairs.

The absorption spectrum of porphyrin-functionalized Au@SiO_2[164] core shell nanoparticles (**187**) in 20 mM HEPES buffer at pH 7.4 showed a strong visible absorption band at 420 nm. When Hg^{2+} was added gradually, the λ_{max} showed a 20 nm red shift and the color of the suspension turned from red to green.

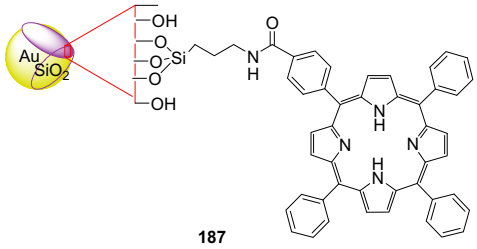

187

Taki's group studied the colorimetric response to Hg^{2+}-induced absorption of triethylene glycol ligands (**188$_n$**-SAu) from an AuNP surface.[165] The color of **188b**-AuNP changed drastically from red to blue on incubation with Hg^{2+}. The colorimetric response of **188a**-AuNP toward Hg^{2+} was less distinct and indiscriminate precipitation immediately occurred, due to irreversible aggregation upon the addition of Hg^{2+}. The Hg^{2+}-induced color change of **188b**-AuNP also appeared in a red-shifted plasmon band of the UV–vis spectrum from 520 (due to dispersed particles) to 580 nm (due to aggregated particles). The **188a**-AuNP was unstable and had a tendency to aggregate, while **188c**-AuNP was too stable to react with Hg^{2+} because of the presence of a long ethylene glycol chain.

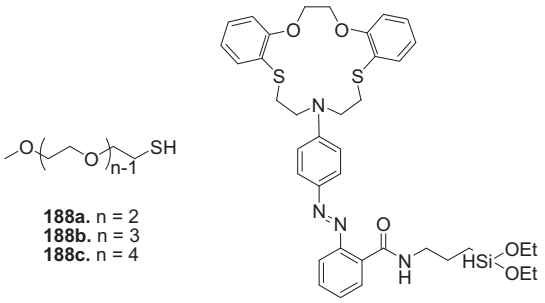

189

Jung et al. selectively detected Hg^{2+} by the immobilization of azo-coupled macrocyclic receptor **189** on silica nanotubes (SNT-**189**).[166] Upon addition of Hg^{2+} in suspension, SNT-**189** underwent a color change from yellow to violet. The Hg^{2+}-loaded SNT-**189** spectrum exhibited an absorption maximum at 542 nm, whereas the absorption peak appeared at 441 nm for the Hg^{2+}-free spectrum. Moreover, the SNT-**189**-coated glass plate underwent a similar color change upon addition of Hg^{2+} ions.

Hg^{2+} and Ag^{+} ions have been selectively detected by using Tween 20-modified AuNPs.[167] Citrate ions adsorbed onto the citrate-capped AuNP surface acted as a reducing agent for Hg^{2+} and Ag^{+} when citrate-capped AuNPs had been modified with Tween 20. Because of the high affinity between Au and Hg, the reduced Hg(0) was directly deposited onto the Au surface through the formation of Hg–Au alloys; meanwhile, Tween 20 molecules were desorbed from the AuNPs. The removal of stabilizer (Tween 20) caused the AuNPs to aggregate under conditions of high ionic strength. Citrate ions have also been used to reduce Ag^{+} onto the Au surface. The formation of Ag-coated AuNPs enabled Tween 20 to be removed from the Au surface, thereby inducing aggregation of the AuNPs in a high ionic strength solution. When Hg^{2+} or Ag^{+} ions were added to Tween 20-AuNPs, the extinction spectra showed a gradual increase in extinction at 650 nm and the color gradually changed from red to purple.

Starch-stabilized AgNPs[168] have been found to selectively recognize Hg^{2+} in aqueous solution. The UV–vis spectrum of AgNPs showed a characteristic peak centered at 400 nm with light yellow color. Upon addition of Hg^{2+} to the solution of AgNPs, the absorbance peak was decreased along with a slight blue shift. Here, Hg^{2+} ions reacted with AgNPs to form metallic mercury. The freshly generated mercury atoms could be strongly bonded on the silver surface to form a solid amalgam-like structure, which could account for the slight blue shift of the surface plasmon absorption band of the AgNPs. The addition of Cd^{2+} resulted in a very small red shift of the absorption band.

Yang and his group determined Hg^{2+} in the presence of Pb^{2+} ions by using unmodified AuNPs as probes and 15-*mer* thrombin-binding aptamer (TBA) as sensing element.[169] The SPR absorption band of an AuNP solution containing TBA and Hg^{2+} or Pb^{2+} under high-salt conditions underwent a red shift and broadening of the band along with a visible color change from red to blue or purple. A comparison of the absorption spectra of the aggregated AuNPs in the presence of Hg^{2+} (800 nm) and Pb^{2+} (650 nm) showed that the characteristic wavelength of the aggregated AuNPs facilitated the determination of Hg^{2+} in the presence of Pb^{2+} ions.

Heterogeneous colorimetric sensors formed by the immobilization of an azobenzene of an azobenzene-coupled receptor onto mesoporous silica (**190**-SiO_2) or titania (**190**-TiO_2) nanoparticles have been used for the selective detection of Hg^{2+}.[170] The aqueous solution of a **190**-SiO_2 suspension (pH 7.4) displayed λ_{max} at 310 nm.

Upon addition of Hg^{2+} in an H_2O suspension, the **190**-SiO_2 resulted in a color change from light yellow to red within 10 s along with an absorption change to 495 nm. The association constant for Hg^{2+} coordination to **190**-SiO_2 was calculated to be log K=5.48. In addition, the absorption or color changes observed in **190**-SiO_2 upon addition of Hg^{2+} were reversible, as observed by the addition of EDTA. Similar absorption and color changes were observed in the case of a portable chemosensor kit, made by coating a 4-μm thick film of **190**-TiO_2 onto a glass substrate, upon addition of Hg^{2+} ions.

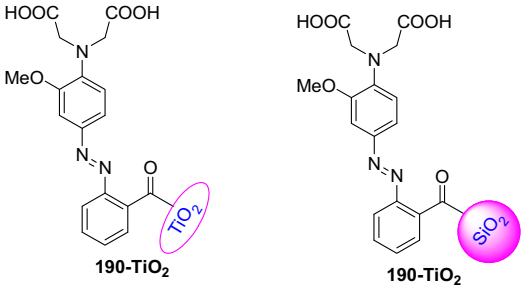

5. Ag^+ metal ion sensing chemosensors

Tripodal receptors **191a**–**c**, based on a mesitylene anchor,[171] containing aza-thioethers as donor atoms and coupled with substituted azophenols acted as selective chromogenic receptors for Ag^+. Addition of Ag^+ to sensor **191c** in dioxane/H_2O (1:9 v/v) caused splitting of the 384 nm band into two new bands at λ_{max} 394 and 510 nm along with a distinct color change from yellow to red. Sensor **191c** was highly Ag^+ selective and did not show any interference from other metal ions, except Cu^{2+}.

The chemosensor **192**, consisting of a poly(olefin) backbone with pendent naphthalene Schiff base receptors, gave chromogenic naked-eye detection of Ag^+ and ratiometric fluorescent detection of Mn^{2+}.[172] The UV–vis spectrum of **192** in THF/H_2O (1:1 v/v, pH 7.0) was characterized by two main bands centered at 308 and 418 nm. Substantial enhancements of the 310 and 418 nm bands were observed upon addition of Ag^+, the former being accompanied by a slight red shift of the absorption maxima. This was accompanied by a distinct change in color of the solution from colorless to dark yellow, while the color of the solutions containing other ions remained relatively unchanged.

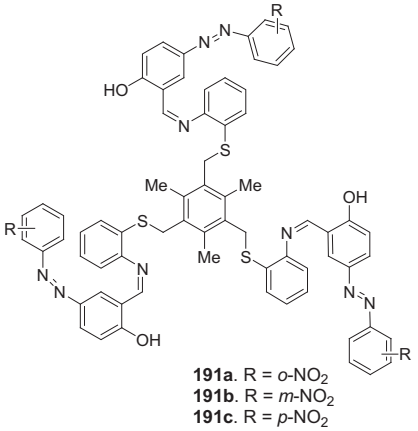

191a. R = *o*-NO_2
191b. R = *m*-NO_2
191c. R = *p*-NO_2

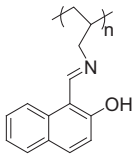

192

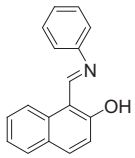

193

In contrast to the selectivity displayed for **192**, monomer **193** was observed to bind to many different ions when examined by UV–vis or fluorescence spectroscopy, suggesting that, for **192**, the availability of multiple binding sites from adjacent receptors was sufficient to complete the coordination sphere of specific metal ions.

In the UV–vis spectrum of a fluorescein derivative possessing thiomorpholine groups (**194**),[173] a red shift of 15 nm was observed when Ag^+ was added. This change was associated with the formation of a dianionic species. In the absence of Ag^+, **194** existed in a monoanionic form because the color of the solution was light yellow. Addition of tetrabutylammonium chloride (TBA^+Cl^-) to the **194**-Ag^+ complex and removal of AgCl changed the color of the solution back to yellow.

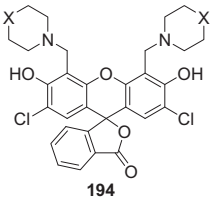

194

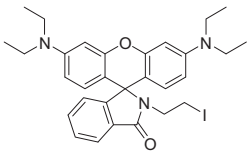

195

Ag^+-promoted spirolactam ring opening[174] has been observed in a Rhodamine B derivative **195** by Ahn et al. Chemodosimeter **195** formed a colorless and non-fluorescent solution in 20% ethanolic water. Addition of Ag^+ ions to this solution led to the development of a pink color (λ_{max}=558 nm) and a strong orange fluorescence (584 nm).

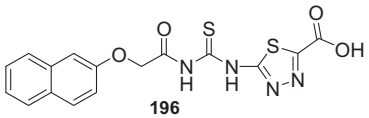

196

Fluorescent organic nanoparticles (**197**) based on a naphthalene-thiourea-thiadiazole-linked molecule (**196**) underwent different color changes upon addition of Ag^+, depending upon the time.[175] After 5 h, the color of the solution of **197** changed from colorless to pink, red-brown, and brown with increasing time. After 24 h, the color of the solution had changed to dark brown. Finally, an appreciable precipitation was formed and visualized by the naked eye. However, addition of other metal ions including Na^+, Ca^{2+}, Co^{2+}, Mn^{2+}, Cd^{2+}, Cu^{2+}, Pb^{2+}, and Hg^{2+} had no effect on the color of the solution of **196** or **197**.

Dong et al. studied unlabeled and labeled sensing strategies for Ag^+ detection by using a DNA-based AuNP colorimetric method.[176] In the unlabeled strategy, C base enriched single-strand DNA (C-ssDNA) was entwined onto AuNPs to form an AuNPs/C-ssDNA complex. In the labeled method, sulphydryl group modified C-ssDNA (HS-C-ssDNA) was covalently labeled on the AuNPS to produce an AuNP-S-C-ssDNA complex. After adding Ag^+ ions and 0.12 M $NaNO_3$ into an AuNP/C-ssDNA solution, the obtained solution turned from red to purple and even dark blue with the presence of higher concentrations of Ag^+ ions. In the UV–vis spectrum, the ratio of AuNP surface plasma absorption (A_{650}/A_{520}) was enhanced with an increase of Ag^+ ions, illustrating the aggregation of the AuNP/C-ssDNA/Ag^+ solution.

However, when Hg^{2+} ions were present, the AuNPs/C-ssDNA/Hg^{2+} solution also turned purple when the salt was added. Additionally, Cu^{2+} ions also displayed a little interference in the UV–vis spectra. The interferences from Hg^{2+}/Cu^{2+} ions could be decreased by adding EDTA to the metal–ion solution directly. The labeled strategy provided more sensitive, stable, and controllable sensing results, compared with the unlabeled method, for the colorimetric detection of Ag^+.

A liquid colorimetric stable yellow copper(I) oxide[177] nanocolloid underwent a marked color change from yellow to dark brown upon addition of only Ag^+. This was associated with a shift of λ_{max} value from 448 to 478 nm.

6. Fe^{2+}/Fe^{3+} metal ion sensing chemosensors

An artificial siderophore[178] **198** is in the form of a squaraine dye chelated to Fe^{3+} between the deprotonated hydroxyl groups on the *ortho* position of the ring adjacent to the carbonyl group of the

cyclobutadiene ring. The UV–vis spectrum of **198** (DMSO) showed a Q band at λ_{max} 651 nm with a broad shoulder at 600 nm, which showed a hypsochromic shift of 101 nm on addition to a solution of DBU (1,8-diazobicyclo[5.4.0]undec-7-ene). This caused a naked-eye color change from dark blue to a purple color. Addition of different metal ions to a solution of **198** resulted in a decrease in absorbance at λ_{max} 555 nm with an increase at λ_{max} 651 nm. The binding affinities showed that there was high affinity of **198** to Fe^{3+} and Zn^{2+} (K_{Fe3+}=8.9×10^7 and K_{Zn2+}4.5×10^8 M^{-1}) as well as Fe^{2+}.

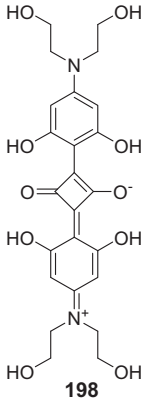

198

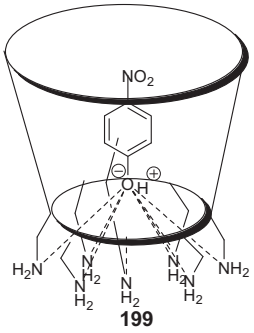

199

Using per-6-amino-β-cyclodextrin as a supramolecular host and *p*-nitrophenol as a spectroscopic probe, colorimetric chemosensor (**199**) was developed by Fe^{3+}/Ru^{3+} in water by Pitchumani.[179] With addition of Fe^{3+} to a solution of **199** in water, the absorbance at 402 nm decreased significantly with the emergence of a new band at 318 nm (corresponding to *p*-nitrophenol). This resulted in a color change from intense yellow to colorless. Similar observations, as in Fe^{3+}, were noticed on addition of Ru^{3+}.

A donor–π–acceptor system possessing a terpyridine group (**200**)[180] underwent a color change of the solution from light yellow to light magenta upon addition of Fe^{2+}/Fe^{3+} along with a sharp new band at 567 nm.

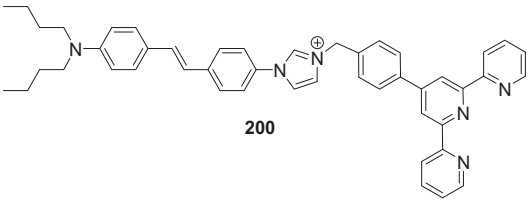

200

Fe^{3+}-induced spirolactam ring opening has been observed in chemodosimeter derivatives **201**–**206**.[181–186] The colorless solutions of chemodosimeters showed no absorption bands above 500 nm. Upon addition of Fe^{3+} ions to solution of chemodosimeters, a new absorption band centered above 500 nm appeared, concomitant with a color change to pink.

Although chemodosimeter **201**[181] has the potential model structure for the Hg^{2+}-promoted guanylation reaction, it exhibited higher binding affinity toward Fe^{3+} than Hg^{2+}. This could be attributed to the addition of a more electron-withdrawing carbonyl group to the thiourea moiety of **201**, resulting in decreased electron density on the sulfur atom of the thiourea group and lowering of the Hg^{2+} affinity.

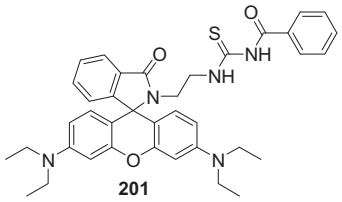

201

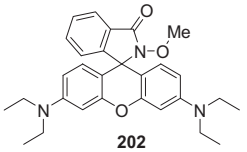

202

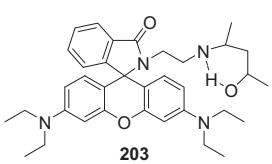

203

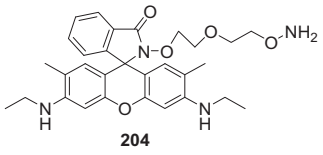

204

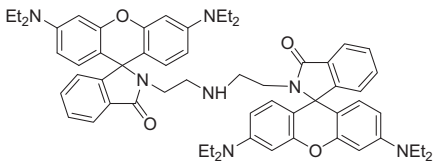

205

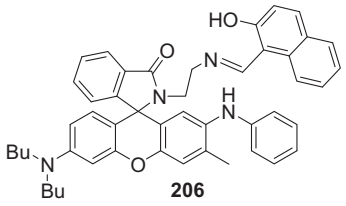

206

A similar type of Fe^{2+}-induced spirolactam ring opening has been observed in a fluoran dye (**206**).[186] However, the absorption maximum showed no obvious changes upon addition of metal ions like Cd^{2+}, Mg^{2+}, Pd^{2+}, Hg^{2+}, Ni^{2+}, Fe^{3+}, Ca^{2+}, Co^{2+} and alkali, and alkaline earth metal ions.

7. Pb^{2+} metal ion sensing chemosensors

Supramolecular systems based on the pyridine-ethenyl-substituted tetrathiafulvalene (TTF) compounds **207a** and **207b** underwent a color change from yellow to deep purple on addition of Pb^{2+}.[187] The bands at λ_{max} 301 nm (absorption band) and 440 nm (CT transition band) red shifted to λ_{max} 330 and 555 nm with Pb^{2+}. The Zn^{2+} and Cd^{2+} ions also induced red shifts of the CT bands by 14 and 8 nm, respectively. The compounds **207a** and **207b** formed respective 2:1 (log *K* 5.42) and 1:1 (log *K* 5.57) complexes with Pb^{2+}.

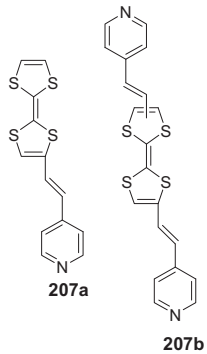

207a

207b

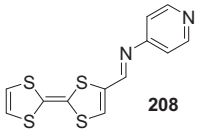

208

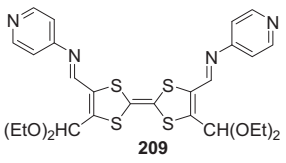

209

However, the TTF derivatives **208** and **209** exhibited a strong absorption band at λ<350 nm and a moderate absorption band in the region 380–650 nm.[188] Upon addition of Pb^{2+} to a solution of **208** in CH_2Cl_2/MeCN (1:1 v/v), the resulting electronic spectra showed the appearance of a new LE band centered on 568 nm, detrimental to the initial ICT band at 484 nm, and the color of the

solution was observed to change from orange to blue. A very similar behavior was observed with the dipyridyl derivative **209**, for which a new band developed at +67 nm.

A colorimetric sensor based on conjugated polydiacetylenes (**210**) displayed a selective and clear blue-to-red transition only with Pb^{2+} in HEPES (pH 7.4) amongst other metal ions.[189] The UV–vis spectrum of **210** showed a decrease of absorption at 620 nm with a simultaneous increase of absorption at 540 nm with the addition of Pb^{2+}.

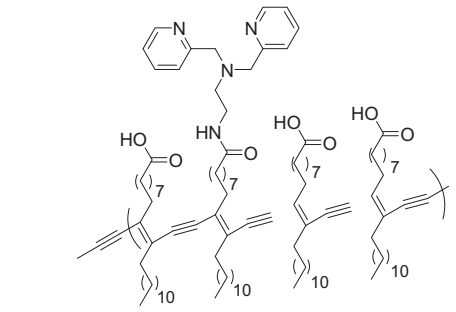

210

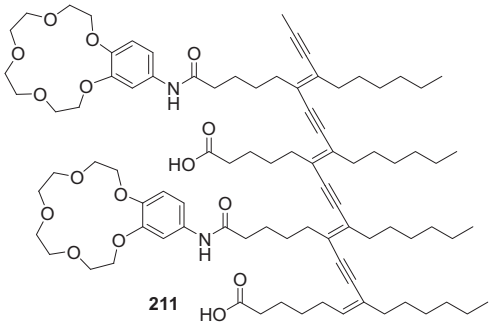

211

Another benzo-15-crown-5-functionalized polydiacetylene-based colorimetric self-assembled vesicular chemosensor (**211**)[190] underwent a blue-to-red color transition along with λ_{max} shift from 640 to 540 nm with the addition of Pb^{2+} ions in buffered water (pH 7.2). Addition of Zn^{2+} and Cu^{2+} exhibited slight changes in the absorption spectra and a slower kinetic response with the color of the solution turning a light purple.

Molina and his group studied different ferrocene-possessing chemosensors (**212**–**219**).[191–193] Significant modifications were observed upon addition of only Cu^{2+}, Hg^{2+}, and Pb^{2+} to a solution of **212** and **213**.[191] The addition of increasing amounts of Pb^{2+} ions to a solution of **212** in MeCN caused the disappearance of the LE band at λ=484 nm along with the progressive appearance of a new band located at 603 nm as well as a decrease of the initial HE band intensity. The new LE band was red shifted by 119 nm and was responsible for the change of color from orange to deep green. Binding assays suggested a 1:1 binding model with log K_a=4.30±0.15. By contrast, addition of Cu^{2+} and Hg^{2+} metal ions to the solution of **212** resulted in the formation of a new ligand to metal (LMCT) band at λ=800 nm with a concomitant decrease of the band at λ=584 nm.

However, the chemosensor **213** displayed a different behavior upon addition of Cu^{2+}, Hg^{2+}, and Pb^{2+} ions than that of chemosensor **212**. In the case of chemosensor **213**, whereas Hg^{2+} and Pb^{2+} promoted a clear complexation process, Cu^{2+} induced oxidation of the chemosensor. However, addition of Hg^{2+} and Pb^{2+} to a solution of **213** induced a red shift of the LE band from 475 to 536 nm ($\Delta\lambda$=61 nm) with a simultaneous change in the color of the solution from orange to deep blue. The binding constants for a 1:1 binding model have been found to be log K_a=5.37±0.21 for Hg^{2+} and log K_a=5.34±0.18 for Pb^{2+}.

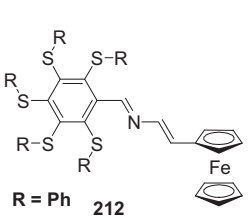

R = Ph **212**

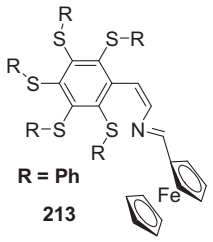

R = Ph **213**

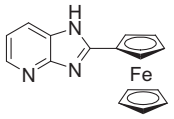

214

The UV–vis spectrum of a ferrocene-possessing receptor having a 1-deazapurine backbone (**214**)[192] in MeCN displayed a strong band at λ=309 nm (HE) and a strong band (LE) of lower intensity at λ=448 nm. Addition of Pb^{2+} to the solution of **214** caused a progressive red shift of the HE band ($\Delta\lambda$=11 nm) and LE band ($\Delta\lambda$=44 nm). These facts were responsible for a perceptible change of color from colorless to orange. The binding constant was calculated to be $K_a=3.3\times10^5$ M^{-1} for the 1:1 complexation mode.

Imidazole-annelated ferrocene derivatives (**215**–**219**) have been used as selective and sensitive multichannel chemical probes for Pb^{2+} ions.[193] The UV–vis spectrum of chemosensor **215** in MeCN displayed an HE band at 305 nm and an LE band at 457 nm. Likewise, the spectrum of chemosensor **216** showed two bands at 309 and at 448 nm. However, a blue-shifted HE band at 292 nm and a red-shifted LE band at 503 nm were present in the absorption spectrum of chemosensor **217** along with a prominent band at 386 nm. The absorption spectrum of 1,1′-disubsituted ferrocene **218** displayed a strong absorption band at 303 nm and a less intense and broad band at 457 nm. Disubstituted chemosensor **219** exhibited an HE band at 260 nm and a red-shifted LE band at 573 nm, between, which a broad band at 397 nm was present.

In the case of chemosensor **215**, addition of aqueous Pb^{2+} induced a small red shift of the LE band by $\Delta\lambda$=15 nm, similar to those observed ($\Delta\lambda$=11 nm) when Zn^{2+}/Hg^{2+} ions were added. However, the absorption spectrum of **216** showed a progressive red shift of the HE band ($\Delta\lambda$=11 nm) and LE band ($\Delta\lambda$=44 nm) with the addition of Pb^{2+} along with a change of color from colorless to orange. The HE and LE bands were also red shifted (6–11 and 29–34 nm, respectively), although without any change of color upon addition of Zn^{2+} and Hg^{2+} ions.

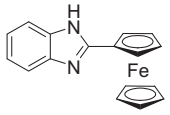

215

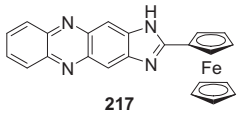

217

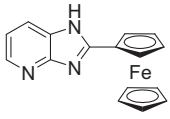

216

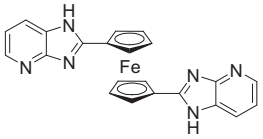

218

On the other hand, addition of Pb^{2+} ions to a solution of the chemosensor **217** caused a progressive appearance of a new strong band located at 404 nm and a red shift of the LE band from 503 to 526 nm. This red shift was responsible for the change of color from pale orange to red. No changes were observed in the absorption spectrum of **217** after the addition of Zn^{2+} and Hg^{2+} ions.

Addition of increasing amounts of Pb^{2+} ions to a solution of the two-armed ferrocene **218** caused a red shift of the LE band by $\Delta\lambda$=23 nm, which was responsible for the change of color from colorless to yellow. The LE band of chemosensor **218** was red shifted ($\Delta\lambda$=7 nm) upon addition of Zn^{2+}. The absorption spectrum of chemosensor **219** in the presence of Pb^{2+} and Zn^{2+} ions underwent a slight blue shift of the LE band ($\Delta\lambda$=7 nm) and a dramatic blue shift of the HE band ($\Delta\lambda$=160 nm), whereas the band located at 397 nm remained unchanged.

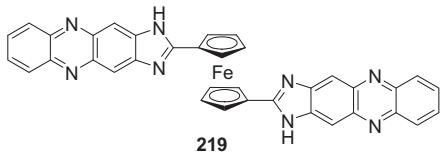

219

Triazole- and azo-coupled calix[4]arene (**220**) recognized Ca^{2+} and Pb^{2+} ions amongst other alkali, alkaline earth, and transition metal ions.[194] The free chemosensor **220** exhibited absorption band at 365 nm in MeCN/$CHCl_3$ (1000:4 v/v). Upon addition of Ca^{2+} to the solution of **220**, the absorption maximum at 365 nm gradually decreased in intensity with the formation of a new absorption band at 527 nm ($\Delta\lambda$=162 nm) along with a color change from light yellow to red. Addition of Pb^{2+} to the solution of **220** induced a bathochromic shift from 365 to 541 nm along with a color change from light yellow to red. The association constants for a 1:1 stoichiometry have been found to be 7.06×10^4 M^{-1} for **220**·Ca^{2+} and 8.57×10^3 M^{-1} for **220**·Pb^{2+} complexes.

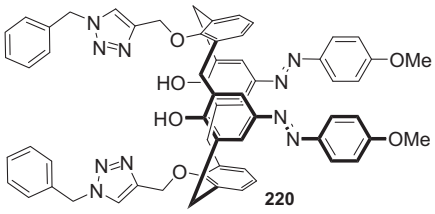

220

The UV–vis spectra of phenanthroline-based chemosensor **221a** in MeCN/H_2O (9:1 v/v, pH 7.4) revealed an absorption band at 352 nm.[195] The addition of Pb^{2+} ions to the solution of chemosensor **221a** resulted in a color change from yellow to red along with the appearance of a new peak at 483 nm (K_a=4.56×10^5 M^{-1}). Chemosensor **221b**, devoid of the *p*-NO_2 group, also displayed a red color with Pb^{2+}, but at a much higher concentration compared to that of **221a**. The binding constant for **221b** and Pb^{2+} was found to be 1.22×10^3 M^{-1}. However, the compound having no ring nitrogen atoms showed a red coloration on prolonged exposure to Pb^{2+} ions.

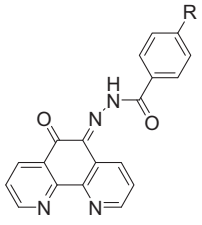

221a. R = NO_2
221b. R = H

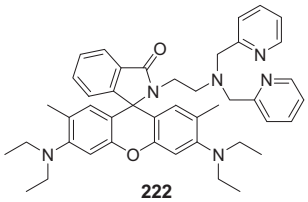

222

Rhodamine-based sensor **222** showed a selectivity for Pb^{2+} over other alkali, alkaline earth, and heavy-metal ions.[196] There was a 120-fold enhancement in the absorbance at λ_{max} 553 nm upon addition of Pb^{2+} to a solution of **222**. This caused the color to change from colorless to pink. An almost, 20-fold enhancement in absorbance was displayed at 553 nm when Zn^{2+} was added. On the other hand, when Cu^{2+} was added, **222** did not display a new peak around 550 nm and only a broad absorption increase was observed around 450 nm.

When different metal ions were added to a solution of podand [2(2-(2-azidoethoxy)-ethoxy)ethanol (OEG)]-triazole-linked AuNPs (**223**),[197] only Pb^{2+} induced a color change from red to navy blue. The color change of the Au colloid was also observed by spotting the colloid onto a solid substrate. The UV–vis spectrum showed that the absorption intensity at 512 nm reduced and the full width at half maximum of plasmon was larger. Due to the interaction induced by Pb^{2+} between two AuNPs, the molecules of **223** aggregated and the color changed.

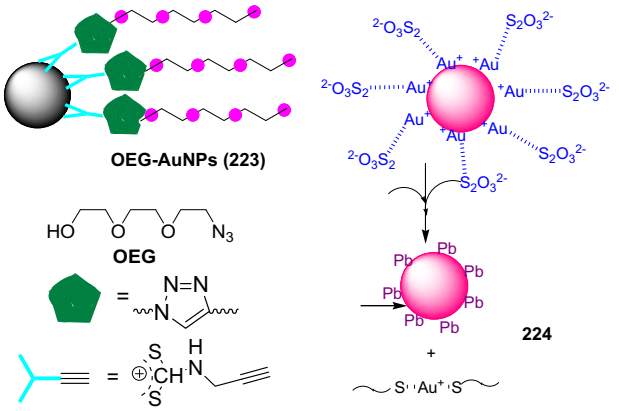

A colorimetric, label-free, and non-aggregation-based AuNP probe (**224**)[198] has been developed for the detection of Pb^{2+} ions in aqueous solution, based on the fact that Pb^{2+} ions could accelerate the leaching rate of AuNPs by thiosulphate ($S_2O_3^{2-}$) and 2-mercaptoethanol (2-ME). When the AuNPs were reacted with $S_2O_3^{2-}$ ions in solution, $Au(S_2O_3)_2^{3-}$ complexes were formed immediately on the AuNP surfaces, leading to a slight decrease in their SPR absorption. After adding Pb^{2+} ions and 2-Me, the AuNPs rapidly dissolved to form Au^+-2-ME complexes in solution. As a result, the SPR absorption decreased dramatically.

A similar phenomenon has been described by Huang's group for the colorimetric detection of Pb^{2+} ions by controlling the ligand shells of AuNPs.[199] When neutral charged 4-mercaptobutanol (4-MB) accessed the surfaces of the AuNPs displacing the citrate ions through the formation of stronger Au–S linkages resulted in reduced surface charge density, thereby inducing aggregation. On the other hand, when negatively charged thiols were bound to the $S_2O_3^{2-}$–AuNPs in the presence of Pb^{2+} ions, the surface charge density did not change and no aggregation was observed. The dispersed AuNPs displayed an extinction band at 520 nm; upon aggregation, the signal underwent a red shift with decreased extinction, while the intensity of the signal at 650 nm increased along with an observable color change.

The citrate-capped AuNPs[200] have been demonstrated to give a pH-dependent response to Pb^{2+} ions. The AuNPs are known to experience a color change upon aggregation induced by metal ions. Fe^{3+}, Cu^{2+}, and Pb^{2+}, upon addition to solution of citrate-capped AuNPs, could induce distinct color changes ($E_{676}/E_{520}>0.6$) of the gold colloidal solution in the range of pH from 6.7 to 9.

The chemical stimuli-responsive disassembly of nanoparticle aggregates using Pb^{2+}-specific DNAzymes has been demonstrated by Lu and Liu[201] Nanoparticles were assembled by DNA base pairing interactions. Dispersed 13 nm nanoparticles had a strong extinction peak at 522 nm. Upon aggregation, the 522 nm peak decreased, while the extinction in the 700 nm region increased. Dispersed nanoparticles had a high extinction ratio and a red color, while aggregated nanoparticles had a low ratio and a blue color. Upon addition of Pb^{2+} to head-to-tail aligned aggregates, no difference was observed in the presence or absence of Pb^{2+}, even in low NaCl concentration buffers.

However, when Pb^{2+} was added to tail-to-tail aligned aggregates suspended in 30 nM NaCl, a slow color change was observed. The color change or disassembly was inhibited in high-salt buffers. Moreover, two 22-*mer* DNAs that were complementary to the cleaved substrate helped to release the cleaved substrate. The disassembly was close to competition in 2 min in the presence of 10 μM of Pb^{2+} and 2 μM of the invasive DNA.

Another colorimetric detection of Pb^{2+} ions by narrowing the size distribution of gallic acid-capped gold nanoparticles (GA-AuNPs)[202] and minimizing the electrostatic repulsion between each GA-AuNP has been demonstrated by Tseng et al. GA-AuNPs in

formic acid (pH 4.5) had a broadened SPR band for 75.1 nm GA-AuNPs as a result of the large size distribution. Although the addition of 1.0 μM Pb^{2+} to this solution caused a red shift of the SPR band, a small increase in extinction at 650 nm was observed. This result indicated the poor sensitivity of GA-AuNPs with a large size distribution in the detection of Pb^{2+}. A similar phenomenon was observed in the case of 150.3 nm GA-AuNPs with a size distribution of 113.5–187.1 nm. However, a narrow SPR band has been observed for 9.3 nm GA-AuNPs because of the narrow size distribution. The addition of Pb^{2+} to a solution of 9.3 nm GA-AuNPs resulted in a large increase in extinction at 600 nm. Moreover, a further enhancement of the colorimetric sensitivity of GA-AuNPs toward Pb^{2+} could be achieved by adding $NaClO_4$ to minimize the electrostatic repulsion between GA-AuNPs, which provided a small energy barrier for Pb^{2+} to overcome.

An allosteric G-quadruplex DNAzyme (PS2.M) gave colorimetric detection of Pb^{2+}.[203] In the presence of K^+, PS2.M folded into an unimolecular G-quadruplex. This K^+-stabilized quadruplex structure bound hemin with high affinity, resulting in a complex that mimicked the horseradish peroxidase and catalyzed the H_2O_2-mediated oxidation of ABTS or luminal to generate a color change. In contrast, the Pb^{2+}-stabilized PS2.M did not bind hemin, thereby exhibiting no DNAzyme activity.

A characteristic SPR band of glutathione-functionalized AuNPs[204] was observed in the spectrum at approximate 520 nm and the color of the solution remained red. However, upon addition of Pb^{2+} to the glutathione-functionalized AuNPs, the solution turned purple and the SPR band shifted to 700 nm, owing to Pb^{2+}-stimulated aggregation.

8. Zn^{2+} metal ion sensing chemosensors

Chemosensor **225** underwent different absorption spectral changes after either reaction with thiol-containing amino acids/peptides or coordination with Zn^{2+}/Co^{2+}.[205] The intensity of the ICT band of **225** around 532 nm was reduced with the appearance of a new absorption band around 394 nm after introducing either Zn^{2+}/Co^{2+} along with a color change from dark purple to yellow. The binding constants of **225** with Zn^{2+} and Co^{2+} for a 1:1 stoichiometry were estimated to be 2.49×10^4 M^{-1} for Co^{2+} and 2.28×10^4 M^{-1} for Zn^{2+}. On addition of cysteine (Cys) and glutathione, the intensity of the ICT band started to decrease gradually, leading to a contrasting color change of the solution of **225**.

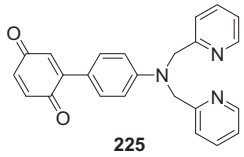

225

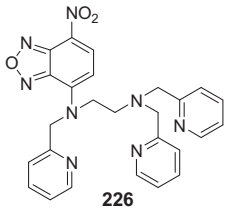

226

The absorption spectrum of 7-nitrobenz-2-oxa-1,3-diazole (**226**)[206] possessed λ_{max} at 350 and 450 nm, the intensity of which decreased upon addition of Zn^{2+} with the concurrent growth of a band at 400 nm, corresponding to a colorimetric change from red to yellow, that is, clearly observable.

Upon addition of Zn^{2+} to a solution of an intensively colored hetarylazo derivative **227** at pH 7.5 in the presence of 0.15 M NaCl, the absorption maximum of **227** considerably reduced in intensity and shifted hypsochromically from 518 to 481 nm along with a naked-eye color change from red to faint orange.[207] However, upon addition of Hg^{2+} at a rather higher concentration compared to Zn^{2+}, the absorption maximum of **227** shifted firstly hypsochromically to 508 nm and then bathochromically to 553 nm. This blue shift resulted in a change of color from red to orange.

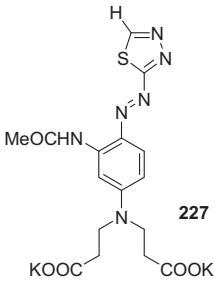

227

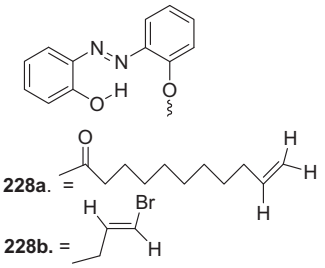

228a. =

228b. =

However, other two azobenzene-containing chemosensors **228a** and **228b** underwent a red shift due to deprotonation induced by metal ions.[208,209] Chemosensor **228a** underwent deprotonation upon coordination with Zn^{2+} and the color of the solution changed from light yellow to reddish orange. However, upon coordination with Cu^{2+}, deprotonation of **228b** was promoted. The absorption spectrum of **228b** underwent a red shift, the typical absorption peak for the hydrazone form of **228b** disappeared and the color of the solution changed from light yellow to light red.

Zn^{2+} ion-induced deprotonation of a secondary amine has been observed in sensors **229** and **230**. On addition of Zn^{2+} ion to the solution of **229** (primrose yellow), the absorption band at λ_{max} 451 nm decreased and two new bands at λ_{max} 309 and 507 nm (pink) appeared.[210] The addition of Cu^{2+}, Co^{2+}, and Ni^{2+} to the solution could also deprotonate the probe **229** and changed the solution color from primrose yellow to pink. However, the absorption spectrum of free **230** exhibited a maximum centered at λ_{max} 460 nm.[211] Addition of Cd^{2+} caused a blue shift of the absorption maximum, whereas Zn^{2+} resulted in a red-shifted absorption band at 492 nm Zn^{2+} and Cd^{2+} could be recognized through a naked-eye color change from green to blue (Cd^{2+}) and to greenish yellow (Zn^{2+}).

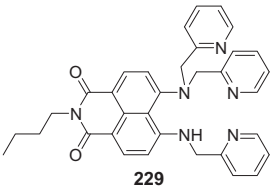

229

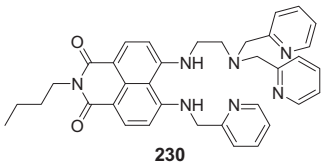

230

The aldimine derivatives **231** and **232** underwent a change in color of the solution from pale red (λ_{max}=496 nm) to deep green (λ_{max}=595 nm) upon selective addition of Zn^{2+} ions.[212] The resulting data suggested a 2:1 binding model for sensor **231** with the association constant being 1.2×10^8 M^{-2}. Similar results were obtained for chemosensor **232** with association constant being 9.3×10^6 M^{-2}.

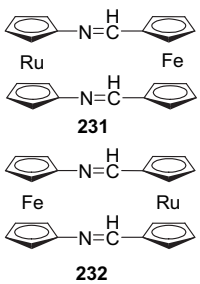

231

232

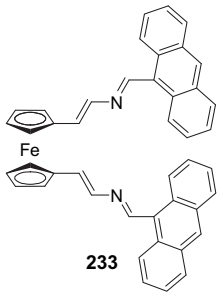

233

After the addition of Zn^{2+} to a solution of the ferrocene derivative **233**,[213] the LE band at 417 nm was red shifted to 487 nm ($\Delta\lambda$=70 nm). In addition, a new and weak lower-energy band appeared at 628 nm. These facts are responsible for the color change from orange to deep purple. On the other hand, with the addition of Cu^{2+}, Ni^{2+}, Co^{2+}, Pb^{2+}, Hg^{2+} or Cd^{2+} metal ions, the absorption maxima did not shift, although the intensity of the absorption band at 417 nm weakens and the shoulder at 510 nm

exhibits a slight increase. No perturbation was observed upon addition of Ca^{2+} and Mg^{2+}.

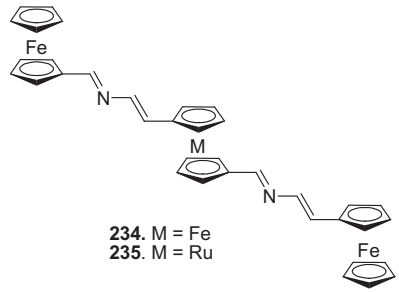

234. M = Fe
235. M = Ru

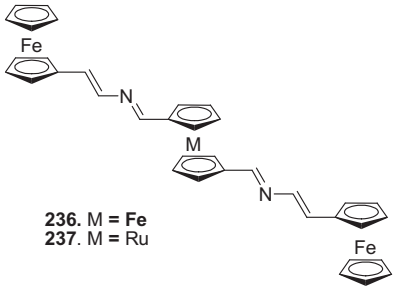

236. M = **Fe**
237. M = Ru

However, addition of Zn^{2+}, Hg^{2+}, and Pb^{2+} ions to solutions of the chemosensors **234** and **235**, in which the central metallocene is placed at the 4-position of the aza bridge, gave rise to the same red shift of the LE band ($\Delta\lambda$=76 and 91 nm, respectively), with simultaneous changes in the color of the solution from orange to deep purple.[214] However, the red shifts promoted for Hg^{2+} and Pb^{2+} metal ions upon addition to the chemosensors **236** and **237**, bearing the central metallocene linked to the 1-position of the aza-diene bridge, were of the same magnitude ($\Delta\lambda$=115 and 114 nm, respectively), but different than those promoted by Zn^{2+} ($\Delta\lambda$=85 and 65 nm, respectively). Hg^{2+} and Pb^{2+} ions promoted a substantial change in the color of solution from yellow to green, whereas Zn^{2+} ions induced a change from yellow to orange.

However, the complexation process of these chemosensors toward the same set of metal cations in MeCN solutions revealed different selectivities. Thus, whereas Li^{+}, Na^{+}, K^{+}, Ca^{2+}, Mg^{2+}, Cd^{2+}, and Ni^{2+} ions did not produce any detectable changes in the UV–vis spectra of these chemosensors, Zn^{2+}, Hg^{2+}, and Pb^{2+} induced the progressive appearance of a new LE band, red shifted with respect to that observed in the free ligand, which in turn decreases continuously until disappearance when the total complexation was achieved.

The absorption spectrum of a coumarin Schiff base derivative **238**[215] showed an intensive absorption band at 374 nm in MeCN, the intensity of which deceased with the addition of Zn^{2+} along with a new absorption peak at 452 nm. The color of the solution changed from colorless to yellow upon addition of 10 equiv of Zn^{2+}. However, upon addition of Co^{2+} and Ni^{2+}, new absorptions at 470 and 480 nm, respectively, were observed, which led to the solution color to change to orange, while upon addition of Fe^{3+}, a new absorption band appeared around 450 nm and the solution color became deep yellow.

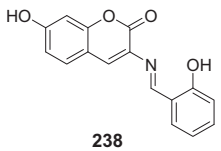

238

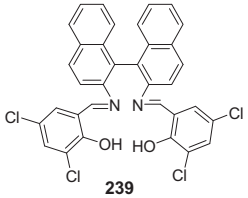

239

However, the UV–vis spectrum of a salen-type Schiff base (**239**)[216] showed a band at 280 nm and two bands centered at 323 and 375 nm. With the addition of Zn^{2+} to a solution of **239**, the 280 nm absorption band increased, the original bands at 323 and 375 nm gradually decreased and a new band centered at 400 nm appeared. This caused a color change of the solution from colorless to light green. However, upon adding Cu^{2+} to the solution of **239**, the absorption band at 280 nm increased in intensity and the original bands at 323 and 375 nm gradually decreased following the formation of a new band centered at 420 nm. At the same time, the colorless solution had become yellow with the addition of Cu^{2+}.

An 8-aminoquinoline-based Schiff base **240**[217] also underwent color and fluorescent changes in the presence of Zn^{2+} ions. The absorption spectrum of **240** exhibited a broad band at 338 nm, which shifted to 455 nm with the addition of Zn^{2+} ions. These changes were accompanied by a visual color change from colorless to yellow.

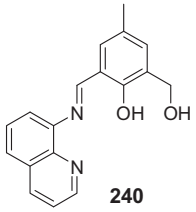

240

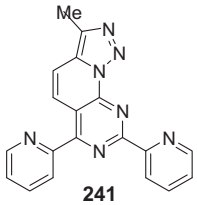

241

The UV–vis spectra of chemosensor **241**[218] consisted of two bands centered at λ_{max} 290 and 373 nm. Addition of Cu^{2+} produced large bathochromic shifts of the band at 373 nm, which appeared at 458 nm. When Zn^{2+} was added to the solution of **241**, the observed shift was less pronounced (382 nm). Nonetheless, the produced shift was large enough to turn the initially colorless solution to yellow.

9. Other transition metal ion sensing chemosensors

A specific ABC triblock copolymer, in which thermomorphic block poly(*N*-isopropylacrylamide) (PNIPA) and hydrophilic poly(-methacrylic acid) (PMAA) mediated the shortest poly(2-hydroxyethyl methacrylate) (PHEMA) bearing pendents of tetra(4-carboxylatophenyl)porphyrins (TCPP) (**242**),[219] upon triggering by metal ions, exhibited fully color-tunable behavior as a cationic detector and colorimeter. Below the low critical soluble temperature of PNIPA (~32 °C), a transparent red-brown solution with a diagnostic TCPP Soret band (λ_{max}=434 nm) was observed. Upon heating above 35 °C, a clear blue shift from 434 to 406 nm was seen. Below 32 °C, the addition of different metal ions (Fe^{3+}, Fe^{2+}, Cu^{2+}, Mn^{2+}, Mg^{2+}, Co^{2+}, Cd^{2+}, Ni^{2+}, and Zn^{2+}) to a solution of **242** led to an unprecedented full spectral color range with the Soret $\pi\rightarrow\pi^{*}$ absorption of the TCPP species showing large variations from 418 to 512 nm upon metal–ion coordination with TCPPs. However, on heating these multicolor nanosensors, discrete thermodynamic characteristics in the temperature range of 35–61 °C with the phase transition point dependent on the metal ion were displayed.

A selective colorimetric solid-phase extraction procedure for the determination of Mo^{6+} in aqueous samples was proposed by Filik et al.[220] Phenylhydrazine (**243**) was used as a coloring reagent for Mo^{6+} sensing and was immobilized onto a commercially available Amberlite XAD-16 resin. The color of this sensing layer changed from yellow to red in the presence of Mo^{6+} solution containing phosphate buffer at pH 2.2, thereby causing an increase in the measured reflectance intensity, i.e., 554.05 nm.

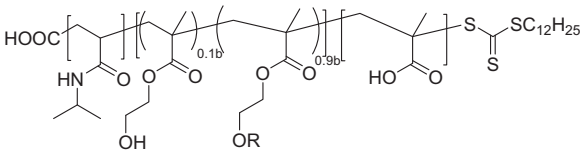

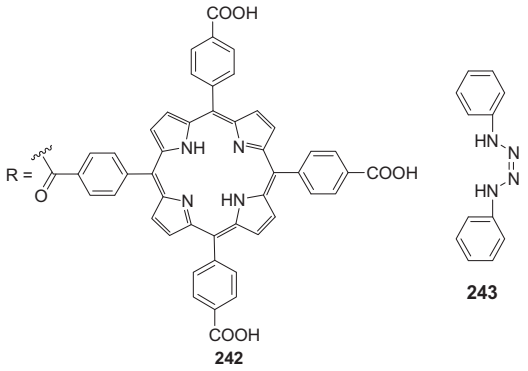

A first-generation poly(propyleneamine) dendrimer, peripherally modified with 4-(butylamino-substituted-1,8-naphthalimide) (**244**) underwent color and fluorescent changes upon addition of different cations in dry DMF solution.[221] Due to the presence of an electron-donating butylamino group, **244** showed absorption maxima in the visible region at λ=423–442 nm in dry DMF. The addition of NaOH changed the color only of its DMF solution from yellow to red, while its fluorescence was quenched. However, the addition of metal ions, such as Zn^{2+}, Co^{2+}, Ni^{2+}, Pb^{2+}, Mn^{2+}, Cu^{2+}, and Fe^{3+} restored the yellow color of the solution and its fluorescence emission increased.

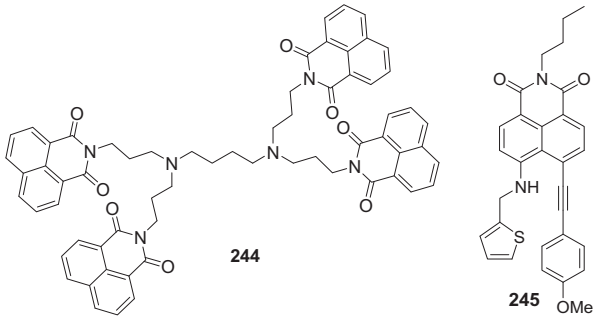

However, naphthalimide derivative **245**[222] had two absorption bands centered at 340 and 458 nm in ethanol/water (60:40 v/v) solution at pH 7.2. The addition of Pd^{2+} to the solution of **245** caused an enhancement in the absorbance at 340 nm with an expansion of the absorbance at 458 nm and meanwhile, a new peak was found in the absorbance at 270 nm. These absorption changes were accompanied by a color change from light yellow to black red with the addition of Pb^{2+} ions.

Metal-induced spirolactam ring opening of rhodamine has been observed in chemodosimeters **246** and **247**. The colorless solution of chemodosimeter **246** showed no absorbance above 500 nm.[223] Upon addition of Pd^{2+} to an aqueous solution of **246**, a strong absorption band centered at 560 nm formed and led to a brilliant purple coloration. The recognition of **246** to Pd^{2+} was based on the π-affinity of Pd^{2+} to allyl groups. Other metal cations with π-affinity, such as Ag^{+}, Ni^{2+}, Co^{2+}, Hg^{2+}, and Pt^{2+}, did not lead to any significant absorption or fluorescence changes.

As the addition of an excess of PPh_3 could reduce Pd^{2+} to Pd^{0}, so a similar absorption and color changes were observed when Pd^{2+} was added to PPh_3-**246** solution. Moreover, the **246**-Pd^{0} system displayed a much stronger fluorescence intensity and higher quantum yield than **246**-Pd^{2+}.

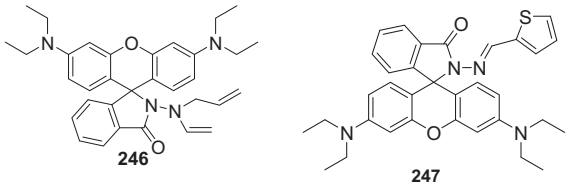

However, the UV–vis spectrum of **247**[224] showed no peak above 400 nm, but, upon addition of Cr^{3+}, a new peak appeared at 559 nm with a shoulder at 520 nm.

The Cr^{3+} chelation-induced aggregation of nanoparticles using 5,5′-dithiobis(2-nitrobenzoic acid)-modified gold nanoparticles (DTNBA-AuNPs) has been demonstrated by Wu et al.[225] By adding DTNBA to AuNPs in solution, functionalized nanostructures, TNBA-AuNPs, were obtained. A solution of TNBA-AuNPs displayed an extinction band at 524 nm, which underwent a red shift ($\Delta\lambda$=125 nm) to 650 nm along with the color of the TNBA-AuNPs changing from pink to blue after 30 min of incubation. The Cr^{3+}-induced value of A_{650}/A_{524} was ~17-fold larger than those achieved by other metal ions.

Bifunctionalized triazole-carboxyl AgNPs (**248**)[226] showed a cooperative effect on recognition of Co^{2+}, resulting in appreciable changes in color and absorption properties over other metal ions. The gradual addition of Co^{2+} to a solution of **248** led to a decrease in the absorption intensity at 405 nm and a dramatic increase in the absorbance intensity at 550 nm. A clear color progression from yellow to orange to red with increasing Co^{2+} concentration was additionally observed.

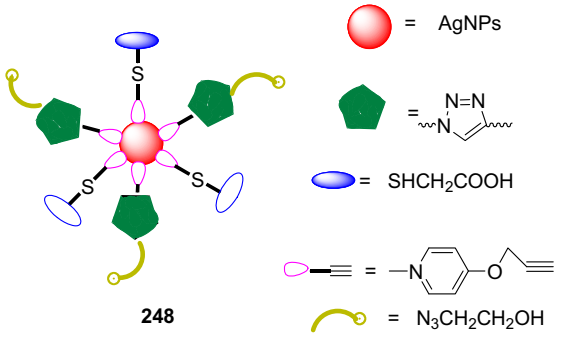

On the other hand, triazole-ester modified silver nanoparticles (**249**)[227] provided a highly selective colorimetric sensor for Cd^{2+}. The absorption spectrum of **249** showed λ_{max} at 394 nm. Amongst a variety of transition and alkali metal ions, only Cd^{2+} ions induced a distinct color change from yellow to red, which corresponded to a dramatic increase of absorption intensity at 550 nm. This was accompanied by a decrease in absorbance intensity at 394 nm.

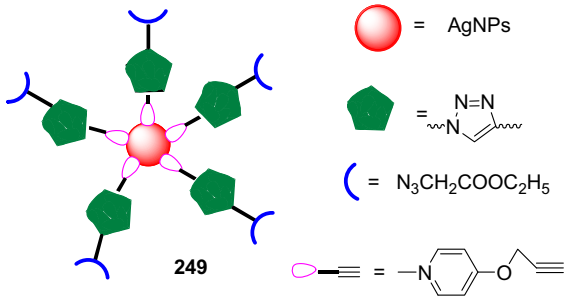

10. Lanthanide ion sensing chemosensors

The UV–vis spectrum of a photochromic Schiff base derivative based on calix[4]arene (**250**)[228] in CH_2Cl_2 possessed λ_{max} at 375 nm. With the addition of Dy^{3+}/Er^{3+} to a solution of **250**, the original peak at 375 nm was decreased and a new broad absorption band

appeared at 450–550 nm. The colorless solution of the chemosensor **250** changed to pink immediately when Dy^{3+} was added and changed to yellow for Er^{3+} after standing in the dark for 24 h.

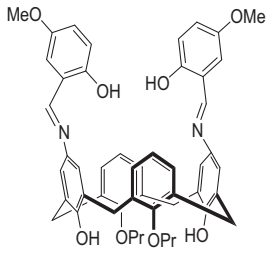

250

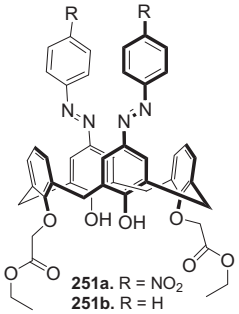

251a. R = NO_2
251b. R = H

Another chromogenic azo-calix[4]arene (**251**) showed complexation toward Cd^{2+}, Pb^{2+}, Mg^{2+}, and Eu^{3+} ions. The UV–vis spectrum of **251a** in MeCN exhibited λ_{max} at 393 nm.[229] Upon addition of Cd^{2+}, Pb^{2+}, Mg^{2+}, and Eu^{3+} ions to the solution of **251a**, a new red-shifted absorption band at 500 nm appeared and increased in intensity with a concomitant decrease of the 393 nm band. Similar changes were observed for chemosensor **251b**. Amongst these metal ions, Eu^{3+} gave maximum changes in the absorption spectrum. The stability constants of chemosensors **251a** and **251b** with Eu^{3+} ions were log K_{2a}=7.9 and log K_{2b}=7.8.

Molina et al. studied the metal–cation coordination properties of 1,4-bis(9-anthryl)-2-aza-1,3-butadiene (**252**),[230] in which two photoactive groups were directly attached by a 2-aza-1,3-butadiene bridge. The UV–vis spectrum of **252** in MeCN exhibited three shoulders at λ=348, 368, and 383 nm, due to the anthracene moiety, along with an intense and broad low-energy band, centered at 420 nm, attributed to the aza bridge, which was responsible for the yellow color of the chemosensor. Gradual addition of only Yb^{3+} and Lu^{3+} to the solution of **252** induced the appearance of a new and weak low-energy band at λ=503 and 508 nm, respectively. This absorption change was responsible for the color change from yellowish to orange. The Job's plot indicated a 1:1 binding model with the association constants being 2.2×10^4 and 1.1×10^4 M^{-1} for Yb^{3+} and Lu^{3+}, respectively.

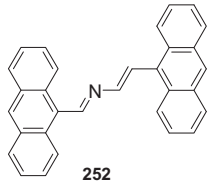

252

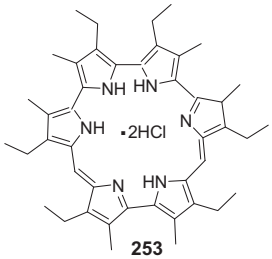

253

Hexaphyrin (1.0.1.0.0.0) (isamethyrin)[231] **253** underwent a significant color change in the presence of UO_2^{2+}, PuO_2^{2+}, and NpO_2^{2+}. The acid salt of isamethyrin exhibited three Soret-like bands at λ_{max} 384 nm, 497 nm and 597 nm. Upon complexation with uranyl ion, the macrocycle underwent spontaneous oxidation, resulting in a change in the overall electronic structure from antiaromatic to aromatic. This resulted in the appearance of one sharp, Soret-like transition at 530 nm and two smaller Q-like bands at 791 and 832 nm. The UO_2^{2+} complex required about 24 h to show a significant color change, whereas the addition of PuO_2^{2+}, NpO_2^{2+}, and Et_3N to a solution of **253** induced an instant color change; Cu^{2+} gave a purple color in comparison to UO_2^{2+}, which gave a more pink color. However, the UV–vis analysis showed a different type of Q-like band in the case of Cu^{2+}, Cd^{2+}, Ni^{2+}, and Pd^{4+}, whereas Gd^{3+} and Zn^{2+} gave a similar Soret band to that seen in UO_2^{2+}, but only a minor peak at 719 nm appeared.

Colorimetric sensors based on uranyl (UO_2^{2+})-specific DNAzyme and gold nanoparticles (AuNPs) have been demonstrated using both labeled and label-free methods by Lu and group.[232] The labeled method resulted in a turn-on sensor, going from purple AuNP aggregates into red disassembled AuNPs upon addition of UO_2^{2+}, whereas the label-free DNAzyme-AuNP sensor resulted in a turn-off sensor; the red AuNPs remained red in the presence of UO_2^{2+}, but changed to blue in the absence of UO_2^{2+}.

The absorption spectrum of malonamide-functionalized AuNPs (**254**)[233] in water revealed a plasmon absorption centered at 520 nm. Upon addition of Eu^{3+} to the solution of **254**, an immediate visible color change from red to blue occurred. In the UV–vis spectrum, the plasmon absorption at 520 nm diminished and broadened, in comparison with the dispersed nanoparticle solution. Moreover, upon addition of other lanthanide ions, such as La^{3+}, Nd^{3+}, Sm^{3+}, Gd^{3+}, Tb^{3+}, Ho^{3+}, and Er^{3+}, the position of the plasmon band shifted from 520 to 540 nm and showed the characteristic broadening and increased baseline.

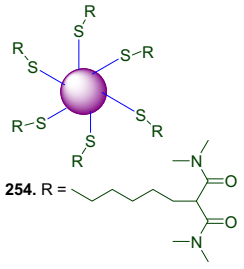

254. R =

255

β-Cyclodextrin-4,4′-dipyridine supramolecular inclusion complex-modified silver nanoparticles (**255**)[234] determined Yb^{3+} ions colorimetrically in aqueous solution via Yb^{3+}-induced aggregation to form chain-like supramolecular aggregates. The UV–vis spectra of **255** displayed λ_{max} at 401 nm. Only Yb^{3+} ions induced a distinct color change from yellow to red, which corresponded to a dramatic increase in the absorbance intensity at ~610 nm. Moreover, the aggregating growth of particles occurred preferentially in the direction of alignment of chemosensor **255**. After the addition of Yb^{3+}, **255** was oriented and assembled to form chain-like aggregates through the coordination linkage of Yb^{3+} ions. Thus, Yb^{3+} ions served as the glue linking the two neighboring Ag nanoparticles.

Acknowledgements

We are thankful to DST, New Delhi for financial assistance.

References and notes

1. Lehn, J.-M. *Chem. Soc. Rev.* **2007**, *36*, 151.
2. Anslyn, E. V. *J. Org. Chem.* **2007**, *72*, 687.
3. Beer, P. D. *Acc. Chem. Res.* **1998**, *31*, 71.
4. Bargossi, C.; Fiorini, M. C.; Montalti, M.; Prodi, L.; Zaccheroni, N. *Coord. Chem. Rev.* **2000**, *208*, 17.
5. Special issue on chemical sensors: *Chem. Rev.* **2000**, *100*, 2477 Guest editors Ellis, A.B.; Walt, D.R.
6. De silva, A. P.; Gunaratne, H. Q. N.; Gunnlaugsson, T.; Huxley, A. J. M.; McCoy, C. P.; Rademacher, J. T.; Rice, T. E. *Chem. Rev.* **1997**, *97*, 1515.
7. Prodi, L.; Bolletta, F.; Montalti, M.; Zaccheroni, N. *Coord. Chem. Rev.* **2000**, *205*, 59.
8. Recent special issues on supramolecular chemistry: (a) *Chem. Soc. Rev.* **2007**, *36*, 125; (b) *Coord. Chem. Rev.* **2006**, *250*, 2917.
9. (a) Pedersen, C. J. *Angew. Chem., Int. Ed. Engl.* **1988**, *27*, 1021; (b) Pedersen, C. J. *J. Am. Chem. Soc.* **1967**, *89*, 2495; (c) Pederson, C. J. *J. Am. Chem. Soc.* **1967**, *89*, 7017.
10. Cram, D. J. *Angew. Chem., Int. Ed. Engl.* **1988**, *27*, 1009.
11. Lehn, J.-M. *Angew. Chem., Int. Ed. Engl.* **1988**, *27*, 89.
12. Martinez-Manez, R.; Sancenon, F. *Chem. Rev.* **2003**, *103*, 4419.
13. Suksai, C.; Tuntulani, T. *Chem. Soc. Rev.* **2003**, *32*, 192.
14. Sancenon, F.; Martinez-Manez, R.; Soto, J. *Chem. Commun.* **2001**, 2262.
15. Liu, H.-H.; Chen, Y. *Eur. J. Org. Chem.* **2009**, 5261.

16. Chawla, H. M.; Sahu, S. N. *J. Inclusion Phenom. Macrocyclic Chem.* **2009**, *63*, 141.
17. Grabchev, I.; Dumas, S.; Chovelon, J.-M. *Dyes Pigm.* **2009**, *82*, 336.
18. Chakrabarti, A.; Chawla, H. M.; Francis, T.; Pant, N.; Upreti, S. *Tetrahedron* **2006**, *62*, 1150.
19. Lee, J. W.; Park, S. Y.; Cho, B.-K.; Kim, J. S. *Tetrahedron Lett.* **2007**, *48*, 2541.
20. Chen, Y. J.; Chung, W.-S. *Eur. J. Org. Chem.* **2009**, 4770.
21. Chang, K.-C.; Su, I.-H.; Wang, Y.-Y.; Chung, W.-S. *Eur. J. Org. Chem.* **2010**, 4700.
22. Takamuki, Y.; Maki, S.; Niwa, H.; Ikeda, H.; Hirano, T. *Tetrahedron* **2005**, *61*, 10073.
23. Hirano, T.; Sekiguchi, T.; Hashizume, D.; Ikeda, H.; Maki, S.; Niwa, H. *Tetrahedron* **2010**, *66*, 3842.
24. Yagi, S.; Nakamura, S.; Watanabe, D.; Nakazumi, H. *Dyes Pigm.* **2009**, *80*, 98.
25. Kar, P.; Suresh, M.; Kumar, D. K.; Jose, D. A.; Ganguly, B.; Das, A. *Polyhedron* **2007**, *26*, 1317.
26. Arunkumar, E.; Ajayaghosh, A.; Daub, J. *J. Am. Chem. Soc.* **2005**, *127*, 3156.
27. Caballero, A.; Tarraga, A.; Velasco, M. D.; Espinosa, A.; Molina, P. *Org. Lett.* **2005**, *7*, 3171.
28. Velu, R.; Ramakrishnan, V. T.; Ramamurthy, P. *Tetrahedron Lett.* **2010**, *51*, 4331.
29. Lin, S.-Y.; Chen, C.-H.; Lin, M.-C.; Hsu, H.-F. *Anal. Chem.* **2005**, *77*, 4821.
30. Wang, L.; Liu, X.; Hu, X.; Song, S.; Fan, C. *Chem. Commun.* **2006**, 3780.
31. Li, T.; Wang, E.; Dong, S. *Chem. Commun.* **2009**, 580.
32. Lee, S. J.; Lee, S. S.; Jeong, I. Y.; Lee, J. Y.; Jung, J. H. *Tetrahedron Lett.* **2007**, *48*, 393.
33. Xu, Z.; Qian, X.; Cui, J. *Org. Lett.* **2005**, *7*, 3029.
34. Mu, H.; Gong, R.; Ma, Q.; Sun, Y.; Fu, E. *Tetrahedron Lett.* **2007**, *48*, 5525.
35. Xu, Z.; Xiao, Y.; Qian, X.; Cui, J.; Cui, D. *Org. Lett.* **2005**, *7*, 889.
36. Huang, J.; Xu, Y.; Qian, X. *Dalton Trans.* **2009**, 1761.
37. Huang, J.; Xu, Y.; Qian, X. *Org. Biomol. Chem.* **2009**, *7*, 1299.
38. Xu, Z.; Pan, J.; Spring, D. R.; Cui, J.; Yoon, J. *Tetrahedron* **2010**, *66*, 1678.
39. Goswami, S.; Sen, D.; Das, N. K.; Hazra, G. *Tetrahedron Lett.* **2010**, *51*, 5563.
40. Wei, Y. L.; Li, Y.; Bo, L. J.; Song, Y. J. *Sci. China, Ser. B: Chem.* **2009**, *52*, 518.
41. Banthia, S.; Samanta, A. *New J. Chem.* **2005**, *29*, 1007.
42. Ghosh, T.; Maiya, B. G.; Samanta, A. *Dalton Trans.* **2006**, 795.
43. Elanchezhian, V. S.; Kandaswamy, M. *Inorg. Chem. Commun.* **2009**, *12*, 161.
44. Basurto, S.; Riant, O.; Moreno, D.; Rojo, J.; Torroba, T. *J. Org. Chem.* **2007**, *72*, 4673.
45. Ros-Lis, J. V.; Martinez-Manez, R.; Benito, A.; Soto, J. *Polyhedron* **2006**, *25*, 1585.
46. Wu, S.-P.; Hunag, R.-Y.; Du, K.-J. *Dalton Trans.* **2009**, 4735.
47. Kumar, M.; Babu, J. N.; Bhalla, V.; Dhir, A. *Inorg. Chem. Commun.* **2009**, *12*, 332.
48. Kim, H. J.; Kim, S. H.; Kim, J. H.; Anh, L. N.; Lee, J. H.; Lee, C.-H.; Kim, J. S. *Tetrahedron Lett.* **2009**, *50*, 2782.
49. Kumar, S.; Kaur, N. *Supramol. Chem.* **2006**, *18*, 137.
50. Kaur, N.; Kumar, S. *Dalton Trans.* **2006**, 3766.
51. Kaur, N.; Kumar, S. *Tetrahedron* **2008**, *64*, 3168.
52. Kaur, N.; Kumar, S. *Tetrahedron Lett.* **2006**, *47*, 4109.
53. Kaur, N.; Kumar, S. *Chem. Commun.* **2007**, 3069.
54. Kaur, N.; Kumar, S. *Tetrahedron Lett.* **2008**, *49*, 5067.
55. Ranyuk, E.; Douaihy, C. M.; Bessmertnykh, A.; Denat, F.; Averin, A.; Beletskaya, I.; Guilard, R. *Org. Lett.* **2009**, *11*, 987.
56. Wu, S.-P.; Du, K.-J.; Sung, Y.-M. *Dalton Trans.* **2010**, *39*, 4363.
57. Wang, W.; Fu, A.; You, J.; Gao, G.; Lan, J.; Chen, L. *Tetrahedron* **2010**, *66*, 3695.
58. Sanna, E.; Martinez, L.; Rotger, C.; Blasco, S.; Gonzalez, J.; Garcia-Espana, E.; Costa, A. *Org. Lett.* **2010**, *12*, 3840.
59. Basurto, S.; Miguel, D.; Moreno, D.; Neo, A. G.; Quesada, R.; Torroba, T. *Org. Biomol. Chem.* **2010**, *8*, 552.
60. Ballesteros, E.; Moreno, D.; Gomez, T.; Rodriguez, T.; Rojo, J.; Garcia-Valverde, M.; Torroba, T. *Org. Lett.* **2009**, *11*, 1269.
61. Wang, H.-H.; Xue, L.; Fang, Z.-J.; Li, G.-P.; Jiang, H. *New J. Chem.* **2010**, *34*, 1239.
62. Kim, M. H.; Noh, J. H.; Kim, S.; Ahn, S.; Chang, S.-K. *Dyes Pigm.* **2009**, *82*, 341.
63. Martinez, R.; Zapata, F.; Caballero, A.; Espinosa, A.; Tarraga, A.; Molina, P. *Org. Lett.* **2006**, *8*, 3235.
64. Guo, Z.-Q.; Chen, W.-Q.; Duan, X.-M. *Org. Lett.* **2010**, *12*, 2202.
65. Shao, N.; Jin, J. Y.; Wang, H.; Zhang, Y.; Yang, R. H.; Chan, W. H. *Anal. Chem.* **2008**, *80*, 3466.
66. Amaya, T.; Saio, D.; Koga, S.; Hirao, T. *Macromolecules* **2010**, *43*, 1175.
67. Mashraqui, S. H.; Khan, T.; Sundaram, S.; Ghadigaonkar, S. *Tetrahedron Lett.* **2008**, *49*, 3739.
68. Kaur, P.; Kaur, S.; Singh, K. *Inorg. Chem. Commun.* **2009**, *12*, 978.
69. Shao, N.; Pang, G.-X.; Wang, X.-R.; Wu, R.-J.; Cheng, Y. *Tetrahedron* **2010**, *66*, 7302.
70. Park, J. S.; Jeong, S.; Dho, S.; Lee, M.; Song, C. *Dyes Pigm.* **2010**, *87*, 49.
71. Lin, W.; Yuan, L.; Cao, X.; Tan, W.; Feng, Y. *Eur. J. Org. Chem.* **2008**, 4981.
72. Goswami, S.; Sen, D.; Das, N. K. *Org. Lett.* **2010**, *12*, 856.
73. Reynal, A.; Etxebarria, J.; Nieto, N.; Serres, S.; Palomares, E.; Vidal-Ferran, A. *Eur. J. Inorg. Chem.* **2010**, 1360.
74. Feng, L.; Zhang, Y.; Wen, L.; Shen, Z.; Guan, Y. *Talanta* **2011**, *84*, 913.
75. Maity, D.; Govindaraju, T. *Chem.—Eur. J.* **2011**, *17*, 1410.
76. Chamjangali, M. A.; Soltanpanah, S.; Goudarzi, N. *Sens. Actuators, B* **2009**, *138*, 251.
77. Wang, Z.; Fan, X.; Li, D.; Feng, L. *Spectrochim. Acta, Part A* **2008**, *71*, 1224.
78. Alvaro, M.; Aprile, C.; Garcia, H.; Peris, E. *Eur. J. Org. Chem.* **2005**, 3045.
79. Choi, S. H.; Pan, K.; Kim, K.; Churchill, D. G. *Inorg. Chem.* **2007**, *46*, 10564.
80. Guliyev, R.; Buyukcakir, O.; Sozmen, F.; Bozdemir, A. *Tetrahedron Lett.* **2009**, *50*, 5139.
81. Rodriguez-Morgade, M. S.; Planells, M.; Torres, T.; Ballester, P.; Palomares, E. *J. Mater. Chem.* **2008**, *18*, 176.
82. Xiang, Y.; Tong, A.; Jin, P.; Ju, Y. *Org. Lett.* **2006**, *8*, 2863.
83. Swamy, K. M. K.; Ko, S.-K.; Kwon, S. K.; Lee, H. N.; Mao, C.; Kim, J.-M.; Lee, K.-H.; Kim, J.; Shin, I.; Yoon, J. *Chem. Commun.* **2008**, 5915.
84. Zeng, X.; Dong, L.; Wu, C.; Mu, L.; Xue, S.-F.; Tao, Z. *Sens. Actuators, B* **2009**, *141*, 506.
85. Chen, X.; Jou, M. J.; Lee, H.; Kou, S.; Lim, J.; Nam, S.-W.; Park, S.; Kim, K.-M.; Yoon, J. *Sens. Actuators, B* **2009**, *137*, 597.
86. Zhao, M.; Yang, X.-F.; He, S.; Wang, L. *Sens. Actuators, B* **2009**, *135*, 625.
87. Zhou, Y.; Wang, F.; Kim, Y.; Kim, S.-J.; Yoon, J. *Org. Lett.* **2009**, *11*, 4442.
88. Yu, Fabiao; Zhang, W.; Li, P.; Xing, Y.; Tong, L.; Ma, J.; Tang, B. *Analyst* **2009**, *134*, 1826.
89. Zhao, Y.; Zhang, X.-B.; Han, Z.-X.; Qiao, L.; Li, C.-Y.; Jian, L.-X.; Shen, G.-L.; Yu, R.-Q. *Anal. Chem.* **2009**, *81*, 7022.
90. Xiang, Y.; Li, Z.; Chen, X.; Tong, A. *Talanta* **2008**, *74*, 1148.
91. Xu, Z.; Zhang, L.; Guo, R.; Xiang, T.; Wu, C.; Zheng, Z.; Yang, F. *Sens. Actuators, B* **2011**, *156*, 546.
92. Tang, L.; Li, F.; Liu, M.; Nandhakumar, R. *Spectrochim. Acta, Part A* **2011**, *78*, 1168.
93. Lin, W.-C.; Wu, C.-Y.; Liu, Z.-H.; Lin, C.-Y.; Yen, Y.-P. *Talanta* **2010**, *81*, 1209.
94. Basu, A.; Das, G. *Dalton Trans.* **2011**, *40*, 2837.
95. Liu, J.; Lu, Y. *Chem. Commun.* **2007**, 4872.
96. Yin, B.-C.; Ye, B.-C.; Tan, W.; Wang, H.; Xie, C.-C. *J. Am. Chem. Soc.* **2009**, *131*, 14624.
97. He, X.; Liu, H.; Li, Y.; Wang, S.; Li, Y.; Wang, N.; Xiao, J.; Xu, X.; Zhu, D. *Adv. Mater.* **2005**, *17*, 2811.
98. Singh, N.; Mulrooney, R. C.; Kaur, N.; Callan, J. F. *Chem. Commun.* **2008**, 4900.
99. Lee, H. Y.; Son, H.; Lim, J. M.; Oh, J.; Kang, D.; Han, W. S.; Jung, J. H. *Analyst* **2010**, *135*, 2022.
100. Yang, H.; Zhou, Z.-G.; Li, F.-Y.; Yi, T.; Huang, C.-H. *Inorg. Chem. Commun.* **2007**, *10*, 1136.
101. Yang, H.; Zhou, Z.-G.; Xu, J.; Li, F.-Y.; Yi, T.; Huang, C.-H. *Tetrahedron* **2007**, *63*, 6732.
102. Basheer, M. C.; Alex, S.; Thomas, K. G.; Suresh, C. H.; Das, S. *Tetrahedron* **2006**, *62*, 605.
103. Min, G.; Wei, X.; Mingyun, G.; Jianhua, S.; Gui, Y. *Chin. J. Chem.* **2009**, *27*, 1773.
104. Lee, S. J.; Jung, J. H.; Seo, J.; Yoon, I.; Park, K.-M.; Lindoy, L. F.; Lee, S. S. *Org. Lett.* **2006**, *8*, 1641.
105. Lee, H. G.; Lee, J.-E.; Choi, K. S. *Inorg. Chem. Commun.* **2006**, *9*, 582.
106. Abalos, T.; Jimenez, D.; Martinez-Manez, R.; Ros-Lis, J. V.; Royo, S.; Sancenon, F.; Soto, J.; Costero, A. M.; Gil, S.; Parra, M. *Tetrahedron Lett.* **2009**, *50*, 3885.
107. Yuan, M.; Li, Y.; Li, J.; Li, C.; Liu, X.; Lv, J.; Xu, J.; Liu, H.; Wang, S.; Zhu, D. *Org. Lett.* **2007**, *9*, 2313.
108. Coronado, E.; Galan-Mascaros, J. R.; Marti-Gastaldo, C.; Palomares, E.; Durrant, J. R.; Vilar, R.; Gratzel, M.; Nazeeruddin, M. K. *J. Am. Chem. Soc.* **2005**, *127*, 12351.
109. Zhang, X.; Hunag, J. *Chem. Commun.* **2010**, 6042.
110. Xiang-Hong, L.; Zhi-Qiang, L.; Fu-You, L.; Xin-Fang, D.; Chun-Hui, H. *Chin. J. Chem.* **2007**, *25*, 186.
111. Zhao, Q.; Cao, T.; Li, F.; Li, X.; Jing, H.; Yi, T.; Huang, C. *Organometallics* **2007**, *26*, 2977.
112. Wang, J.; Qian, X.; Cui, J. *J. Org. Chem.* **2006**, *71*, 4308.
113. Kim, S. H.; Kim, J. S.; Park, S. M.; Chang, S.-K. *Org. Lett.* **2006**, *8*, 371.
114. Ruan, Y.-B.; Maisonneuve, S.; Xie, J. *Dyes Pigm.* **2011**, *90*, 239.
115. Tatay, S.; Gavina, P.; Coronado, E.; Palomares, E. *Org. Lett.* **2006**, *8*, 3857.
116. Li, Y.; He, S.; Lu, Y.; Zeng, X. *Org. Biomol. Chem.* **2011**, *9*, 2606.
117. Shunmugam, R.; Gabriel, G. J.; Smith, C. E.; Aamer, A.; Tew, G. N. *Chem.—Eur. J.* **2008**, *14*, 3904.
118. Zou, B. Y.; Wan, M.; Sang, G.; Ye, M.; Li, Y. *Adv. Funct. Mater.* **2008**, *18*, 2724.
119. Liu, S.-J.; Fang, C.; Zhao, Q.; Fan, Q.-L.; Huang, W. *Macromol. Rapid Commun.* **2008**, *29*, 1212.
120. Bingol, H.; Kocabas, E.; Zor, E.; Coskum, A. *Talanta* **2010**, .
121. Bajaj, L.; Chawla, H. M.; Francis, T.; Venkatesan, N. *ARKIVOC* **2005**, *iii*, 200.
122. Kao, T.-L.; Wang, C.-C.; Pan, Y.-T.; Shiao, Y.-J.; Yen, J.-Y.; Shu, C.-M.; Lee, G.-H.; Peng, S.-M.; Chung, W.-S. *J. Org. Chem.* **2005**, *70*, 2912.
123. Nuriman; Kuswandi, B.; Verboom, W. *Anal. Chim. Acta* **2009**, *655*, 75.
124. Caballero, A.; Lloveras, V.; Curiel, D.; Tarraga, A.; Espinosa, A.; Garcia, R.; Vidal-Gancedo, J.; Rovira, C.; Wurst, K.; Molina, P.; Veciana, J. *Inorg. Chem.* **2007**, *46*, 825.
125. Zapata, F.; Caballero, A.; Espinosa, A.; Tarraga, A.; Molina, P. *Inorg. Chem.* **2009**, *48*, 11566.
126. Romero, T.; Caballero, A.; Espinosa, A.; Tarraga, A.; Molina, P. *Dalton Trans.* **2009**, 2122.
127. Martinez, R.; Zapata, F.; Caballero, A.; Espinosa, A.; Tarraga, A.; Molina, P. *ARKIVOC* **2010**, *iii*, 124.
128. Caballero, A.; Martinez, R.; lloveras, V.; Ratera, I.; Vidal-Gancedo, J.; Wurst, K.; Tarraga, A.; Molina, P.; Veciana, J. *J. Am. Chem. Soc.* **2005**, *127*, 15666.
129. Martinez, R.; Espinosa, A.; Tarraga, A.; Molina, P. *Org. Lett.* **2005**, *7*, 5869.
130. Sheng, R.; Wang, P.; Liu, W.; Wu, X.; Wu, S. *Sens. Actuators, B* **2008**, *128*, 507.
131. Huang, J.; Xu, Y.; Qian, X. *J. Org. Chem.* **2009**, *74*, 2167.
132. Martinez, R.; Espinosa, A.; Tarranga, A.; Molina, P. *Tetrahedron* **2010**, *66*, 3662.
133. Cheng, Y.-F.; Zhao, D.-T.; Zhang, M.; Liu, Z.-Q.; Zhou, Y.-F.; Shu, T.-M.; Li, F.-Y.; Yi, T.; Huang, C.-H. *Tetrahedron Lett.* **2006**, *47*, 6413.
134. Zheng, H.; Qian, Z.-H.; Xu, L.; Yuan, F.-F.; Lan, L.-D.; Xu, J.-G. *Org. Lett.* **2006**, *8*, 859.

135. Wu, J.-S.; Hwang, I.-C.; Kim, K. S.; Kim, J. S. *Org. Lett.* **2007**, *9*, 907.
136. (a) Yang, Y.-K.; Yook, K.-J.; Tae, J. *J. Am. Chem. Soc.* **2005**, *127*, 16760; (b) Ko, S.-K.; Yang, Y.-K.; Tae, J.; Shin, I. *J. Am. Chem. Soc.* **2006**, *128*, 14150.
137. Soh, J. H.; Swamy, K. M. K.; Kim, S. K.; Kim, S.; Lee, S.-H.; Yoon, J. *Tetrahedron Lett.* **2007**, *48*, 5966.
138. Kim, S. K.; Swamy, K. M. K.; Chung, S.-Y.; Kim, H. N.; Kim, M. J.; Jeong, Y.; Yoon, J. *Tetrahedron Lett.* **2010**, *51*, 3286.
139. Chen, X.; Nam, S.-W.; Jou, M. J.; Kim, Y.; Kim, S.-J.; Park, S.; Yoon, J. *Org. Lett.* **2008**, *10*, 5235.
140. (a) Zhan, X.-Q.; Qian, Z.-H.; Zheng, H.; Su, B.-Y.; Lan, Z.; Xu, J.-G. *Chem. Commun.* **2008**, 1859; (b) Shi, W.; Ma, H. *Chem. Commun.* **2008**, 1856.
141. Chen, X.; Baek, K.-H.; Kim, Y.; Kim, S.-J.; Shin, I.; Yoon, J. *Tetrahedron* **2010**, *66*, 4016.
142. Ahamed, B. N.; Ghosh, P. *Inorg. Chim. Acta* **2011**, *372*, 100.
143. Jiang, L.; Wang, L.; Zhang, B.; Yin, G.; Wang, R.-Y. *Eur. J. Inorg. Chem.* **2010**, 4438.
144. Kim, H. N.; Nam, S.-W.; Swamy, K. M. K.; Jin, Y.; Chen, X.; Kim, Y.; Kim, S.-J.; Park, S.; Yoon, J. *Analyst* **2011**, *136*, 1339.
145. Wang, H.; Li, Y.; Xu, S.; Li, Y.; Zhou, C.; Fei, X.; Sun, L.; Zhang, C.; Li, Y.; Yang, Q.; Xu, X. *Org. Biomol. Chem.* **2011**, *9*, 2850.
146. Peng, X.; Wang, Y.; Tang, X.; Liu, W. *Dyes Pigm.* **2011**, *91*, 26.
147. Liu, B.; Tian, H. *Chem. Commun.* **2005**, 3156.
148. Lee, M. H.; Lee, S. W.; Kim, S. H.; Kang, C.; Kim, J. S. *Org. Lett.* **2009**, *11*, 2101.
149. Guo, Z.; Zhu, W.; Zhu, M.; Wu, X.; Tian, H. *Chem.—Eur. J.* **2010**, *16*, 14424.
150. Lee, M. H.; Cho, B.-K.; Yoon, J.; Kim, J. S. *Org. Lett.* **2007**, *9*, 4515.
151. Cheng, C.-C.; Chen, Z.-S.; Wu, C.-Y.; Lin, C.-C.; Yang, C.-R.; Yen, Y.-P. *Sens. Actuators, B* **2009**, *142*, 280.
152. Ros-Lis, J. V.; Marcos, D.; Martinez-Manez, R.; Rurack, K.; Soto, J. *Angew. Chem., Int. Ed.* **2005**, *44*, 4405.
153. Ahamed, B. N.; Arunachalam, M.; Ghosh, P. *Inorg. Chem.* **2010**, *49*, 4447.
154. Shi, H.-F.; Liu, S.-J.; Sun, H.-B.; Xu, W.-J.; An, Z.-F.; Chen, J.; Sun, S.; Lu, X.-M.; Zhao, Q.; Huang, W. *Chem.—Eur. J.* **2010**, *16*, 12158.
155. Leng, B.; Zou, L.; Jiang, J.; Tian, H. *Sens. Actuators, B* **2009**, *140*, 162.
156. Yu, C.-J.; Cheng, T.-L.; Tseng, W.-L. *Biosens. Bioelectron.* **2009**, *25*, 204.
157. Huang, C.-C.; Chang, H.-T. *Chem. Commun.* **2007**, 1215.
158. Lee, J.-S.; Han, M. S.; Mirkin, C. A. *Angew. Chem., Int. Ed.* **2007**, *46*, 4093.
159. Lu, N.; Shao, C.; Deng, Z. *Analyst* **2009**, *134*, 1822.
160. Li, Tao; Dong, S.; Wang, E. *Anal. Chem.* **2009**, *81*, 2144.
161. Wang, H.; Wang, Y. X.; Jin, J.; Yang, R. H. *Anal. Chem.* **2008**, *80*, 9021.
162. Xue, X.; Wang, F.; Liu, X. *J. Am. Chem. Soc.* **2008**, *130*, 3244.
163. Xu, X.; Wang, J.; Jiao, K.; Yang, X. *Biosens. Bioelectron.* **2009**, *24*, 3153.
164. Cho, Y.; Lee, S. S.; Jung, J. H. *Analyst* **2010**, *135*, 1551.
165. Hirayama, T.; Taki, M.; Kashiwagi, Y.; Nakamoto, M.; Kunishita, A.; Itoh, S.; Yamamoto, Y. *Dalton Trans.* **2008**, 4705.
166. Lee, S. J.; Lee, J.-E.; Seo, J.; Jeong, I. Y.; Lee, S. S.; Jung, J. H. *Adv. Funct. Mater.* **2007**, *17*, 3441.
167. Lin, C.-Y.; Yu, C.-J.; Lin, Y.-H.; Tseng, W.-L. *Anal. Chem.* **2010**, *82*, 6830.
168. Fan, Y.; Liu, Z.; Wang, L.; Zhan, J. *Nanoscale Res. Lett.* **2009**, *4*, 1230.
169. Wang, Y.; Yang, F.; Yang, X. *Biosens. Bioelectron.* **2010**, *25*, 1994.
170. Kim, E.; Seo, S.; Seo, M. L.; Jung, J. H. *Analyst* **2010**, *135*, 149.
171. Bhardwaj, V. K.; Singh, N.; Hundal, M. S.; Hundal, G. *Tetrahedron* **2006**, *62*, 7878.
172. Singh, N.; Kaur, N.; Choitir, C. N.; Callan, J. F. *Tetrahedron Lett.* **2009**, *50*, 4201.
173. Swamy, K. M. K.; Kim, H. N.; Soh, J. H.; Kim, Y.; Kim, S.-J.; Yoon, J. *Chem. Commun.* **2009**, 1234.
174. Chatterjee, A.; Santra, M.; Won, N.; Kim, S.; Kim, J. K.; Kim, S. B.; Ahn, K. H. *J. Am. Chem. Soc.* **2009**, *139*, 2040.
175. Qu, F.; Liu, J.; Yan, H.; Peng, L.; Li, H. *Tetrahedron Lett.* **2008**, *49*, 7438.
176. Li, B.; Du, Y.; Dong, S. *Anal. Chim. Acta* **2009**, *644*, 78.
177. Andal, V.; Buvaneswari, G. *Sens. Actuators, B* **2011**, *155*, 653.
178. Wallace, K. J.; Gray, M.; Zhong, Z.; Lynch, V. M.; Anslyn, E. V. *Dalton Trans.* **2005**, 2436.
179. Suresh, P.; Azath, I. A.; Pitchumani, K. *Sens. Actuators, B* **2010**, *146*, 273.
180. Liang, Z.-Q.; Wang, C.-X.; Yang, J.-X.; Gao, H.-W.; Tian, Y.-P.; Tao, X.-T.; Jiang, M.-H. *New J. Chem.* **2007**, *31*, 906.
181. Tang, L.; Li, Y.; Nandhakumar, R.; Qian, J. *Monatsh. Chem.* **2010**, *141*, 615.
182. Bae, S.; Tae, J. *Tetrahedron Lett.* **2007**, *48*, 5389.
183. Dong, L.; Wu, C.; Zeng, X.; Mu, L.; Xue, S.-F.; Tao, Z.; Zhang, J.-X. *Sens. Actuators, B* **2010**, *145*, 433.
184. Moon, K.-S.; Yang, Y.-K.; Ji, S.; Tae, J. *Tetrahedron Lett.* **2010**, *51*, 3290.
185. Xiang, Y.; Tong, A. *Org. Lett.* **2006**, *8*, 1549.
186. Wang, S.; Gwon, S.-Y.; Kim, S.-H. *Spectrochim. Acta, Part A* **2010**, *76*, 293.
187. Xue, H.; Tang, X.-J.; Wu, L.-Z.; Zhang, L.-P.; Tung, C.-H. *J. Org. Chem.* **2005**, *70*, 9727.
188. Balandier, J.-Y.; Belyasmine, A.; Salle, M. *Eur. J. Org. Chem.* **2008**, 269.
189. Lee, K. M.; Chen, X.; Fang, W.; Kim, J.-M.; Yoon, J. *Macromol. Rapid Commun.* **2011**, *32*, 497.
190. Pan, X.; Wang, Y.; Jiang, H.; Zou, G.; Zhang, Q. *J. Mater. Chem.* **2011**, *21*, 3604.
191. Caballero, A.; Espinosa, A.; Tarraga, A.; Molina, P. *J. Org. Chem.* **2008**, *73*, 5489.
192. Zapata, F.; Caballero, A.; Espinosa, A.; Tarraga, A.; Molina, P. *Org. Lett.* **2008**, *10*, 41.
193. Zapata, F.; Caballero, A.; Espinosa, A.; Tarraga, A.; Molina, P. *J. Org. Chem.* **2009**, *74*, 4787.
194. Chang, K.-C.; Su, I.-H.; Lee, G.-H.; Chung, W.-S. *Tetrahedron Lett.* **2007**, *48*, 7274.
195. Goswami, S.; Chakrabarty, R. *Eur. J. Org. Chem.* **2010**, 3791.
196. Kwon, J. Y.; Jang, Y. J.; Lee, Y. J.; Kim, K. M.; Seo, M. S.; Nam, W.; Yoon, J. *J. Am. Chem. Soc.* **2005**, *127*, 10107.
197. Li, H.; Zheng, Q.; Han, C. *Analyst* **2010**, *135*, 1360.
198. Chen, Y.-Y.; Chang, H.-T.; Shiang, Y.-C.; Hung, Y.-L.; Chiang, C.-K.; Huang, C.-C. *Anal. Chem.* **2009**, *8*, 9433.
199. Hung, Y.-L.; Hsiung, T.-M.; Chen, Y.-Y.; Huang, C.-C. *Talanta* **2010**, *82*, 516.
200. Guan, J.; Jiang, L.; Zhao, L.; Li, J.; Yang, W. *Colloids Surf., A* **2008**, *325*, 194.
201. Liu, J.; Lu, Y. *J. Am. Chem. Soc.* **2005**, *127*, 12677.
202. Huang, K.-W.; Yu, C.-J.; Tseng, W.-L. *Biosens. Bioelectron.* **2010**, *25*, 984.
203. Li, T.; Wang, E.; Dong, S. *Anal. Chem.* **2010**, *82*, 1515.
204. Chai, F.; Wang, C.; Wang, T.; Li, L.; Su, Z. *ACS Appl. Mater. Interfaces* **2010**, *2*, 1466.
205. Zeng, Y.; Zhang, G.; Zhang, D.; Zhu, D. *Tetrahedron* **2008**, *49*, 7391.
206. Xu, Z.; Kim, G.-H.; Han, S. J.; Jou, M. J.; Lee, C.; Shin, I.; Yoon, J. *Tetrahedron* **2009**, *65*, 2307.
207. Kaur, P.; Kaur, S.; Mahajan, A.; Singh, K. *Inorg. Chem. Commun.* **2008**, *11*, 626.
208. Wang, J.; Ha, C.-S. *Tetrahedron* **2009**, *65*, 6959.
209. Wang, J.; Ha, C.-S. *Sens. Actuators, B* **2010**, *146*, 373.
210. Xu, Z.; Qian, X.; Cui, J.; Zhang, R. *Tetrahedron* **2006**, *62*, 10117.
211. Lu, C.; Xu, Z.; Cui, J.; Zhang, R.; Qian, X. *J. Org. Chem.* **2007**, *72*, 3554.
212. Oton, F.; Espinosa, A.; Tarraga, A.; Molina, P. *Organometallics* **2007**, *26*, 6234.
213. Zapata, F.; Caballero, A.; Espinosa, A.; Tarranga, A.; Molina, P. *Org. Lett.* **2007**, *9*, 2385.
214. Caballero, A.; Espinosa, A.; Tarranga, A.; Molina, P. *J. Org. Chem.* **2007**, *7*, 6924.
215. Li, H.-Y.; Gao, S.; Xi, Z. *Inorg. Chem. Commun.* **2009**, *12*, 300.
216. Wang, S.; Men, G.; Zhao, L.; Hou, Q.; Jiang, S. *Sens. Actuators, B* **2010**, *145*, 826.
217. Zhou, X.; Yu, B.; Guo, Y.; Tang, X.; Zhang, H.; Liu, W. *Inorg. Chem.* **2010**, *49*, 4002.
218. Chadlaoui, M.; Abaraca, B.; Ballesteros, R.; Arellano, C. R. D. *J. Org. Chem.* **2006**, *71*, 9030.
219. Yan, Q.; Yuan, J.; Kang, Y.; Cai, Z.; Zhou, L.; Yin, Y. *Chem. Commun.* **2010**, 2781.
220. Filik, H.; Aksu, D.; Apak, R.; Boz, I. *Sens. Actuators, B* **2009**, *141*, 491.
221. Grabchev, I.; Bosch, P.; Mckenna, M.; Staneva, D. *J. Photochem. Photobiol., A* **2009**, *201*, 75.
222. Duan, L.; Xu, Y.; Qian, X. *Chem. Commun.* **2008**, 6339.
223. Li, H.; Fan, J.; Du, J.; Guo, K.; Sun, S.; Liu, X.; Peng, X. *Chem. Commun.* **2010**, 1079.
224. Weerasinghe, A. J.; Schmiesing, C.; Sinn, E. *Tetrahedron Lett.* **2009**, *50*, 6407.
225. Dang, Y.-Q.; Li, H.-W.; Wang, B.; Li, L.; Wu, Y. *ACS Appl. Mater. Interfaces* **2009**, *1*, 1533.
226. Yao, Y.; Tian, D.; Li, H. *ACS Appl. Mater. Interfaces* **2010**, *2*, 684.
227. Li, H.; Yao, Y.; Han, C.; Zhan, J. *Chem. Commun.* **2009**, 4812.
228. Liang, Z.; Liu, Z.; Gao, Y. *Tetrahedron Lett.* **2007**, *48*, 3587.
229. Rouis, A.; Mlika, R.; Dridi, C.; Davenas, J.; Ouada, H. B.; Halouani, H.; Bonnamour, I.; Jaffrezic, N. *Mater. Sci. Eng. C* **2006**, *26*, 247.
230. Zapata, F.; Caballero, A.; Espinosa, A.; Tarraga, A.; Molina, P. *Eur. J. Inorg. Chem.* **2010**, 697.
231. Sessler, J. L.; Melfi, P. J.; Seidel, D.; Gorden, A. E. V.; Ford, D. K.; Palmer, P. D.; Tait, C. D. *Tetrahedron* **2004**, *60*, 11089.
232. Lee, J. H.; Wang, Z.; Liu, J.; Lu, Y. *J. Am. Chem. Soc.* **2008**, *130*, 14217.
233. Lisowski, C. E.; Hutchison, J. E. *Anal. Chem.* **2009**, *81*, 10246.
234. Han, C.; Zhang, L.; Li, H. *Chem. Commun.* **2009**, 3545.

Biographical sketch

Dr. Navneet Kaur received her M.Sc. (Hons. School) from Guru Nanak Dev University, Amritsar, India in 2003. She completed her Ph.D. (2008) under the supervision of Professor Subodh Kumar at the Department of Chemistry, Guru Nanak Dev University, Amritsar, where she worked on the synthesis and photophysical studies of colorimetric chemosensors for metal ions. She is presently working as assistant professor in Panjab University, Chandigarh, Punjab, India. Her research activities focus on the development of molecular chemosensors and their applications as multiple-mode molecular logic systems.

Professor Subodh Kumar after obtaining his Ph.D. (1985) from Guru Nanak Dev University, Amritsar, India joined the Department of Chemistry, Guru Nanak Dev University, Amritsar as a Lecturer. He is presently Professor and head in the same department. His research activities focus on the development of organic materials for applications as molecular sensors, organic light-emitting diodes, and molecular logic systems. He is the recipient of Bronze Medal of Chemical Research Society of India (2004), Bhagya Tara award, Punjab University (2008) and Professor M.S. Wadia award, University of Pune (2008). He is a fellow of 'The National Academy of Science', Allahabad (2003).